


 Cite this: *RSC Adv.*, 2024, 14, 31877

# Current and emerging trends of inorganic, organic and eco-friendly corrosion inhibitors†

 Mahmoud A. Ahmed, \*<sup>ab</sup> Sherif Amin<sup>b</sup> and Ashraf A. Mohamed \*<sup>a</sup>

Effective corrosion control strategies are highly desired to reduce the fate of corrosion. One widely adopted approach is the use of corrosion inhibitors, which can significantly mitigate the detrimental effects of corrosion. This systematic review provides a thorough analysis of corrosion inhibitors, including both inorganic and organic compounds. It explores the inhibition mechanisms, highlighting the remarkable inhibitive efficiency of organic compounds attributed to the presence of heteroatoms and conjugated  $\pi$ -electron systems. The review presents case studies and investigations of corrosion inhibitors, shedding light on their performance and application potential. Moreover, it compares the efficacy, compatibility, and sustainability of emerging environmentally friendly corrosion inhibitors, including biopolymers from natural resources as promising candidates. The review also highlights the potential of synergistic impacts between mixed corrosion inhibitors, particularly organic/organic systems, as a viable and advantageous choice for applications in challenging processing environments. The evaluation of inhibitors is discussed, encompassing weight loss (WL) analysis, electrochemical analysis, surface analysis, and quantum mechanical calculations. The review also discusses the thermodynamics and isotherms related to corrosion inhibition, further improving the understanding of inhibitor's behavior and mechanisms. This review serves as a valuable resource for researchers, engineers, and practitioners involved in corrosion control, offering insights and future directions for effective and environmentally friendly corrosion inhibition strategies.

 Received 5th August 2024  
 Accepted 23rd September 2024

DOI: 10.1039/d4ra05662k

[rsc.li/rsc-advances](https://rsc.li/rsc-advances)
<sup>a</sup>Chemistry Department, Faculty of Science, Ain Shams University, Cairo 11566, Egypt. E-mail: mahmoudmahmoud\_p@sci.asu.edu.eg; aamohamd@sci.asu.edu.eg

<sup>b</sup>Veolia Water Technologies, Cairo 11835, Egypt

 † Electronic supplementary information (ESI) available. See DOI: <https://doi.org/10.1039/d4ra05662k>

**Mahmoud A. Ahmed**

Mahmoud Adel Ahmed earned his PhD degree in 2024. He has been actively engaged in research for the past eight years and his research focuses on the synthesis, characterization, and environmental applications of nanomaterials and their composites in water treatment and remediation. He has authored several reviews and book chapters on these topics. He also serves as a senior service engineer at Veolia Environmental Services, managing various sectors like reverse osmosis, boilers, cooling towers, and wastewater plants.


**Sherif Amin**

Sherif Amin is a seasoned professional with over 20 years of experience in the water treatment field. He obtained his B.Sc. in Chemistry from Al-Azhar University in 2001. For the past 15+ years, Amin has served as a Chemical Service Manager for Veolia Environment, managing various sectors including reverse osmosis, boilers, cooling towers, and wastewater plants. Amin has extensive experience in the application of chemical processes such as corrosion inhibitors, scale inhibitors, coagulants, flocculants, and dispersants. He has authored numerous publications on water treatment.



# 1. Introduction

Corrosion is a complex phenomenon that takes many forms, including uniform and localized corrosion, where atmospheric, galvanic, microbiological, pitting, crevice, erosion, intergranular, and stress-cracking corrosion types are most common.<sup>1</sup> Corrosion causes irreversible degradation of materials, affecting not only the structural integrity of buildings, bridges, and infrastructures but also posing risks to human safety and life.<sup>2,3</sup> In addition to the direct costs associated with replacing corroded parts and maintaining equipment, corrosion has indirect economic consequences.<sup>4</sup> Corrosion-related equipment breakdowns reduce industry efficiency and cause lost productivity. Furthermore, corrosion's detrimental consequences on the environment should not be ignored. Corrosion-induced leaks and spills have the potential to pollute soil, water, and air, causing ecological disruption and posing health risks. When toxic substances from corroded materials leak into the surroundings, it can have lasting impacts on the ecosystem, necessitating extensive cleanup and mitigation activities. Because of the serious consequences of corrosion, governments and corporations all over the world are focusing their efforts on developing innovative corrosion avoidance and management approaches.<sup>5</sup> While corrosion cannot be completely eradicated, several approaches can greatly reduce its incidences and consequences.<sup>6</sup> These approaches often include changing the potential, surface coating, improved structural design, proper material selection, modifying the surrounding environment, and the use of corrosion inhibitors as potent protection measures, as shown in Fig. 1.<sup>7-9</sup>

Corrosion inhibitors are one of the popular approaches that have been thoroughly explored and are commonly employed for mitigating various types of uniform and localized corrosion. These inhibitors are chemical species that interact with the material's surface and/or change the characteristics of the surrounding environment to substantially boost a material's corrosion resistance in a particular environment. When applied

in tiny concentrations, these inhibitors prevent or retard corrosion without substantially altering the concentration of other corrosive agents. An ideal corrosion inhibitor should be economical, simple to use, eco-friendly, and highly efficient at low dosages. Corrosion inhibitors found applications in various industrial, and pipe-line protection applications, including the oil and gas industry, cooling systems, potable water production, and the processing of metal surfaces before coating application, such as protecting reinforced concrete structures.<sup>10,11</sup> Corrosion inhibitors can be classified according to their chemical composition (organic or inorganic), their oxidizing/non-oxidizing properties, or their application field (descaling, pickling, cooling water systems, acid cleaning, among others). Corrosion inhibitors stop or retard the anodic oxidation and/or cathodic reduction processes and may lead to the formation of a protective layer or film on the exposed metal surface. Thus, inhibitors may be classified as: anodic, cathodic, or mixed inhibitors. However, the most used classification scheme is that based on chemical composition. Organic inhibitors work mainly by adsorption mechanisms, whereas inorganic inhibitors typically work with electrochemical mechanisms. When it comes to performance, inorganic inhibitors have been long used since they work better over a wider temperature range and for longer periods. However, despite their relatively higher cost, organic inhibitors are thought to be safer.<sup>12-14</sup> The performance of organic inhibitors relies on their composition, which typically includes various polar groups such as  $-OH$ ,  $-OCH_3$ ,  $-COOH$ ,  $-COOC_2H_5$ ,  $-NH_2$ ,  $-CONH_2$ , among others.<sup>14-16</sup> These groups contain heteroatoms and non-bonding and  $\pi$ -electrons that enable extensive interactions.<sup>17,18</sup> When these organic inhibitors contact a metallic surface, they can form adsorption layers or protective films that shield the metal from its corrosive environment and prevent its oxidation. Organic inhibitors can bind to metal surfaces by chemisorption and/or physisorption. The former involves coordinate-type bonding, *e.g.*, sharing the inhibitor's  $\pi$ - and non-bonding electrons with the metal d-orbitals, whereas the latter involves physical electrostatic attraction between the inhibitor and the metal surface.<sup>13</sup> Inorganic inhibitors such as chromates, molybdates, phosphates, nitrites, nitrates, borates, and silicates were commonly used to combat corrosion.<sup>19,20</sup> These substances interact with metal surfaces with various mechanisms that prevent corrosion. Due to cost considerations, more feasible alternatives such surface active chelates, gluconates, polyacrylates, polyphosphates, carboxylates, and phosphonates gradually replaced many of the older inhibitors. Some of the latter substances act as precipitating inhibitors that typically produce precipitates at the metal–environment interface, while others can act as passivators, scavengers, corrosion poisons, or blockers.<sup>13,21,22</sup> Moreover, some old inhibitors, *e.g.*, chromates, have frequently raised environmental concerns due to detrimental impacts on soil and aquatic life.<sup>23,24</sup> In response to these concerns, researchers are actively exploring environmentally friendly inhibitors as alternatives to traditional inhibitors. These eco-friendly alternatives offer numerous advantages, including ready availability of resources, non-toxicity, renewability, friendly synthesis processes, cost-effectiveness, and development of



Ashraf A. Mohamed

*Ashraf A. Mohamed is a professor of environmental analytical chemistry, at the Department of Chemistry, Faculty of Science, Ain Shams University, Cairo, Egypt. He earned his MSc degree in 1991 and his PhD degree in 1995. He has been actively engaged in research for the past 35 years and his current research interests include analytical chemistry, nanomaterials, layered double hydroxides, molecularly imprinted polymers,*

*water treatment and analysis, optical sensors, and paper microfluidics. He has authored several reviews and book chapters on these topics.*



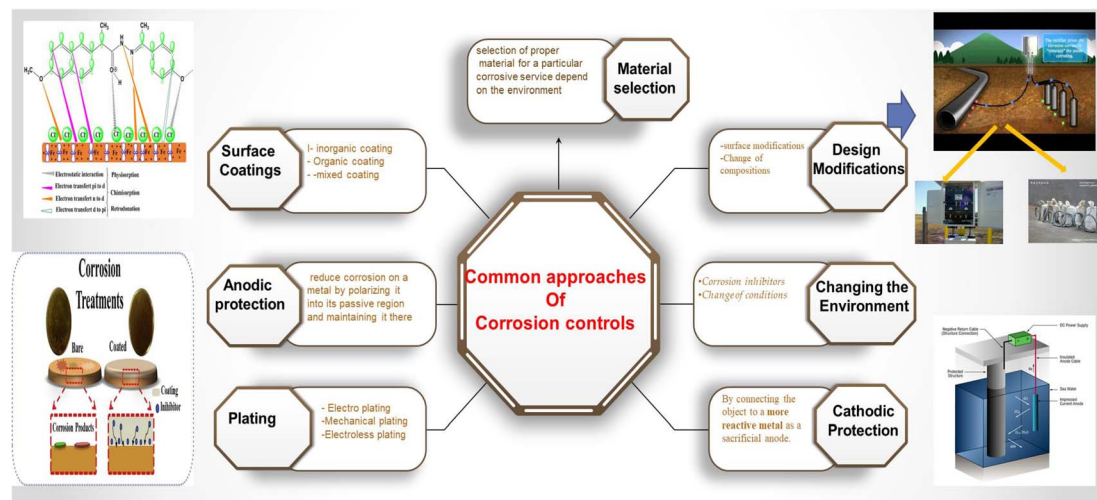


Fig. 1 Common approaches of corrosion control.

environmentally acceptable products.<sup>24</sup> Some well-researched eco-friendly substitutes for harmful corrosion inhibitors include natural polymers, polysaccharides, amino acids and their derivatives, and Arabic gums.<sup>25,26</sup> Green corrosion inhibitors may generally be divided into two primary groups: inorganic or organic green corrosion inhibitors. A typical example is biopolymers, which are naturally occurring compounds synthesized by cells of plants and animals, offering eco-friendly appropriate substitutes for a range of industrial uses. In contrast to synthetic polymers, they are biodegradable and do not accumulate within living organisms. Prominent examples of biopolymers encompass polypeptides, polysaccharides such as cellulose, starch, and chitosan, natural rubber, nucleic acids such as RNA and DNA, and lignin.<sup>27</sup> The incorporation of heteroatoms within the complex structure of biopolymers confers enhanced adsorption capabilities and plays an integral role in corrosion inhibition.<sup>28,29</sup> Consequently, extensive research has focused on exploring the anticorrosive features of biopolymers.<sup>29</sup> Furthermore, corrosion inhibitors are generally added to materials such as plastics, paper, *etc.*, for metal rust protection. The process of releasing corrosion inhibitors from materials to the metal surface will also have an impact on its corrosion inhibition.<sup>30</sup> Fig. 2 shows comparison between various types of inhibitors.

This review delves deeply into the world of corrosion inhibitors, aiming to shed light on their various types, mechanisms, performance, and potential applications. To better understand the inhibitor's efficiency and mode of action, the review critically analyzes the numerous mechanisms involved in corrosion inhibition. Further, the review evaluates and compares the performance of various corrosion inhibitors, both organic and inorganic, through insightful case studies and investigations. Furthermore, this review highlights the use of emerging eco-friendly corrosion inhibitors derived from natural resources such as biopolymers, plant extracts, and drugs as potential corrosion inhibitors. To comprehensively evaluate a corrosion inhibitor's performance, the review highlights various

analytical tools such as WL analysis, electrochemical analysis, and surface analysis. Additionally, the review discusses thermodynamics and isotherms related to corrosion inhibition, which advances our comprehension of inhibitors' behaviors and mechanisms. Furthermore, the review highlights the importance of computational studies in predicting new inhibitor's performance, thereby saving time and effort. This review bridges the gap between theory and practice, allowing researchers and practitioners to make informed decisions, develop effective corrosion inhibition strategies, and pave the way for a future in which viable inhibitors protect materials and structures from the detrimental effects of corrosion.

## 2. Corrosion inhibition mechanisms

The inhibition of metal corrosion can be achieved through one or more of the following mechanisms:

### 2.1 Adsorption mechanism of corrosion inhibition

There are multiple paths in which corrosion inhibitors can adsorb onto metal surfaces. These include strong chemisorption bonds due to chemical interactions of the metal surface and the inhibitor, as well as weak physical adsorption forces, such as hydrogen bonding, electrostatic attractions, or van der Waals interactions. Although, recent studies have shown that van der Waals interaction has little impact on identifying preferential sites compared to electrostatic interactions, it still plays a role.<sup>31,32</sup> Commonly, organic inhibitor molecules comprise  $\pi$ -electrons and/or lone-pair electrons of heteroatoms (N, O, S, P, ...), where the latter can participate in protolytic equilibria yielding positively or negatively charged moieties depending on the medium pH.<sup>33,34</sup> Metallic species that experienced partial oxidation acquire positively charged surface sites that can attract negatively charged counterions like chloride and sulfate, as well as electron-pair donor moieties from inhibitors. In some cases, however, these counterions adhering to the metal surface result in negative charges that strongly



## Difference Between Various type of inhibitor

Difference	Inorganic	organic	Biopolymer
Effectiveness	-Often highly effective at providing immediate and long-lasting protection due to the formation of stable passive films -they can be less versatile in different environmental conditions	-Offer good protection against corrosion by adsorption on the metal surface. They are versatile and can be tailored to specific substrates and conditions for effective use.	-Effectiveness may vary depending on the type of biopolymer and the specific application conditions.
Compatibility	-Can sometimes be limited in compatibility with certain metals or coatings, requiring careful selection for optimal performance	-can be more versatile and compatible with a wide range of metal substrates and coatings, providing effective protection in various applications.	-may have specific interactions with different metal surfaces, requiring thorough testing for compatibility and performance
Cost and Availability	-Generally more costly due to the production processes and raw materials involved	-Costs can vary, but organic inhibitors are often more readily available and cost-effective compared to inorganic inhibitors	-Availability and costs may vary depending on the production methods and sources of biopolymers
Environmental Impact	-Typically have a higher environmental impact due to their toxicity, disposal issues, and potential harm to ecosystems	-Generally considered more environmentally friendly compared to inorganic inhibitors, but biodegradability and persistence in the environment should be considered	-more sustainable and less harmful to the environment. They offer a greener alternative for corrosion inhibition.
Long-Term Stability	- Known for their long-term stability and durability in providing corrosion protection over extended periods.	-May require monitoring and replenishment over time to maintain effectiveness, as they can degrade or leach from the metal surface.	- Long-term stability can vary depending on the biopolymer and application conditions, requiring further study for reliable and consistent performance.

Fig. 2 Comparison between various types of inhibitors.

interact with protonated groups of some organic inhibitors.<sup>35</sup> Additionally, the inhibitor's electron-pair donor moieties can participate in coordinate bond formation with metals' low-energy empty orbitals. The adhesion forces between the substrate and the inhibitor molecules demonstrate greater potency in chemisorption than in physisorption processes. Consequently, chemisorption boasts heightened adsorption energy, thereby establishing itself as a superior approach for corrosion inhibition.<sup>36</sup> Furthermore, an important aspect of some adsorption processes is referred to as retro-donation, which involves electron transfer from occupied metal orbitals to unoccupied anti-bonding orbitals of the inhibitor's heteroatoms. This retro-donation results in a synergistic chemical bonding effect.<sup>13</sup> Fig. S1† depicts possible corrosion inhibition mechanisms *via* chemisorption and physisorption pathways involving organic inhibitors.<sup>36</sup> Furthermore, the inhibitor's adsorbed molecules may create a protective layer on the metal surface, which might serve as a physical barrier.<sup>37</sup>

In another instance, XPS examination was carried out to identify the adsorption of Isatin-CS self-assembled monolayers (SAMs) on Q235 carbon steel. The physical and chemical interactions are evidenced through the presence of two types of nitrogen in the XPS data, reflecting that the Isatin-CS SAM are adsorbed onto the surface of steel *via* both mechanisms<sup>38</sup> In another study, the N (403 eV)/N (398.1 eV) peak area ratio stays the same at varying inhibitor concentrations. This indicates that when the steel surface is fully coated, the proportion of molecules in different orientations is constant. Hence for nitrogen-functional inhibitors, adsorption can happen *via* electrostatic bonding between the steel surface and the N group<sup>39</sup> XPS analysis results confirm the chemisorption of DAPO (2,5-bis(4-dimethylaminophenyl)-1,3,4-oxadiazole) on the MS surface. The existence of an N-Fe bond complex reflects that

DAPO was chemisorbed onto MS surface, corroborating the thermodynamic findings. Furthermore, the addition of DAPO promotes the generation of a robust and insoluble oxide layer (Fe<sub>2</sub>O<sub>3</sub>, FeOOH) on the MS surface, thereby promoting its corrosion resistance.<sup>40</sup> A similar study showed that the peak at 710.28 eV (N-Fe/S-Fe) also reflects that the inhibitor interacts with the metal surface to form coordination bonds.<sup>41</sup>

The majority of organic inhibitors adhere to the target metal surface by displacing water on the surface and creating a tight barrier, as revealed by many studies.<sup>42</sup> The physical barrier prohibits corrosive substances like oxygen, water, and aggressive anions from approaching the metal surface. These barriers can affect both anodic and cathodic processes, thus slowing down both the chemical and electrochemical corrosion processes. The corrosion inhibitor's chemistry plays a crucial role in its inhibition performance. The inhibitor's specific chemical structure, functional groups, electron density, and molecular weight can all affect its ability to adsorb onto the metal surface and form a protective layer or film.<sup>43</sup>

To summarize, in corrosion inhibition by adsorption, the inhibitor's molecules or their ions adhere to anodic or cathodic sites, resulting in the blocking of active zones, a shift in anodic and/or cathodic potentials, and/or the formation of a protective barrier or film.<sup>43</sup>

For instances, the researchers examined the mechanism of *Euphorbia heterophylla* L. extract as a potent inhibitor for mild steel (MS) when exposed to a 1.5 M HCl solution and proved physical adsorption as the dominant mechanism behind the inhibition process.<sup>44</sup> Furthermore, polyaspartic acid (PASP) was explored as an environmentally friendly MS corrosion inhibitor in a 3% NaCl solution.<sup>45</sup> By establishing an adsorption layer on the metal surface, PASP demonstrated a moderate inhibitory efficacy of 61% at a concentration of 2.0 g L<sup>-1</sup>. However, at



a concentration of 0.5 g L<sup>-1</sup> PASP, the addition of zinc ions further increased the inhibitory efficiency to 97%, indicating a synergistic effect between PASP and Zinc ions. As shown in Fig. S2a–d,† when compared to a blank specimen, scanning electron microscopy (SEM) images verified that a protective inhibitor coating (PSAP or PSAP/Zn) was present on the MS surface. Zinc ions, in particular, produced a thicker PSAP/Zn protective layer that functioned synergistically as a cathodic inhibitor.<sup>45</sup> In another study,<sup>46</sup> the researchers explored the effectiveness of PASP and threonine (Thr) in preventing corrosion within simulated cooling water. The findings demonstrated that the PASP-Thr exhibited superior corrosion inhibition compared to PASP alone. This synergism can be attributed to the ability of PASP-Thr to create a protective film on the carbon steel surface, utilizing a combination of chemical and physical–chemical adsorption approaches, as shown in Fig. S2e.† The unique characteristics of PASP-Thr, such as its abundance of polar groups, and considerable molecular weight facilitate strong adherence and uniform coverage on the carbon steel surfaces.<sup>46</sup>

Thermodynamic information can be utilized to determine the type of adsorption exhibited by a corrosion inhibitor, whether it is chemisorption or physical adsorption. When the absolute value of  $\Delta G_{\text{ads}}^0$  is larger than 40 kJ mol<sup>-1</sup>, chemisorption takes place, signifying the creation of a chemical bond between the inhibitor and the metal surface.<sup>47</sup> In contrast, physisorption happens when the absolute value of  $\Delta G_{\text{ads}}^0$  is lower than 20 kJ mol<sup>-1</sup>, suggesting an electrostatic interaction between the inhibitor's molecules and the metal surfaces.<sup>46</sup> However, in many cases, the adsorption mechanism was found to be a combination of both physical and chemical interactions between the inhibitor and the metal surface.<sup>16,47</sup>

## 2.2 Electrochemical mechanisms of corrosion inhibition

Through an electrochemical mechanism, corrosion inhibitors smoothly suppress corrosion on metal surfaces by suppressing the anodic and/or cathodic reactions occurring during a corrosion process. This is achieved by inhibiting the cathodic reduction reaction rate and/or preventing the anodic oxidative metal dissolution.<sup>32,48</sup> Corrosion inhibition employing cathodic inhibitors involves several mechanisms. Firstly, these inhibitors increase the overpotential of the cathodic reaction, making corrosion more difficult to occur. By raising the overpotential, the rate of corrosion is effectively decreased. Cathodic inhibitors, *e.g.*, polyphosphates, zinc salts and cerium(III) salts, also work by blocking the cathodic reaction through deposition at cathodic sites, *e.g.*, through the formation of insoluble compounds, or by increasing the metal liability to hydrogen.<sup>37,49</sup> This blocking action effectively hinders corrosion by lowering the availability of the cathodic reactant. The presence of cathodic inhibitors acts as a barrier, disrupting the flow of electrons and ultimately reducing the overall corrosion rate. Conversely, anodic protection takes place when a corrosion inhibitor is adsorbed on the surface and forms an oxide film on the metal surface. This protective film acts as a protective barrier, inhibiting the anodic reaction. Anodic inhibitors can be

categorized into non-oxidizing ions (silicates, tungstates, and phosphates) which demand oxygen for protection, and oxidizing anions (*e.g.*, nitrites, and chromates) that can protect metals without external oxygen. Regardless of the type, anodic inhibitors may cause pitting issues and accelerated corrosion rate if concentrations are too low. Therefore, monitoring inhibitor levels is crucial.

For instance, polarization curves of MS in simulated cooling water (SCW) with various concentrations of silicate or phosphate inhibitors demonstrated that the cathodic Tafel slopes decreased, while, it was observed that an increase in the concentration of SiO<sub>3</sub><sup>2-</sup> or PO<sub>4</sub><sup>3-</sup> led to an enhancement in the values of anodic Tafel slope, with phosphate having a greater effect. This implies that both SiO<sub>3</sub><sup>2-</sup> or PO<sub>4</sub><sup>3-</sup> act as anodic inhibitors by impacting the anodic reaction of metal dissolution.<sup>50</sup> Another study researched the synergized inhibition of Ce<sup>4+</sup>/melamine on the corrosion behavior of aluminum alloy (AA2024) in a 3.5% NaCl solution.<sup>51</sup> The results showed that the corrosion current density of the sample was significantly lowered compared to the blank or single inhibitor samples. Additionally, examination of Tafel lines of polarization curves of samples in different inhibitor's concentrations showed that the anodic branches of all curves exhibited similar behavior, but with a decrease in the corrosion current density ( $I_{\text{corr}}$ ) attributable to a reduction in the cathodic current. These findings suggest that Ce<sup>4+</sup>/melamine solution acts as a cathodic-type inhibitor.<sup>51</sup> However, in a study of N80 steel corrosion in a concentrated tetrapotassium pyrophosphate solution and its corrosion control by vanadate, the addition of 0.5 wt% NaVO<sub>3</sub> caused a drop in the passive current density by 10–100, showing that NaVO<sub>3</sub> functioned as an anodic inhibitor.<sup>52</sup>

## 2.3 Summaries of corrosion mechanisms

Corrosion inhibitors can be classified into different categories based on their mechanism of action, including anodic, cathodic, and mixed inhibitors. Anodic inhibitors work by inhibiting the anodic metal dissolution reaction. Cathodic inhibitors work by inhibiting the reduction reaction, which is a crucial step in corrosion processes. Mixed inhibitors work by reducing both the anodic and cathodic reactions, leading to a more comprehensive corrosion inhibition. The synergistic interplay between the anodic and cathodic processes can result in a higher overall inhibition efficiency. Based on the mode of protection, inhibitors can form a passive layer, adsorb on the metal surface, or form a protective layer. Fig. 3 illustrates a scheme of corrosion inhibitor's role.

## 3. Type of corrosion inhibitors

In the realm of inhibition, we can differentiate between organic and inorganic inhibitors. Inorganic inhibitors exert their influence by retarding or preventing the anodic and/or the cathodic reactions of a corrosion cell. Conversely, organic inhibitors possess a multifaceted nature, displaying adsorption action, cathodic, anodic effects, or a mix of them. By classifying



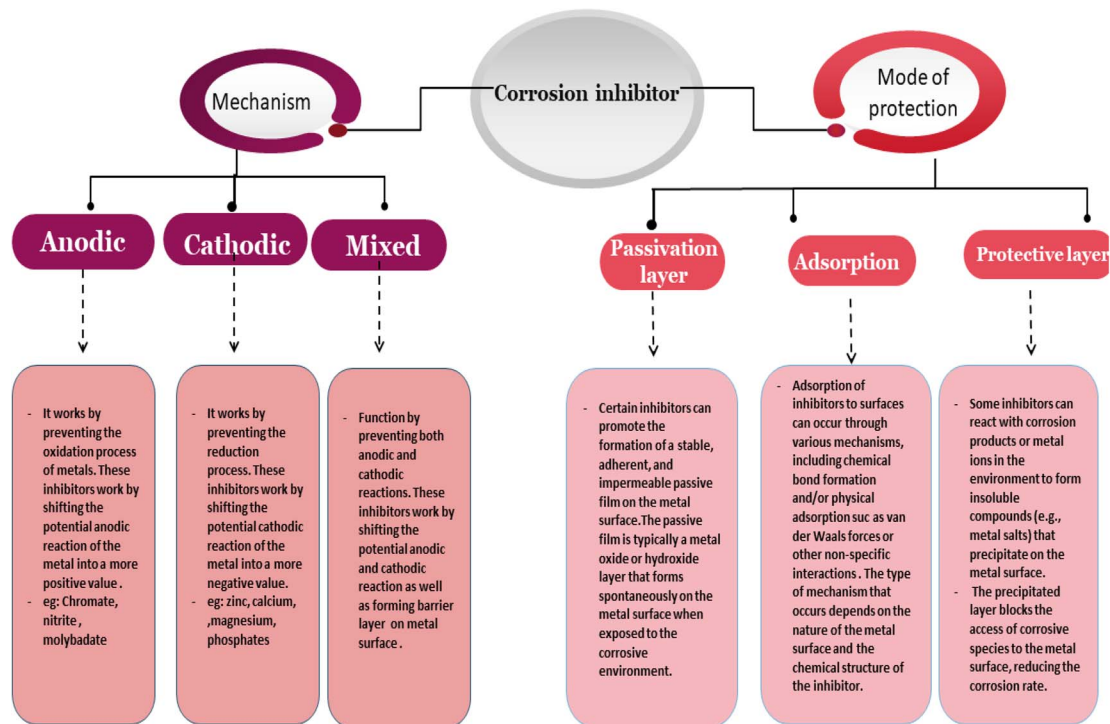


Fig. 3 Scheme of corrosion inhibitor role.

inhibitors into these categories, we gain a clearer understanding of their mechanisms and functionalities.

### 3.1 Inorganic inhibitors

An anodic inhibitor causes passivation by coating the metal surface with a protective layer, e.g., oxide layer. Anodic or passivation inhibitors include nitrite, silicate, phosphate, chromate, and molybdate, among others. On the other hand, cathodic inhibitors operate through various approaches, such as cathodic precipitation, cathodic poisons, or oxygen scavenging. Cathodic inhibitors include salts of magnesium, calcium, zinc, and others. Table 1 lists some of the common inorganic corrosion inhibitors along with their important characteristics.

**3.1.1. Nitrite inhibitors.** Nitrite, a widely studied inorganic inhibitor, has received considerable attention in scientific literature owing to its affordability and effective inhibition features.<sup>69,70</sup> Nitrite inhibitors tend to minimize the corrosion current density and move  $E_{\text{corr}}$  to a noble direction.<sup>54</sup> For instance, potentiodynamic polarization (PDP) curves were employed to examine how the addition of  $\text{NaNO}_2$  impacts the corrosion inhibition of carbon steel in de-aerated SCW.<sup>54</sup> When  $\text{NaNO}_2$  was absent, the metal easily corroded; however, when  $\text{NaNO}_2$  was introduced at levels of 10 and 100 ppm, carbon steel exhibited a transition from active to passive behavior. Remarkably, carbon steel displayed powerful passivation features when  $\text{NaNO}_2$  was added at a level of 1000 ppm.<sup>54</sup> The mechanism behind nitrite's inhibitory action has been the subject of investigation by numerous researchers.<sup>53,71</sup> Specifically, in the case of iron, it has been proposed that nitrite ion

serves as an oxidizing agent, facilitating the conversion of ferrous to ferric ions and thus playing a key role in the formation of a sturdy and enduring oxide passive film on steel surfaces.<sup>37</sup> The resulting protective film was primarily composed of magnetite in both of the outer and inner layers.<sup>53</sup> The environmental parameters including the metal or alloy type and composition, medium pH, aggressive ion type and concentration, and the temperature have a great impact on the performance of nitrite inhibitor.<sup>55,71–73</sup> For instance, it was shown that when chloride ions exist at great levels, while using insufficient amounts of nitrite promoted the likelihood of encountering pitting phenomena owing to the proximity of pitting potential ( $E_{\text{pit}}$ ) to the open circuit potential (OCP).<sup>71</sup> Furthermore, the nitrite was found to be more resistant than chromate to the damage caused by chloride ions; however, it was of marginally less resistant to the effects of sulfate ions.<sup>74</sup> Moreover, when the nitrite level was equal to or less than  $53 \text{ mmol L}^{-1}$ , it was demonstrated that the sulfate-generated corrosion was more likely to occur than that of chloride.<sup>75</sup> Furthermore, in SCW solution containing chloride ions, the effect of nitrite ions on MS corrosion was examined and demonstrated that in alkaline and near-neutral media (pH 6 and above), nitrite ions efficiently inhibited steel corrosion; however, in acidic environments (pH 4 and below), nitrite ions promoted corrosion.<sup>56</sup> A prolonged soaking period, up to 24 hours, enhanced the inhibitory effect of  $\text{NaNO}_2$  afterward, for all nitrite levels at and above pH 6, it stayed comparatively steady.<sup>56</sup> Additionally, through PDP curves' analysis, the researchers found that the addition of nitrite to de-aerated tap water containing carbon steel, caused the corrosion potential to move toward the noble region, resulting in a minimized



Table 1 Characteristics of some representative examples of inorganic corrosion inhibitors

Inhibitor	Environment	Nature of adsorption	Conc.	Method of corrosion monitoring	IE%	Ref.
Zn <sup>2+</sup>	Carbon steel/sea water	N. A., cathodic inhibitor	6 ppm	PDP, EIS	83.3%	49
Sodium silicate	Carbon steel/simulated cooling water	Langmuir, anodic inhibitor	1 × 10 <sup>-2</sup> M	PDP	74.0%	50
Sodium phosphate					95%	
Silicate-phosphate					62.3%	
Sodium vanadate	N80 steel/concentrated K <sub>4</sub> P <sub>2</sub> O <sub>7</sub> solution	N. A., anodic inhibitor	0.5 wt%	WL, PDP, EIS, XPS, SEM	99.85	52
Sodium nitrite	Carbon steel/5 mM chloride	N. A., anodic inhibitor	9 mM	PDP, EIS, SEM	90%	53
Sodium nitrite	Carbon steel/simulated primary cooling water ductile cast iron/simulated primary cooling water	N. A., anodic inhibitor	1000 ppm 10 000 ppm	EIS, DFT, PDP, EIS, XPS, SEM	N. A.	54
Sodium nitrite	Carbon steel/250 NaCl	N. A., anodic inhibitor	175 ppm	PDP	99.061	55
Sodium nitrite	Carbon steel/simulated cooling water	N. A., anodic inhibitor	500 ppm	PDP	90%	56
Sodium nitrite	Carbon steel/tab water	N. A., anodic inhibitor	200	EIS, PDP, EIS, XPS, SEM	N. A.	57
Sodium nitrite	Carbon steel	N. A., anodic inhibitor	2 g L <sup>-1</sup>		65%	58
Sodium nitrite			2 g L <sup>-1</sup>		53%	
Nitrite + molybdate			<2 g L <sup>-1</sup>		93%	
Sodium molybdate	Carbon steel/0.1 M HCl	Langmuir, anodic inhibitor	300 ppm	WL, PDP	93.28	59
	0.2 M HCl				97%	
	0.3 M HCl				94.65%	
	0.4 M HCl				93.29%	
	0.5 HCl				88.99	
Sodium tungstate	Carbon steel/0.1 M HCl		300 ppm		79%	
	0.2 M HCl				86.8%	
	0.3 M HCl				83.06	
	0.4 M HCl				81.17%	
	0.5 HCl				71.87%	
Sodium molybdate	Carbon steel/Ca(OH) <sub>2</sub> + H <sub>2</sub> SO <sub>4</sub> + HNO <sub>3</sub> (pH = 8)	N. A., anodic inhibitor	0.04%	EIS, PDP	80%	60
Sodium molybdate	Carbon steel/Saturated Ca(OH) <sub>2</sub> + 0.5 M NaCl (pH = 12.5)	N. A., anodic inhibitor	2882 ppm	EIS, PDP, XPS	97%	61
Sodium molybdate	Carbon steel/0.01 M NaCl + 0.1 M NaHCO <sub>3</sub>	N. A., anodic inhibitor	2059 ppm	EIS, PDP, SEM-EDX	97.9%	62
Sodium molybdate	Carbon steel/simulated cooling water	N. A., anodic inhibitor	400 ppm	WL, SEM	98.5%	63
Sodium tungstate	Iron-based alloys/10% H <sub>2</sub> SO <sub>4</sub> (pH < 1)	N. A., anodic inhibitor	33 × 10 <sup>3</sup> ppm	PDP, SEM-EDX	97%	64
Sodium tungstate	Carbon steel/1 M NaOH (pH = 14)	Langmuir, anodic inhibitor	100	WL, OCP, PDP	30.71	65
			200		45.75%	
			400		62.41%	
			800 ppm		73%	
Sodium tungstate + ZnSO <sub>4</sub>	Mild steel/natural seawater	N. A., mixed type inhibitor	1000 ppm + 300 ppm ZnSO <sub>4</sub>	WL, EIS, PDP, XPS	84.81	66
Sodium nitrite sodium silicate	Carbon steel/3% NaCl	N. A., anodic inhibitor	0.5%	WL	94.1%	67
			2%		92.5%	
Sodium silicate	Carbon steel/3.5% NaCl	Langmuir/anodic inhibitor	1250 ppm	WL, EIS, PDP, SEM	92%	68

corrosion rate (Fig. S3a†).<sup>57</sup> SEM examination unveiled that the nitrite inhibitor facilitated the creation of a  $\gamma$ -Fe<sub>2</sub>O<sub>3</sub> passive film at nitrite levels of 100–200 ppm, while lower nitrite levels of ≤50 ppm led to the formation of corrosion products owing to uniform corrosion (Fig. S3c and d†).<sup>57</sup> In terms of electrochemical impedance spectroscopic (EIS) studies, it was observed that the carbon steel with <100 ppm nitrite exhibited a higher vulnerability to localized corrosion due to its smaller anode area and larger cathode area, whereas a submerged solution containing <50 ppm nitrite primarily experienced uniform corrosion. In another study, the impact of temperature

on the ability of nitrite to inhibit corrosion was examined and the researchers found that as the temperature of the medium increased,  $I_{\text{CORR}}$  increased, while  $E_{\text{CORR}}$  was shifted towards more negative values.<sup>53</sup> It became evident that both  $\beta_c$  and  $\beta_a$  increased with temperature, but the increase in  $\beta_a$  was significantly greater than that of  $\beta_c$ , revealing that higher temperatures generally promote the dissolution of metal ions by enhancing the activation of the tested metal surface, resulting in a minimization in the resistance of the oxide film existing on the metal surface. In this respect, the primary focus has been placed on regulating the level of nitrite within an optimal range



to achieve superior inhibitory characteristics and consequently mitigate the likelihood of pitting corrosion. In addition, nitrite has been employed collaboratively with other inhibitors, such as molybdate, to mitigate mild-steel and carbon-steel corrosion in chloride solutions lacking ample oxygen.<sup>58,76,77</sup>

**3.1.2. Molybdate inhibitors.** Due to its low toxicity and environmental friendliness, the molybdate ion has been extensively examined as a corrosion inhibitor for a variety of metals and alloys in a range of adverse environments.<sup>78–80</sup> The first exploration of the inhibitory impact of molybdate on carbon steel corrosion in a neutral medium was carried out in 1953 (ref. 81) and its inhibition mechanism was ascertained in 1955.<sup>82</sup> The researchers found that although molybdate was less effective in de-aerated water, it demonstrated high performance in aerated water. Subsequently, numerous studies have explored the application of molybdate as a powerful inhibitor for steel corrosion.<sup>59,83</sup> Molybdate falls under the category of oxidizing anodic inhibitors, requiring the existence of external oxygen to generate a protective oxide layer on iron alloys. As the anode undergoes a chemical reaction, ferrous ions are produced ( $\text{Fe}^0 \rightarrow \text{Fe}^{2+} + 2e^-$ ). These ferrous ions then interact with molybdate ions, resulting in the generation of a molybdate–ferrous complex that does not provide adequate protection.<sup>84</sup> Subsequently, this complex undergoes oxidation when it comes into contact with dissolved oxygen to yield a thin protective and insoluble molybdate–ferric complex, which combines with ferric oxide to provide an enhanced corrosion protection.<sup>85</sup> Thus, a molybdate thin layer on the surface of MS considerably impeded localized corrosion in NaCl solutions.<sup>86</sup> This protective molybdate film demonstrated a dual-layer structure: the outer layer primarily contained  $\text{Fe}_2(\text{MoO}_4)_3$ , while the inner layer consisted of ferric hydroxide/oxide.<sup>76,77</sup> In another investigation, the researchers found that  $\text{MoO}_2$ ,  $\text{MoO}_4^{2-}$ , and  $\text{MoO}_3$  made up the protective coating of carbon steel that developed in a solution containing 0.5 M  $\text{NaHCO}_3$ , 0.5 M  $\text{NaCO}_3$ , and 1.5 M NaCl.<sup>87</sup> Interestingly, it was demonstrated that the  $\text{MoO}_4^{2-}$  peak had a greater intensity than any other species in the protective layer. Additionally, after being subjected to the molybdate solution, MS specimens were examined employing Auger Electron Spectroscopy (AES). The findings demonstrated that a 3 nm molybdenum oxide layer was discovered next to a 6 nm layer of iron oxide.<sup>88</sup> Furthermore, molybdate is thought to fortify the topmost layer of hydrated iron oxide by establishing hydrogen bonds with hydroxide groups present on the surface. This reinforcement imparts a negative surface charge, effectively preventing aggressive anions such as chloride and sulfate from approaching the metal surface and inhibiting the departure of ferrous ions from the metal.<sup>85,87</sup> Molybdate aids in slowing down pits formation by releasing adsorbed molybdate when a breach in the protective layer arises as evidenced by shifts of the pitting potential ( $E_{\text{pit}}$ ) to the positive direction.<sup>87</sup> This molybdate then precipitates as complexed iron-molybdates within the tiny pit, preventing further corrosion propagation.<sup>85,89</sup> The effective range of molybdate levels is wide because it is significantly affected by the presence of high levels of aggressive anions. For instance, the researchers reported that in deionized or low-electrolyte

water, a 70 ppm molybdate was an effective inhibitor; however, in the presence of 200 ppm chloride, a 466 ppm molybdate was necessary to achieve corrosion inhibition.<sup>85</sup> Similarly, other researchers found that when the chloride levels was around 200 ppm, a minimum of 1000 ppm molybdate was required to provide adequate protection; however, at lower levels of 70 ppm  $\text{Na}_2\text{SO}_4$  and 30 ppm NaCl, effective inhibition can be achieved with only 200 ppm  $\text{Na}_2\text{MoO}_4$ .<sup>90</sup>

**3.1.3. Silicate inhibitors.** Alkali silicates are water soluble, nonflammable, non-toxic, and exhibit a prolonged shelf-life. There are many commercially available grades of sodium silicates (SS), which may be identified by their  $\text{SiO}_2/\text{Na}_2\text{O}$  weight ratio. These ratios commonly fall between 1.00 : 2.00 to 3.75 : 1.00, where grades with ratios less than 2.85 : 1.0 are termed alkaline, while those having higher ratios are neutral.<sup>20</sup> Silicate inhibitors are a popular category of inorganic substances utilized to mitigate corrosion. These inhibitors function by creating a protective silicate coating on the metal surface, which effectively shields it from the harmful effects of the corrosive surroundings.<sup>20</sup> However, certain studies reported that an iron oxide layer with a thin film of  $\gamma\text{-Fe}_2\text{O}_3$  (ref. 85 and 91) or a structured  $\text{Fe}_2\text{O}_3/\text{FeO}/\text{Fe}^{20}$  arrangement is responsible for the protective action of sodium silicate. A possible pathway for silicate protective film development includes the displacement of water at the interface between steel and the surrounding solution, where silicates are adsorbed onto the target metal surface, resulting in a reduction in the film capacitance.<sup>20</sup> X-ray photoelectron spectroscopic (XPS) analysis of the silicate protective layers on steel revealed that silicon makes up the majority of the outer film's composition that can be formed by (1) diffusion of silicate ions to steel surface with subsequent interaction with  $\text{Fe}^{3+}$ ,  $\text{Fe}^{2+}$ , and  $\text{OH}^-$  ions to form insoluble silicate compounds that settle on steel surfaces and/or (2) silica hydrolysis on steel surface and formation of a protective mixed layer made of hydrated silica gel and iron oxides.<sup>92</sup> Furthermore, it has been proposed that silica that is continually added to the system has self-healing qualities in addition to creating a protective coating.<sup>93–95</sup> This implies that if film damage occurs (for example, from erosion or corrosion), the silicate found in the surrounding medium slowly creates a new film to heal the protective layer where the damage was caused. The generation of the healing protective film by sodium silicate inhibitor might occur gradually, over several weeks.<sup>20,85</sup>

**3.1.4. Tungstate inhibitors.** Sodium tungstate has proved as a promising corrosion inhibitor in various industries for easy application and integration into various corrosion prevention methods, such as immersion, spraying, or dipping.<sup>96</sup> Its unique characteristics make it a competent option for protecting various metals, *e.g.*, steel, aluminum, copper, and nickel, from corrosion in different environments.<sup>96–98</sup> Moreover, tungstate exhibits favorable performance in both acidic and alkaline environments. It possesses excellent chemical stability, enabling it to resist deterioration and maintain its protective properties in highly corrosive media. This feature makes sodium tungstate particularly useful in industries where corrosive agents vary or fluctuate, providing consistent corrosion protection regardless of the pH conditions. Additionally,



sodium tungstate is known for its inhibiting effects on localized corrosion mechanisms such as pitting and crevice corrosion. These types of corrosion can occur in specific areas where the protective oxide layer is compromised, leading to severe damage if left unmitigated.<sup>96</sup> Furthermore, the good thermal stability of tungstate's make it a suitable choice for applications in high-temperature environments, where many corrosion inhibitors can lose their effectiveness.<sup>96</sup> When tungstate is introduced into a corrosive environment, it tends to undergo polymerization that results in the generation of polytungsten anions like  $[W_7O_{24}]^{6-}$  and  $[W_{10}O_{32}]^{4-}$  along with the parent monomeric form  $WO_4^{2-}$ .<sup>96</sup> The corrosive anions compete with tungstate-based anions to adsorb at the corroding interface of the metal sample. The existence of tungstate's lowers the adsorption of corrosive ions on the target surface and simultaneously generates an insoluble protective tungstate layer by binding to metal ions, and effectively hindering the attack of corrosive anions.<sup>99</sup> Thus, tungstate's can effectively fill in gaps and fix any flaws in the protective layer.<sup>64</sup> Just like  $MoO_4^{2-}$  inhibitors, tungstate is also considered risky as it can boost corrosion when not applied in an optimum dosage. Moreover, instances of failures have been reported at high tungstate levels, under unique conditions.<sup>100</sup>

**3.1.5. Phosphate inhibitors.** Phosphates are widely used as steel corrosion inhibitor in concrete protection, and boiler's water, potable water, and cooling water systems, as well as other water distribution systems.<sup>101-103</sup> Thus, sodium hydrogen phosphate, disodium hydrogen phosphate, sodium phosphate, polyphosphate, and monofluorophosphate, have been used successfully in various applications. Phosphates are classified as non-oxidative anodic inhibitors that are usually effective when oxygen is present.<sup>104-106</sup> Numerous investigations have been conducted to comprehend the corrosion inhibitory role of phosphates on the iron surfaces within diverse environments.<sup>102,107</sup> Generally, it is widely acknowledged that the protective layer generated on the iron surface in alkaline conditions consists of a dual component structure: an internal section comprising iron oxides such as  $Fe_3O_4$  or/and  $(Fe_2O_3)$  and an exterior section comprising various iron phosphate complexes, *e.g.*,  $Fe_3(PO_4)_2$ ,  $FeHPO_4$ , and  $FePO_4$ , where various oxidation states of iron and various protolytic equilibrated forms of phosphate are involved depending on the levels of dissolved oxygen and the medium pH.<sup>108-110</sup> Various analytical techniques, including AES and XPS analysis,<sup>111</sup> ellipsometric,<sup>112</sup> Raman spectra,<sup>113</sup> and XRF,<sup>104</sup> have verified the existence of phosphate inside the outer layer's structure. Nevertheless, the features of this protective film are contingent upon various elements, namely the temperature and pH of the medium, alongside the type and concentration of electrolyte ions.<sup>114,112,114</sup> Phosphates, however, may also serve as cathodic corrosion-inhibitors, under certain circumstances. In these situations, a film forms on cathodic sites, probably due to a reaction between the metal and phosphate ions in a medium.<sup>105</sup> The degree of inhibition is determined by how well the film works, particularly how well it serves as a barrier. Furthermore, it was found that the inhibitory effects of polyphosphate are further promoted when divalent  $Ca^{2+}$  or  $Zn^{2+}$  cations are found in the

solution.<sup>115</sup> This phenomenon is associated with the formation of (1) a shield on the cathodic areas, thereby raising its over-potential, and/or (2) a shield on the anodic areas by preventing oxygen from reaching the anodic sites, thereby inhibiting corrosion.<sup>115</sup> Thus, when iron was placed in a dilute ortho-phosphate medium containing  $Ca^{2+}$ , the cathodic process was impeded by the formation of a sparingly soluble calcium phosphate film, which covered the iron surface limiting its accessibility and reaction with dissolved oxygen.<sup>116</sup> Additionally,  $Na_3PO_4$  solution inhibited the cathodic reduction reaction of oxygen for iron corrosion in tap water medium, probably due to the cathodic adhesion of positively charged magnesium and calcium with phosphate anions and raising the cathodic over-potential. Interestingly, the formation of these sparingly soluble particles and their subsequent adhesion to the tested metal surfaces is independent of the oxygen content of the medium.<sup>117</sup>

**3.1.6. Zinc ion inhibitor.** In aqueous environments, zinc salts that dissolve in water are commonly employed as inhibitors to minimize corrosion.<sup>118</sup> These salts function by forming insoluble metal hydroxides on the surface of the targeted metal. This chemical reaction takes place when the zinc salts come into contact with  $OH^-$  formed during the cathodic reduction of  $O_2$  molecules. When combined with other inhibitors like organic and inorganic anions, such as molybdate, phosphonates, and other polymeric species, zinc salts can offer promoted defense against corrosion. However, there is a growing inclination to minimize the employment of zinc-based inhibitors. This is driven by concerns regarding their environmental impact and the potential risks associated with the presence of biogenically produced  $H_2S$  in the water, as well as water contamination caused by substances containing sulfide. These factors can result in a significant drop in the level of zinc ions, thereby compromising the performance of the inhibitor.

**3.1.7. Summary of inorganic inhibitors.** Inorganic inhibitors perform an essential role in protecting metals in harsh circumstances. Their corrosion resistance, nonvolatility, and thermal stability make them preferred over organic inhibitors in certain applications. Understanding the impact of these inhibitors on the cathodic and anodic polarization branches are keys to predicting their corrosion prevention performance. By altering the reactions in each branch, inhibitors can either impede or prevent the corrosion process, making them valuable tools for safeguarding metals. There are three main forms of inorganic inhibitors: anodic, cathodic, and mixed inhibitors. However, environmental concerns and the high concentrations often required hinder their application. Further, the utilization of anodic inhibitors at low levels can induce the stimulation of corrosion, notably the formation of pits, constituting a substantial hazard. Considering these factors, the selection and utilization of inorganic inhibitors require careful assessment and consideration.

## 3.2 Organic inhibitors

**3.2.1. Organic phosphonate.** Phosphonates are widely recognized and commonly employed organic inhibitors for



water systems to minimize corrosion. These include compounds like HEDP (1-hydroxyethane-1,1-diphosphonic acid), AMP (amino trimethylene phosphonic acid), ADMP (amino-di(methylenephosphonic) acid), ATMP (amino-tris(methylene-phosphonic)acid), EDTP (ethylendiamine-*N,N,N',N'*-tetrakis(methylenephosphonic)acid), HMDTP (hexaethylenediamine-*N,N,N',N'*-tetrakis(methylenephosphonic) acid), PBTC (2-phosphonobutane-1,2,4-tricarboxylic acid), and HPAA (hydroxyphosphono-acetic acid), along with the metal cation complexes they form.<sup>119</sup> Their exceptional stability, owing to strong carbon–phosphorus bonds, allows them to withstand even the harshest conditions. The activity of inhibitors containing phosphonic acid groups is primarily attributed to their ability to attach to oxidized metal surfaces through –P–O–M bonds (where M stands for metals).<sup>120</sup> This assertion has been supported by various surface analytical techniques.<sup>22,121</sup> For example, the impacts of HEDP to minimize steel corrosion in a soft water medium was investigated.<sup>122</sup> According to the EIS measurements, there is a lowering in capacitance as the level of HEDP rises, which might be caused by the integration of organic phosphorous into the surface. The maximum inhibition of 62.59% was observed at concentrations of 25 ppm HEDP. Nevertheless, as the HEDP level rises to greater levels, a negative impact on inhibition was shown. This is because as the HEDP level rises, soluble complexes with ferrous ions are generated rather than the protective layer covering the surface. Furthermore, an ideal phosphonate inhibitor of the “complexing type” should have various features including the ability to create dense and structurally robust thin films of metal phosphonate on the surface, and should not form highly soluble metal complexes that remain soluble in the bulk without depositing onto the metal surface.<sup>123</sup> If the generated film is uneven or porous, it could create localized oxygen permeation sites, leading to potential pitting of the metal surface.<sup>123</sup> The performance of phosphonate-based inhibitor systems can be boosted through the existence of metal cations in solution. Thus, the researchers have extensively studied the synergistic effects of HEDP and calcium ions.<sup>124</sup> Their findings reflected that the optimal anticorrosion impact is achieved when the molar ratio of Ca : HEDP was 1 : 1 under neutral conditions. Subsequent studies on MS revealed that larger Ca/HEDP solution concentrations induce the inhibitor film to develop thicker and the oxide portion in the surface layer to rise.<sup>123,125</sup> In isolation, HEDP functions as an anodic corrosion inhibitor, impeding the dissolving of metals. But when paired with calcium ions, it suppresses the cathodic O<sub>2</sub> reduction and lowers the anodic current. As a consequence, both components lessen the corrosion current.<sup>125,126</sup> Furthermore, a protective layer on steel surface was formed by a synergistic combination of zinc ions and imino dimethyl phosphonic acid (IDMPA) inhibitor, where the formed [Zn(II)–IDMPA] complex spread onto steel surface and combined with the generated Fe<sup>2+</sup>/Fe<sup>3+</sup> at the anodic sites to form another protective complex proposed as [Fe(II)/Fe(III)/Zn(II)–IDMPA].<sup>127</sup> In the meantime, the bulk solution's free Zn<sup>2+</sup> ions combine with OH<sup>–</sup> ions generated at the cathodic regions, resulting in the generation of Zn(OH)<sub>2</sub> precipitate. Further, the combination of zinc ions and propyl phosphonic acid (PPA) has

demonstrated performance inhibition for steel at pH 6–8, where a protective film of [Fe(III)Fe(II)Zn(II)–PPA], Zn(OH)<sub>2</sub>, and iron oxides/hydroxides was generated on steel surfaces.<sup>128</sup> This film minimized the double-layer capacitance and promoted resistance to charge transfer, resulting in enhanced anti-corrosion features.<sup>128</sup> It is worthy to note that, the molar ratio of zinc to phosphonate is crucial in determining the composition of the complexes responsible for film formation and inhibition effectiveness. Additionally, the levels of phosphonate and zinc individually impact the anti-corrosion effect, with higher zinc levels enhancing inhibition activity. The formed layers impede both of the iron anodic dissolution and the cathodic oxygen reduction processes.

**3.2.2. Heterocyclic inhibitors.** Metallic corrosion can be retarded or inhibited by a variety of heterocyclic compounds. These inhibitors are organic substances that have a ring structure containing one or more heteroatoms (P, S, N, or O). Because heteroatoms are part of their structure, heterocyclic inhibitors may interact with metal ions more easily to develop stable, insoluble complexes that upon adsorption on metallic surfaces can prevent corrosion. The presence of lone pair electrons on heteroatoms enables them to readily interact with metal and results in powerful chemical adsorption. There is a well-known empirical rule regarding the inhibition performance of molecules including heteroatoms, ordering the sequence of increasing efficacy as O < N < S < P, revealing that the atoms with lower electronegativity exhibit great charge transfer and great hindering effectiveness.<sup>43,129</sup> Additionally, when heteroatoms are subjected to alkaline or acidic environments, they can participate in protolytic equilibria to acquire negative or positive charges *via* deprotonation or protonation processes. Through reverse donation, *e.g.*, dπ–pπ, the heteroatom (pπ-orbital) can accept electrons from the metal (dπ-orbital). On the other hand, if the heteroatom is negatively charged, it contributes electrons to the metal surface. Powerful adsorption is advantageous for inhibition in both scenarios. It should be mentioned that heterocycles including sulfur are preferable for hindering corrosion in sulfuric acid, whereas heterocycles including nitrogen have proven to be more efficient as inhibitors in hydrochloric acid media. Still, it is thought that heterocycles with both nitrogen and sulfur atoms are considerably more potent. Numerous variables, such as the temperature, inhibitor concentration, pH, and the metal surface's features, impact the adsorption phenomena. Heterocyclic corrosion inhibitors of various kinds have been thoroughly investigated and applied to prevent corrosion. However, ring strain causes four- or three-membered heterocycles to be lower in stability than six- or five-membered rings, which lessens their significance as types of heterocyclic inhibitors (HCIs).

Within the five-membered heterocycles, nitrogen-containing compounds—triazoles, imidazoles, tetrazoles, pyrazoles, and so on—are the significant chemicals that hinder corrosion.<sup>130</sup> Thiazoles, oxazoles, thiadiazoles, and other heterocycles are examples of compounds that include sulfur or oxygen atoms in addition to nitrogen atoms. Important compounds that suppress corrosion are fused-ring heterocycles such as



benzotriazole, indole, benzoxazole, and benzimidazole. Six-membered heterocycles are the most essential type of these inhibitors because they undergo the least amount of ring strain. Tetrazines, pyridine, diazines, triazines, and their counterparts are a few examples of these.<sup>130</sup> Fused ring quinoline inhibitors are routinely employed found widespread use as corrosion inhibitors.

Moreover, the existence of polar groups likes OH,  $-\text{NH}_2$ ,  $-\text{OCH}_3$ , and others, as well as unsaturation through triple and double bonds, allows these inhibitors to readily donate electrons and be protonated in aggressive corrosive environments. Electron-donating substituents such as  $-\text{OH}$ ,  $-\text{NH}_2$ , and others, promote the electron density at the active site, facilitating the interaction between the metal substrate and inhibitor molecules.<sup>43,131</sup> Conversely, electron-withdrawing substituents like  $-\text{NO}_2$ ,  $-\text{CN}$ ,  $\text{COOH}$ , and others, minimize the electron density at the inhibitor's active sites, leading to a minimized rate of adherent on metal surfaces.<sup>132,133</sup> The availability of substituents in the side chain(s) and the number of heteroatoms can determine the formation of poly, mono-, and bi-dentate complexes.

The impact of certain common substituents on the inhibition potential of some heterocyclic inhibitors is schematically depicted in Fig. 4. The literature review demonstrated that the values of  $\Delta G_{\text{ads}}$  for the adhered of various heterocycle ranges between  $-40$  and  $-20$   $\text{kJ mol}^{-1}$ , reflecting that their adsorption phenomena predominantly follow the physiochemisorption.

**3.2.3. Summary of organic inhibitors.** Phosphonic acids are successful corrosion inhibitors because of their commercial availability, low toxicity, and good efficacy. The reason phosphonate inhibitors are employed is because they adsorb on targeted surfaces and create insoluble protective layers that augment activation energy and minimize the active area of targeted metal. These inhibitors have a combination of anti-scaling and anti-corrosion features, as well as a robust protective capability across a variety of salinities and temperatures. However, there are several drawbacks, such as the potential for localized corrosion, minimized performances in areas of stagnant electrolytes, and the existence of hydrogen sulfide, even in minute amounts. Furthermore, phosphonate inhibitors may break down in the presence of oxidizing biocides. Further,

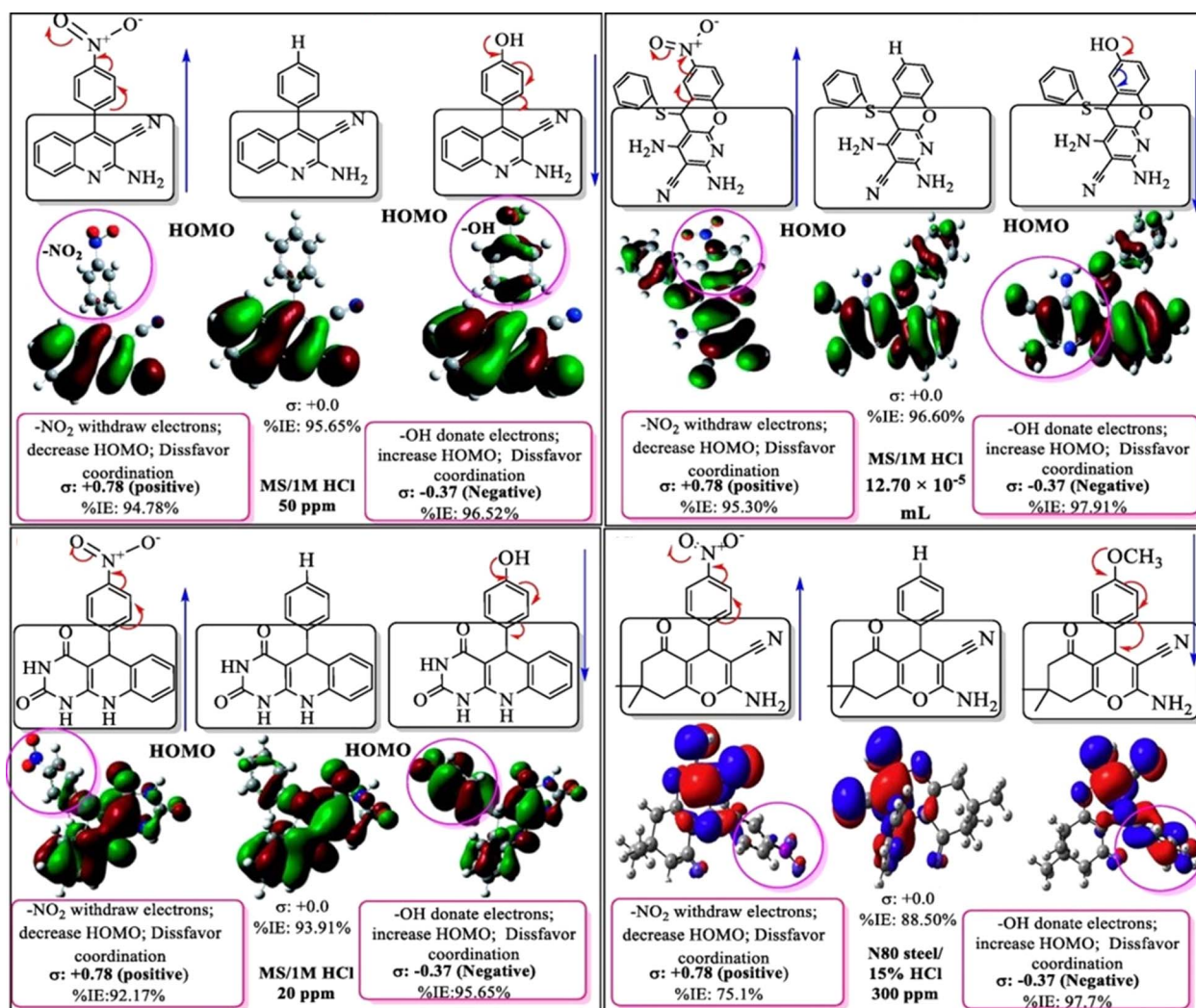


Fig. 4 Adsorption and coordination bonding behavior of pyridine, triazine and quinoline and their mono- and di-substituted derivative.<sup>134</sup>



Table 2 Characteristics of some representative examples of organic corrosion inhibitors

Inhibitor	Environment	Nature of adsorption	Conc.	Method of corrosion monitoring	IE %	Ref.
Phosphonate anion (PHOS)	Mild steel/SCW	Langmuir/anodic inhibitor	$10^{-3}$ M	WL, SEM-EDX, PDP, EIS, MD	88%	135
Pyridine	Mild steel/1 M HCl	Langmuir/mixed type inhibitor	$10^{-2}$ M	SEM-EDX, PDP, EIS, MD	46%	136
Quinoline			$10^{-2}$ M		64%	
1,10-Phenanthroline			$10^{-2}$ M		80.4	
3-Pyridylalldoxime (3POH)	Mild steel/1 M HCl	Langmuir/mixed type inhibitor	200 ppm	PDP, EIS	94%	137
1-Benzylimidazole	Carbon steel/1 M HCl	Langmuir/mixed type inhibitor	500 ppm	WL, PDP, EIS	82.0%	138
3-Amino-5-mercapto-1,2,3-triazole (AMTA)	Carbon steel/2 M $H_2SO_4$	N. A./mixed type inhibitor	$5 \times 10^{-3}$ M	SEM-EDX, PDP, EIS	76.67%	139
Benzotriazole (BZT)	Carbon steel/2 M HCl	Chemisorption/mixed type inhibitor	500 ppm	WL, PDP, EIS, LPR, DFT, CS	78.1%	140
5-Methyl-1H-benzotriazole (5MBZT)					91.8%	
3-Amino-5-methylthio-1H-1,2,4-triazole (3AMT)					24.8%	
Allyl-6-nitro-1H-indazole	Carbon steel (C38)/1 M HCl	Langmuir/mixed type inhibitor	$10^{-3}$ M	WL, PDP, EIS, XPS, SEM	95%	141
1-Ethyl-5-nitro-1H-benzimidazole-2-thiol			$10^{-3}$ M		97.5%	
Pyridine	MS/0.1 M $HClO_4$	N. A./mixed type inhibitor	0.05 M	PDP, DFT, MD	27.5%	142
2-Amino-5-chloropyridine					68.3%	
2-Amino-3,5-dichloropyridine					52.1%	
2-Amino-3-benzyloxy pyridine					42.4%	
Imidazole-4-methylimine thiourea (MIT)	Mild steel/1 M HCl	Langmuir/mixed type inhibitor	200 ppm	SEM, EISDPD, DFT, MD	93.7%	143

heterocyclic agents are also employed as inhibitors in aggressive media. The wide use of inhibitors is attributed to their ease of application, reasonable cost, and efficiency. Studies have demonstrated that inhibitors containing heteroatoms (N, P, O, S) and lone electrons are essential for physisorption or chemical adsorption to form a protective barrier on certain metal surfaces. Inhibitors frequently come into touch with caustic substances including acids, oxidizing agents, and aggressive ions during industrial operations. A heterocyclic structure must be carefully designed to account for various reactions that can make the inhibitor ineffective or exacerbate the effects of corrosion. Functional groups in the structure directly impact its adherence to metal surfaces. Certain functional groups can be added to heterocyclic agents to boost their design and synthesis while minimizing interfering issues. Furthermore, to guarantee safety, it is crucial to do biological toxicity testing before utilizing heterocyclic inhibitors. Table 2 lists some of the common organic corrosion inhibitors along with their important characteristics.

### 3.3 Adverse effects of inorganic and organic corrosion inhibitors

Inorganic corrosion inhibitors can have significant adverse effects, particularly on the environment and human health. One of the primary concerns is the environmental impact of these inhibitors. Many inorganic corrosion inhibitors, such as chromates and phosphates, can accumulate in the environment and lead to the contamination of water bodies, soil, and air. Chromates, for instance, are known to be carcinogenic and can pose a serious threat to both ecological systems and human health.<sup>144</sup>

The release of these harmful substances into the environment can have far-reaching consequences, disrupting delicate ecosystems and potentially exposing human populations to toxic substances through various exposure pathways, such as drinking contaminated water, ingesting contaminated foods or inhaling polluted air. In addition to the adverse environmental impact, inorganic corrosion inhibitors can also exhibit direct toxicity to living organisms. Substances like nitrite and zinc salts can be toxic to a wide range of organisms, including aquatic life, plants, and humans, depending on the concentration level and exposure route.<sup>145</sup> Ingestion or inhalation of these inhibitors can lead to various health problems, such as respiratory issues, skin irritation, and gastrointestinal disorders. This toxicity affects not only the workers who handle these inhibitors but also the general public and the surrounding communities where these substances are used or disposed of.

Further, organic corrosion inhibitors, while offering alternative solutions to inorganic inhibitors, also can have their own set of adverse effects that must be considered. One significant concern is the toxicity and environmental persistence of some organic inhibitors, such as imidazolines and quaternary ammonium compounds. These substances can be toxic to aquatic organisms and may bioaccumulate in the environment, leading to long-term impacts on ecosystems. Another adverse effect of some organic corrosion inhibitors is their potential to cause foaming or fouling in various industrial systems, such as heat exchangers, pipelines, or boilers. This can lead to operational issues, reduced efficiency, and the need for additional maintenance and cleaning, which can be time-consuming and costly. Furthermore, the use or decomposition of organic



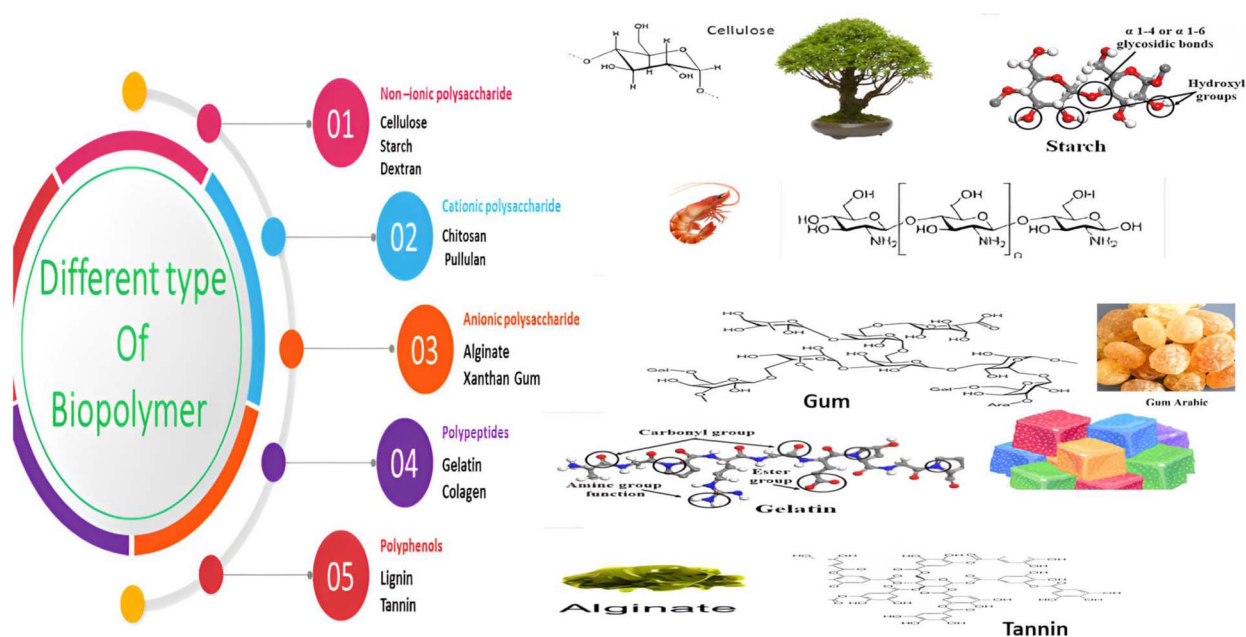


Fig. 5 Various types of biopolymers.

corrosion inhibitors can result in the formation of potentially harmful byproducts. These byproducts may have adverse environmental or health implications, as they can be carcinogenic, ecotoxic, or have other undesirable properties. The disposal and waste management of spent or unused corrosion inhibitors also present challenges. These substances may require specialized treatment or containment to prevent environmental contamination, and improper disposal can result in the release of harmful substances into the environment, further exacerbating the risks to ecosystems and human health.<sup>146–150</sup> To address these adverse effects and promote sustainable corrosion management practices, it is crucial to carefully evaluate the specific application, environmental conditions, and potential risks associated with both inorganic and organic corrosion inhibitors before selection and use. Proper handling, disposal, and the development of environmentally friendly alternative inhibitors can help mitigate the associated risks and ensure the safe and effective use of these substances.

### 3.4 Environmentally friendly corrosion inhibitors

**3.4.1. Polysaccharides inhibitors.** Biopolymers are natural polymers derived from renewable sources like plants, animals, and microorganisms. These materials have garnered attention due to their unique properties and environmental sustainability. Some common examples of biopolymer types include alginate, chitosan, lignin, cellulose, and starch (Fig. 5). These materials possess the ability to form protective layers on metal surfaces, effectively preventing the entry of corrosive chemicals. Biopolymers offer sustainable and effective alternatives to other inhibitors. Their capacity to adhere to metal surfaces and create protective barriers helps to hinder the electrochemical processes that lead to corrosion. The adsorption on surfaces is impacted by various elements, such as pH, polymer

concentration, temperature, and surface charge. Through hydrogen bonding, electrostatic forces, and other molecular interactions, biopolymers can effectively block the penetration of corrosive substances. The utilization of carbohydrates as inhibitors presents an attractive alternative due to their abundance, renewability, and low environmental impact. Carbohydrates can be derived from numerous sources, including plant materials (e.g., starch and cellulose), marine crustacean shells (e.g., chitosan and alginate), and even from bacterial fermentation processes.<sup>151–153</sup> To optimize the corrosion inhibition properties of carbohydrates, chemical modifications can be employed. By targeting specific functional groups, such as hydroxyl, carboxyl, or amino groups, within the carbohydrate structure, their inhibitory effects can be enhanced. For instance, the introduction of amino groups can improve adsorption characteristics, facilitating the formation of more effective protective films and increasing corrosion resistance. Numerous studies have investigated the corrosion inhibition potential of different carbohydrates for several metals, including steel, in various corrosive environments such as acidic, alkaline, and saline solutions.<sup>154,155</sup> Chitosan (CS), a derivative of chitin found in crustacean shells, has also gained attention as an effective corrosion inhibitor. Chitin is derived primarily from shrimp and other crustacean shells (Fig. 6a). For the partial deacetylation of Chitin, it is common to employ an alkaline solution. With their remarkable qualities, both chitin and CS prove to be exceptional candidates for a wide array of biological and industrial applications, including the prevention of corrosion. Chitosan consists of various reactive groups: a primary  $\text{CH}_2\text{OH}$ , a secondary  $\text{CH}-\text{CH}_2\text{OH}$ , and an amino group ( $-\text{NH}_2$ ), attached to carbon atoms.<sup>153</sup> The use of CS as a corrosion inhibitor is justified for various reasons; for instance, owing to its polymer nature, power to fully adsorb



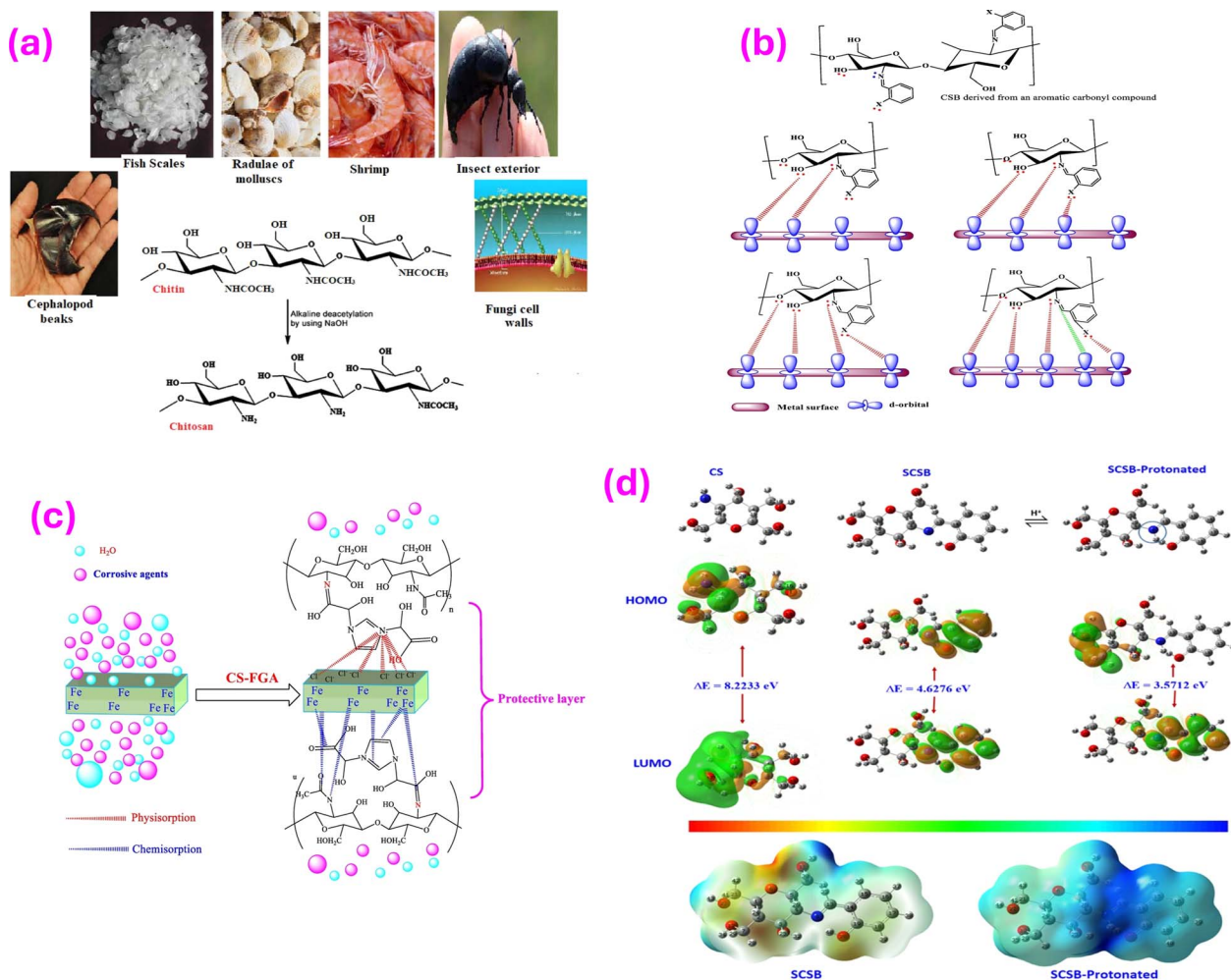


Fig. 6 (a) Various sources of chitosan, reprinted with the permission of ref. 156, copyright 2024, Elsevier; (b) illustration of formation of chelating complexes of chitosan Schiff bases, reprinted with the permission of ref. 157, copyright 2024, Elsevier; (c) adsorption mode of CS-FGA molecule on the MS surface, reprinted with the permission of ref. 158, copyright 2024, Elsevier; (d) optimized geometry; HOMO and LUMO orbitals of neutral and protonated SCSB; and MEP images of neutral and protonated SCSB, reprinted with the permission of ref. 159, copyright 2024, Elsevier.

onto and cover various metallic surfaces, and efficient corrosion protection.<sup>157,160</sup> In fact, these biomacromolecules contain polar moieties that can act as sites for adsorption when they interact with metal surfaces. Chitosan, a versatile material, exhibits both physisorption and chemisorption properties. Chemisorption occurs through the sharing of electrons between the N and O atoms of CS, leading to coordination bonding.<sup>161,162</sup> Physisorption, on the other hand, is driven by electrostatic interactions between the charged CS and surface.<sup>163</sup> Polar groups like –OH and –NH<sub>2</sub> have the capacity to be protonated in aqueous solutions, which may contribute to the creation of cationic forms.<sup>164</sup> On the other hand, the buildup of counter ions from the electrolyte ions at the positive surface causes the metal surface to turn negatively charged. The interplay between charge interactions and chemisorption and physisorption adds to chitosan's adaptability and adsorption power across a range of applications.<sup>158</sup> The natural antimicrobial features of CS can help prevent MIC by limiting the growth of corrosive microorganisms on metal surfaces. Its diverse inhibitive mechanisms

contribute to its performance in various corrosive environments.<sup>134</sup> Several factors including concentration level, pH, duration of exposure, and temperature may impact the performance of CS.<sup>134</sup> For instance, when applied to MS protection, CS exhibited 96% and 93% corrosion inhibition efficiency at 60 °C and 70 °C, in an HCl environment.<sup>165</sup> Using polarization analyses, it was proposed that CS served as a mixed inhibitor, affecting both the cathodic and anodic reactions. Impedance measurements reflected that CS adsorption occurred at the solution/metal interface. The Langmuir isotherm model was noticed to agree with CS adherence onto MS surfaces. Thus, when 200 ppm CS was employed as a corrosion inhibitor in a 1 M sulfamic acid medium, there was significant inhibitory performance of 73.8% noticed for MS.<sup>166</sup> The research demonstrated that CS operated by obstructing the active sites of the metal, thus mimicking both the anodic and cathodic processes that take place on the surface of tested MS. To further confirm this, surface examinations using atomic force microscopy (AFM) and SEM were conducted, revealing the creation of



a protective film on steel surface owing to the existence of the inhibitor. Additionally, the study determined that the CS adsorption adhered to the Langmuir model. However, a major drawback of CS is its inadequate solubility in many liquids, which greatly limits its use as a corrosion inhibitor.<sup>154</sup> CS has a unique property – it is insoluble water, but it can dissolve in a slightly acidic medium (with a pH below 6.5). This is owing to  $-NH_2$  in the CS converting to a soluble glucosamine- $NH_3^+$  form under these mildly acidic conditions.<sup>134</sup> The solubility of CS in aqueous electrolytes is robustly impacted by the level of deacetylation (% DD) – the robust the % DD, the greater the solubility.<sup>134,167</sup> Commercially useful grades of CS typically have a % DD between 60–100% and a molecular weight range of 3800–20000 Da.<sup>168,169</sup> Researchers have been actively exploring approaches to further enhance the solubility of CS. One common approach is to chemically modify the CS structure by introducing more polar substituent groups, such as ester ( $-COOR$ ), hydroxyl ( $-OH$ ), amino ( $-NH_2$ ), ether ( $-O-$ ), nitrile ( $-CN$ ), amide ( $-CONH_2$ ), and nitro ( $-NO_2$ ) groups.<sup>48,49</sup> These phenomena can make soluble better by improving the bond between the changed CS and the water, or by turning the CS into even more watery forms.<sup>161,170,171</sup> For instance, To enhance chitosan's solubility, a chitosan salt was fabricated and tested as an effective corrosion inhibitor for N80 steel in seawater.<sup>161</sup> Results revealed that CS served as a mixed-type inhibitor with a notable inhibitory impact on the anodic reaction. Notably, at a concentration of 1000 ppm, CS displayed an impressive inhibition performance of 96.68%. Currently, there is a significant focus on the chemical bonding of organic compounds with CS and their potential as agents to mitigate corrosion. To achieve this, CS undergoes an operation called cross-linking, wherein an organic polyol-linker is employed to connect multiple CS chains. This type of cross-linking boosted the solubility and protective capabilities of the CS derivatives. Therefore, the use of polyethylene glycol (PEG) cross-linked-CS was tested as a corrosion inhibitor for steel, at a dosage of  $200\text{ mg L}^{-1}$ , and exhibited a high inhibition performance of 93.9%.<sup>172</sup> The adherence of CS-PEG on the steel surface and the generation of a protective film were accountable for the significant enhancement in surface smoothness noticed at the optimal CS-PEG level. The transfer of d-orbital electrons from iron to unoccupied antibonding orbitals of CS inhibitor promoted adherent phenomena, while heteroatoms with free lone pair electrons present on employed CS inhibitor supported chemical adherence.

Various works reported that chitosan-based Schiff bases (CSBs) exhibit outstanding stability and resist deterioration. The fact that CSBs are composed of polymers, which enables them to offer superior covering and protection for metal surfaces, is one of its benefits. Additionally, polar substituents found in CSBs can serve as adsorption sites when they engage and form bonds with metal surfaces. Furthermore, these substituents aid in making CSBs more soluble in electrolytes containing water. It's vital to remember that CS may be made more soluble and corrosion-resistant by altering its structure. As seen in Fig. 6b, CSBs are able to make powerful connections with metal surfaces because they have several electron-rich

moieties.<sup>157</sup> Moreover, in this bonding process, the imine bond ( $>C=N-$ ) is very significant. For instance, Chitosan-Salicylaldehyde-Schiff base (CS-SB) was investigated as a corrosion inhibitor of steel in 3.5% NaCl solution saturated with  $CO_2$ .<sup>159</sup> The researchers found that the existence of CS-SB significantly enhanced the surface morphologies of the steel, as noticed through SEM and AFM analysis. Additionally, the results from PDP tests reflected that CS-SB served as a mixed-type inhibitor, effectively minimizing the corrosion process. At a level of  $150\text{ mg L}^{-1}$ , CS-SB exhibited an inhibition performance of 95.2% and a corrosion rate of 0.444 mm per year. Among the isotherm models tested, the Langmuir model offered a great fit for the experimental data. Luo and colleagues<sup>158</sup> developed a CS-FGA through a straightforward amidation reaction. The protonated CS-FGA molecules with  $-N^+=$  species can physically adhere to the pre-adsorbed  $Cl^-$  ions. Additionally, the heteroatoms and polar groups in the CS-FGA can accept and donate electrons, leading to chemical adsorption through electron mobility between the Fe atoms and heteroatoms or the polar groups. The adsorption mode of CS-FGA is illustrated in Fig. 6c. Furthermore, SCSB was fabricated, and its inhibition impact was analyzed using various approaches. Computational investigation revealed the excellent adsorption of the protonated form of the inhibitor (Fig. 6d). The inclusion of the salicylaldehyde moiety has significantly promoted the size of the resulting SCSB molecule, leading to a planar structure. The enhanced structural planarity and size are likely to promote the coverage of the surface.<sup>159</sup>

On the other hand, cellulose is a valuable carbohydrate-based polymer with various applications. It consists of  $\beta$ -D-glucose units linked by a  $\beta$ -(1-4)-glycosidic bond to form a linear chain polysaccharide. Cellulose is a key component of Oomycetes, plant cell walls, and algae. It is abundantly found in nature, with approximately 40–50% found in wood, 90% found in cotton, and 57% in hemp.<sup>173</sup> Carboxymethyl cellulose (CMC) is one of the derivatives of cellulose that contains carboxymethyl bonded to the glucopyranose units in the structure.<sup>174</sup> For instance, cellulose extracted from pistachio nut shells was employed as a corrosion inhibitor of steel.<sup>175</sup> The researchers found that the inhibitor adhered to the Langmuir isotherm and exhibited a mixed-type inhibition behavior. Furthermore, 800 ppm level of inhibitor resulted in a significant 92% performance. Additionally, the inhibitor exhibited both chemisorption and physisorption characteristics onto the tested metal surface. Furthermore, the use of hydroxyethyl cellulose (HEC) as a corrosion inhibitor for A1020 steel in an acidic medium was investigated.<sup>176</sup> The researchers found that the inhibition performance was promoted with higher HEC levels but minimized with rising temperature. HEC was identified as a mixed-type inhibitor, mainly anodic, based on PDP investigations. In an acidic medium, HEC exists in a protonated form and interacts electrostatically with  $Cl^-$  ions already adherent to the metal surface. Protonated HEC competes with  $H^+$  ions for electrons on the surface, resulting in the release of  $H_2$  gas. This phenomenon returns HEC to their neutral form and promotes chemisorption by oxygen atoms, which have a free lone pair of electrons. Additionally, the accumulation of electrons on the



steel surface leads to a more negative charge. As a result, an electron from the d-orbital of Fe may move to a vacant anti-bonding orbital of the inhibitor. Similar, carboxymethyl cellulose (CMC) was employed as an inhibitor for steel in a 3.5% NaCl medium saturated with CO<sub>2</sub>.<sup>177</sup> The inhibitor's adherence obeyed Langmuir's isotherm. In another study, the researchers examined how the addition of halide (Cl<sup>-</sup>, Br<sup>-</sup>, and I<sup>-</sup>) impacted the performance of CMC in an acidic medium.<sup>178</sup> They noticed that the existence of iodide ions promoted the inhibition provided by CMC, resulting in a synergistic impact. However, the existence of chloride had the opposite impact, causing an antagonistic impact on inhibition. The effectiveness of CMC, as displayed by the inhibition efficiency (%  $\eta$ ) value, was promoted over time as the MS was immersed in the medium containing CMC and iodide ions, as well as other halide ions.

On the other hand, lignin is a 3D aromatic biopolymer that can be found in a variety of materials, including bagasse, wood, and sugar cane. It is ideally suited as coating and corrosion inhibitor owing to its accessibility, environmental friendliness,

and anti-corrosion features.<sup>179–181</sup> While lignin already possesses natural functional groups (*e.g.*, aromatic sites, –OH, and –OCH<sub>3</sub>) that contribute to its beneficial properties, efforts have been made to introduce new functionalities to enhance its anticorrosion potential.<sup>182,183</sup> These polar functional groups within lignin are particularly essential for its corrosion suppression mechanism, as they facilitate adherence onto metallic surfaces.<sup>184,185</sup> Despite lignin's demonstrated corrosion inhibition properties, ongoing research focus on exploring various strategies to further enhance its effectiveness as a corrosion inhibitor.<sup>186–188</sup> For instance, lignin as an inhibitor was applied to ferrous metal surfaces exposed to acidic conditions.<sup>189</sup> Lignin is obtained from bagasse through an acidification approach and its functional groups are confirmed through FTIR analysis. The researchers evaluate the corrosion inhibition performance of lignin by varying its levels and the duration of immersion. Through the weight-loss approach, they demonstrated that the most optimal inhibition performance was achieved with a lignin level of 10 g L<sup>-1</sup> and a metal immersion time of 6 hours, resulting in an impressive 80.79% corrosion

Table 3 Extract of data of some polysaccharides evaluated as corrosion inhibitors

Inhibitor	Environment	Nature of adsorption	Conc.	Method of corrosion monitoring	IE %	Ref.
Chitosan	Mild steel, 0.1 M HCl	Langmuir	1.8 mM	WL, EIS, PDP, AFM and EDS	92.1	194
Chitosan	1 M HCl, carbon steel	Langmuir	5000 ppm	WL	93.2	195
CH + KI	Mild steel, 1 M sulfamic acid	Langmuir	200 ppm CH + 5 ppm KI	WL, EIS, PDP, AFM and SEM	91.6	166
Chitosan + KI	15% H <sub>2</sub> SO <sub>4</sub>	Langmuir	5 g CH + 5 mM KI	WL, DEIS, PDP, AFM, SEM and EDS	97.6	196
Chitosan–polyaniline (PANI/CTS)	0.5 M HCl, mild steel	Mixed-type inhibitor	200 ppm	EIS, PDP, SEM and DFT	79.02%	197
Chitosan Schiff base (ChTSB)	Mild steel, 1 M HCl	Temkin isotherm, mixed-type	1500 ppm	EIS, PDP, AFM, SEM and EDS	86.94%	198
Salicylaldehyde-chitosan Schiff base (SCBS)	Carbon steel (J55 steel), 3.5% NaCl	Langmuir, mixed type	150 ppm	XPS, EIS, PDP, AFM, SEM and EDS	95.4%	159
CS-2	Mild steel & 1 M HCl	Langmuir, mixed type	150 ppm	XPS, EIS, PDP, MD, AFM, and SEM	98.0%	154
Chitosan-cinnamaldehyde Schiff base	Carbon steel & 3.5% NaCl	Langmuir, mixed type, cathodic predominantly	600 ppm + 10 mM KI	DFT, EIS, PDP, MD, SEM and EDS	92.67%	199
4-(Dimethylamino)benz-aldehyde-chitosan	Mild steel/1 M HCl	Langmuir	50 ppm	PDP, EIS, WL, SEM and EDS	90.65	200
Carboxymethyl chitosan (CMC)	3.5% NaCl, carbon steel	Langmuir, mixed type inhibitor	80 ppm	PDP, EIS	85.57%	201
Chitosan (CH)	5% NaCl + CO <sub>2</sub> aPI 5 L X60	Langmuir, mixed type	100 ppm	EIS, PDP and SEM	45%	177
carboxymethylcellulose (CMC)	pipeline steel	inhibitors	100 ppm		39%	
Ethyl hydroxyethyl cellulose (EHEC)	1 M H <sub>2</sub> SO <sub>4</sub> /mild steel	Langmuir, slightly cathodic	2500	WL, EIS, PDP and DFT	68.19%	202
Carboxymethyl cellulose (CMC)	2MH <sub>2</sub> SO <sub>4</sub> /mild steel	Langmuir	500 ppm	WL and hydrogen evolution	65%	178
Exudate gum from <i>Araucaria heterophylla</i> tree (AH-gum)	Mild steel/1 M H <sub>2</sub> SO <sub>4</sub>	Langmuir, mixed type	0.05% v/v	WL, EIS, PDP, DFT, MD, AFM, SEM	79%	203
Exudate gum from Terminalia mentalya tree (TM-gum)	Carbon steel/1 M HCl	Langmuir and Temkin, mixed type	2000 ppm	WL, EIS, PDP, SEM	96%	204
Mangifera indica gums tree (MA-gum)	Carbon steel/1 M HCl	Langmuir and Temkin, mixed type	1000 ppm	WL, LP, OP	98%	205
Gellan gum	Cast iron/1 M HCl	Langmuir, mixed type	5000 ppm	WL, PDP, EIS, SEM	81%	206
Gum acacia	Mild steel/1 M HCl	Langmuir, mixed type	1000 ppm	WL, PDP, EIS	97%	207
Xanthan gum (XG)	Mild steel/1 M HCl	Langmuir, mixed type	1000 ppm	WL, PDP, EIS, SEM	74.24	208



inhibition. The Langmuir adsorption isotherm described the adherence of lignin onto the surface of tested MS.<sup>190</sup> Further, the research showed that the existence of lignin can significantly impact the texture and features of the target metal surface. SEM images have revealed that when lignin was added to a solution, it effectively minimizes the roughness of the metal surface, leading to enhanced homogeneity and smoothness. This is a strong indication of lignin's potential in inhibiting corrosion consequently minimizing the oxidative metal dissolution.<sup>191,192</sup> Furthermore, AFM analysis has demonstrated that in the absence of lignin inhibitors, the surface undergoes deterioration due to acidic conditions. However, the addition of lignin inhibitors to the solution successfully mitigates surface corrosion. Lignin has been found to diminish the maximum height scales of surface roughness when compared to samples without inhibitors.<sup>180,193</sup> Table 3 lists some of the common polysaccharide corrosion inhibitors along with their important characteristics.

Alginate, a naturally occurring polysaccharide derived from brown seaweed, has emerged as a promising and eco-friendly inhibitor.<sup>209</sup> As industries and researchers seek alternatives to traditional and hazardous corrosion inhibitors, the use of alginate has gained significant attention due to its unique properties and eco-friendly nature.<sup>210</sup> This biopolymer derived from brown seaweed, with its unique structure imparts sodium alginate (SA) many desirable features, such as biodegradability, robust solubility, non-toxicity, and biocompatibility. Recent works have highlighted the successful employing of SA as a novel and powerful biological inhibitor for MS in challenging environments, including saline media and hydrochloric acid pickling.<sup>211,212</sup> The primary mechanism by which alginate inhibits corrosion is the formation of a protective, passivation layer on the metal surface. Alginate's long, linear polysaccharide chains are composed of two main types of monomer units: guluronic acid (G) and mannuronic acid (M).<sup>213</sup> These monomers possess various functional groups, such as carboxyl and hydroxyl groups, which allow alginate to adsorb strongly onto metal surfaces through chemical and physical interactions.<sup>210,214</sup> The adsorption of alginate on the metal surface creates a barrier that separates the metal from the corrosive environment, effectively shielding it from direct contact with corrosive agents like oxygen, moisture, and attacking ions.<sup>215</sup> This physical barrier inhibits the electrochemical processes that drive corrosion, slowing down the anodic and cathodic reactions responsible for metal dissolution and the formation of corrosion products.<sup>216</sup> Namely, Alginate's corrosion inhibition mechanism involves the modulation of both the anodic and cathodic reactions that occur during the corrosion process. The adsorption of alginate on the metal surface can block the active sites and alter the kinetics of both of the anodic (metal dissolution), and cathodic (oxygen reduction) reactions, thereby reducing the overall corrosion rate.<sup>211,217</sup> Moreover, the adsorption of alginate on the metal surface can promote the formation of a stable, protective passive film. This passive film acts as an additional barrier, further enhancing the corrosion resistance of the metal. The synergistic effect of these multifaceted mechanisms, including adsorption, chelation, anodic and cathodic

inhibition, and pH buffering, contributes to the exceptional corrosion inhibition performance of alginate. The understanding of these underlying mechanisms is crucial for the rational design and optimization of alginate-based corrosion inhibitors, enabling their effective deployment in a wide range of industrial applications. For instance, using polarization studies, the SA mitigation performance on MS in 1 M HCl medium was explored and revealed an impressive performance of 90.9% inhibition at a level of 1500 mg L<sup>-1</sup> SA, highlighting its potential as a powerful inhibitor in acidic medium.<sup>218</sup>

Furthermore, natural gums are complex polymers composed of long polymeric sugar chains with enormous molecular weights, which are formed of monosaccharide units joined by glycosidic linkages.<sup>219,220</sup> Based on their environmental friendliness and wide availability, natural gums have drawn attention in corrosion inhibitor research. These natural gums' molecular weight, chemical makeup, and molecular and electrical structures all have a significant impact on how well they prevent corrosion.<sup>221</sup> These gums have chemical components that prevent corrosion by creating hydrophobic barriers, which limit the entrance of molecules and ions that cause corrosion at the metal–solution interface. Furthermore, certain gums have polar functional groups that attach to metal surfaces to promote protection by improving electron or charge transport.<sup>221,222</sup> The performance of natural gums as inhibitors is significantly influenced by temperature and duration of immersion.<sup>223</sup> However, natural gums do not show remarkable inhibition when employed in their pure form because of things like quick hydration, microbial and algal contamination, pH-dependent solubility, and heat instability.<sup>224</sup> A variety of modification techniques—which fall into the categories of physical or chemical strategies—are used to get over these obstacles.<sup>225</sup> To provide a synergistic impact, physical tactics entail combining and mixing natural gums with materials like surfactants and halides. Conversely, the chemical approach makes use of natural gums' many qualities to enhance their inhibitory qualities.<sup>225</sup> This method frequently makes use of procedures including grafting, crosslinking, esterification, and etherification. Creating composites and nano-composites—wherein inorganic components at the nanoscale are integrated into the gum matrix—is a more modern technique for modification.

For instance, several gum types were studied as mild steel corrosion inhibitors, including AF-gum (*Albizia ferruginea* gum), KS-gum (*Khaya senegalensis* gum), Daniella Oliveri gum, AL-gum (*Anogessus leocarpus* gum), FTP-gum (*Ficus tricopoda* gum), CS-gum (*Canarium schweinfurthii* gum), KI-gum (*Khaya ivorensis* gum), FP-gum (*Ficus platyphylla* gum), and CA-gum (*Commiphora Africana* gum).<sup>225–230</sup> In general, as the dosage is increased, their inhibitory performances get better, but when the temperature of the solution increases, they get worse. The inhibitory property arises from the adsorption of heteroatom-rich molecules, which act as the anchor point for the adsorption process.<sup>225</sup> The inhibition efficiency falls between 66% and 84%. They adsorb spontaneously, according to the physical adsorption mechanism, and their ideal concentration is 0.50 g L<sup>-1</sup>.



**3.4.2. Amino acid and proteins inhibitor.** Proteins have gained attention as inhibitors owing to their low environmental impact. They offer features such as high effectiveness, low toxicity, and biocompatibility. Proteins can generate a protective layer on the treated metal surface, hindering corrosion processes.<sup>231</sup> Apart from their crucial functions such as catalyzing metabolic reactions and DNA replication within living organisms, various proteins have been explored for their inhibitory features in various corrosive environments.<sup>232</sup> On the other hand, amino acids, the building units of proteins, are organic compounds that are characterized by specific side chains unique to each amino acid, where these side chains consist of functional groups such as carboxyl groups ( $-\text{COOH}$ ) and amino groups ( $-\text{NH}_2$ ), among other groups. The structure of amino acids includes elements such as nitrogen, oxygen, hydrogen, carbon, and possibly other atoms that are present in the side chains.<sup>233</sup> Peptide bonds, also known as amide bonds, form when the  $-\text{COOH}$  of one amino acid molecule reacts with the  $-\text{NH}_2$  of another amino acid molecule.<sup>234</sup> According to studies, side chains containing "R" groups and a large number of linked amino acids form polypeptides.<sup>235</sup> Ultimately, polypeptides come together to form linear biopolymers known as proteins.

The impacts of casein on the corrosion behavior of steel in an acidic medium were investigated using various analytical techniques.<sup>236</sup> The WL results reflected that as the level of casein increased from 50 to 400 ppm, the rate of corrosion inhibition declined from 34.3 mpy to 3.9 mpy. However, when the temperature of the test medium was raised from 298 K to 343 K, the surface coverage and consequently the casein inhibition role were negatively impacted. Thermodynamic calculations displayed that in the presence of 400 ppm casein, the enthalpy of activation and activation energy enhanced from  $5.95 \text{ kJ mol}^{-1}$  to  $43.23 \text{ kJ mol}^{-1}$  and from  $8.61 \text{ kJ mol}^{-1}$  to  $45.89 \text{ kJ mol}^{-1}$ , respectively. The functional groups of casein enhanced electrostatic adherence to the employed metal surface (physisorption). Additionally, in the chemisorption operation, heteroatoms in casein, such as oxygen, donated their lone-pair electrons to the metal-vacant d-orbitals. In another investigation, EIS was used to explore the behavior of steel in an HCl solution in the presence of gelatin.<sup>237</sup> It was noticed that the existence of gelatin led to the creation of a protective layer on the surface of the tested MS, which slowed down the charge movement reaction between the medium and metal. Gelatin was found to serve as a mixed-type inhibitor, blocking both the cathodic and anodic sites, and its adsorption features followed the Langmuir model. The polypeptide chain's backbone amide linkages were believed to account for gelatin adherence onto the metal surface. It is noteworthy to emphasize that the number of papers on the anticorrosive behavior of proteins is comparatively lower than that on the performance of amino acids (AAs) in inhibiting corrosion.<sup>238</sup> The AAs can be viewed as comparatively more affordable, soluble, and environmentally friendly substitutes.<sup>239,240</sup> Besides the environmental aspects, the inclusion of heteroatoms such as sulfur (S), nitrogen, conjugated  $\pi$ -electron systems, and oxygen (O), plays an essential role in the

performance of amino acid inhibitors. Amino acids can be classified into three main groups: acidic, neutral, and basic (Fig. 7a).<sup>241</sup> The classification is based on the relative abundance of amino ( $-\text{NH}_2$ ) groups and carboxyl ( $-\text{COOH}$ ) within the amino acid structure. Basic amino acids contain more  $-\text{NH}_2$  groups than  $-\text{COOH}$  groups, while acidic amino acids exhibit the opposite trend.<sup>241,243</sup> Neutral amino acids are characterized by a balanced ratio of amino to carboxyl groups. This unique structural feature of amino acids suggests their potential as powerful inhibitors. The adsorption mechanism of these substances on MS is particularly intriguing, granting them the remarkable ability to function as natural inhibitors. The adsorption phenomenon is driven by the binding of the N atom within AAs to the MS. This adsorption phenomenon facilitates the creation of a robust layer on the metal surface, effectively slowing down the rate of corrosion.<sup>241,242</sup> The physisorption interaction will occur more quickly and effectively with amino acids than with traditional inhibitors because they are already charged particles. Furthermore, it is possible to propose that amino acids have at least two adsorption sites, while traditional inhibitors only have one by treating charged moieties as adsorption centers. Additionally, some specialized subgroups of amino acids, called amino alcohols, have been found to have remarkable corrosion inhibition performance.<sup>238,241,244</sup> They achieve this through a two-pronged strategy. First, they replace chloride ions that play a critical role in the corrosion phenomenon. Second, they block specific locations where  $\text{O}_2$  gains electrons, thus hindering overall corrosion. This dual approach allows these AAs to be promising inhibitors.

For instance, the ability of leucine, alanine, and glycine to suppress steel corrosion in an acidic medium was analyzed, where Langmuir's isotherm best fitted amino acids adsorption on steel.<sup>245</sup> Furthermore, AAs and their derivatives such as heterocyclic amino acids substances can also form powerful chelating complexes that excellently bind to metal surfaces.<sup>246</sup> Fig. 7b shows the advantages and limitations of AA-based heterocycles and bare amino acids as corrosion inhibitors.<sup>241</sup> Specific amino acids like tryptophan, histidine, and proline, as well as their derivatives, have been widely utilized for corrosion hindering owing to their capacity to bind to surfaces and create these chelating complexes.<sup>247</sup> For instance, proline can form a bidentate chelating complex employing its carboxyl and amino groups.<sup>248</sup> Tryptophan and histidine can form even robust tridentate chelating complexes owing to another N in their indole and imidazole structures, respectively.<sup>249</sup> The adsorption phenomenon of these compounds primarily follows the Temkin and Langmuir adsorption isotherms, and they function as mixed-type inhibitors. While amino acids substances are known for their ability to coordinate with substrates, they are generally not recommended for commercial uses owing to their relatively lower molecular size and small coverage of surface. However, the heterocyclic substances derived from amino acids often have acceptable molecular sizes, allowing them to more effectively protect surfaces.<sup>241</sup> The semi-synthetic nature of the heterocyclic substances derived from AAs is believed to make them more friendly alternatives to conventional, harmful inhibitors. For example, a separate study



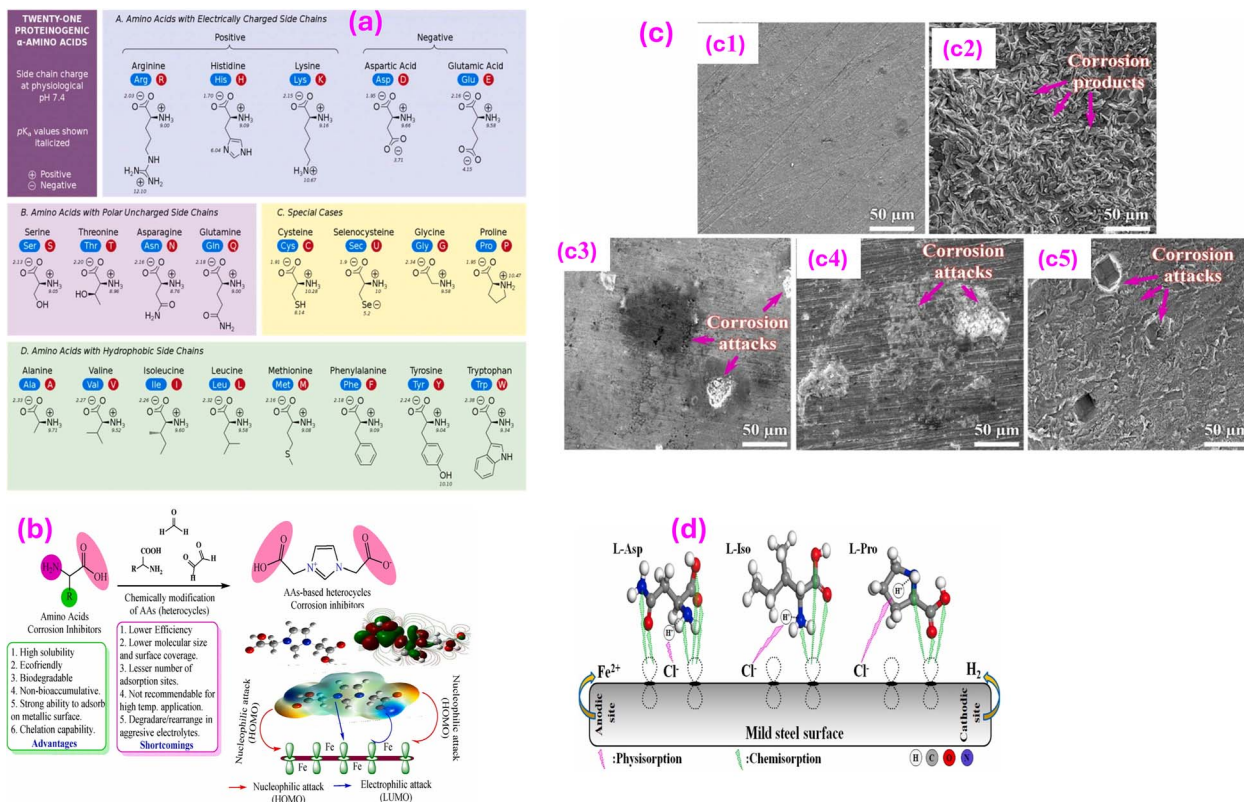


Fig. 7 (a) Chemical structure and classification of amino acids, reprinted with the permission of ref. 241, copyright 2024, Elsevier, (b) advantages and limitations of AA-based heterocyclic and bare amino acids, reprinted with the permission of ref. 241, copyright 2024, Elsevier; (c) surface morphology of Ms: (c1) before immersion, and after immersion in: (c2) 0.5 M HCl, (c3) L-Asp, (c4) L-Iso, and (c5) L-P, reprinted with the permission of ref. 242, copyright 2024; (d) inhibition mechanism of L-Asp, L-Iso, and L-Pro inhibitors in 0.5 M HCl solution, reprinted with the permission of ref. 242, copyright 2024.

demonstrated the ability of the amino acid proline to minimize corrosion. Consistent with expectations, the researchers noticed that rising the pH from 2 to 5 led to an improvement in the inhibition performance, rising from 16% to 65%.<sup>248</sup> The corrosion inhibition of L-isoleucine (L-Iso), L-proline (L-Pro) and L-asparagine (L-Asp) on steel immersed in 0.5 M HCl was also investigated.<sup>242</sup> At 1000 ppm, L-Pro, L-Iso and L-Asp showed 91%, 93% and 95% inhibition, respectively. Fig. 7c shows the surface morphology of MS before and after immersion of each inhibitor at 1000 ppm. XPS studies showed that the acceptor–donor interactions between surface iron atoms and AAs heteroatoms play a key role in the chemisorption phenomenon (Fig. 7d).<sup>242</sup> Furthermore, the inhibition capabilities of unmodified proline against corrosion have been explored.<sup>250,251</sup> Likewise, the bare amino acid histidine is commonly utilized, solely or alongside other substances designated as synergists, as a method of combating corrosion.<sup>252–254</sup> Tryptophan (Trp) possesses a unique chemical composition, featuring an indole group integrated within its side chain. This indole group is formed by the fusion of a benzene ring and a pyrrole ring. Due to this distinctive structural attribute, Trp has the potential to serve as a more robust inhibitor compared to histidine (His) and proline (Pro). Consequently, numerous studies have been dedicated to exploring the role of Trp in mitigating corrosion in aqueous environments.<sup>255,256</sup> Table 4 lists some of the common amino

acids-based corrosion inhibitors along with their important characteristics.

**3.4.3. Polyphenols inhibitors.** Tannins are complex combinations of organic polyphenolic substances isolated from plants.<sup>270,271</sup> They can be classified into two main types: hydrolyzable and condensed tannins. Hydrolyzable tannins originate mostly from pods and fruits, while condensed tannins are found in significant amounts in the wood and bark of various trees such as black wattle.<sup>271,272</sup> These condensed tannins have been extensively studied as corrosion inhibitors in different environments.<sup>273,274</sup> The researchers attributed the tannins' inhibitory effect to their electron-rich heteroatoms and double bonds, which facilitate adsorption on the metal surface, thereby contributing to the inhibition process.

## 4. Synergistic inhibition effects

Herein, the term synergy refers to the collaborative impact of multiple corrosion inhibitors working together to promote their ability to hinder corrosion. When these inhibitors are combined, their combined impact is more robust than when employed individually. This collaborative impact can be attributed to the many ways in which these inhibitors work, which complement and promote each other's actions. By employing these inhibitors together, they offer extra protection



Table 4 Extract of data of some amino acids and proteins evaluated as corrosion inhibitors

Inhibitor	Environment	Nature of adsorption	Conc.	Method of corrosion monitoring	IE %	Ref.
Glycine	Mild steel/0.5 M HCl	N. A.	N. A.	PDP	53.9%	257
Phenylalanine					74.8%	
Glutamic acid					8.2%	
Glutamic acid with Zn <sup>2+</sup>	Carbon steel/sea water	N. A.	200 ppm glutamic acid with 25 ppm Zn <sup>2+</sup>	WL, EIS, PDP, AFM, SEM	87%	258
Methionine methyl ester (MME) methionine ethyl ester (MEE)	Iron/9 g L <sup>-1</sup> NaCl	Frumkin model	10 <sup>-2</sup> M	PDP	80%	259
Poly(vinyl alcohol-histidine)	Mild steel/1 M HCl	Temkin isotherm/mixed-type inhibitor	0.6% wt	WL, EIS, PDP, SEM	40%	260
Cysteine	Mild steel/1 M HCl	Langmuir	0.1 M	MD, EIS	90.4%	261
Polyspartic acid	Mild steel/0.5 M H <sub>2</sub> SO <sub>4</sub>	N. A.	2000 ppm	WL. PP. EIS. SEM. XPS. FT-IR.	88%	262
Glutamine	Mild steel/1 M HCl	Langmuir	100 ppm	PDP, SEM	96%	263
OPEM	Mild steel/15% M HCl	Langmuir/mixed-type inhibitor	200 ppm	PDP, SEM, EIS	97.5%	264
OPEA					95.5%	
Phenylalanine (PA) + Zn <sup>2+</sup> ions	Carbon steel/Well water	N. A., anodic inhibitor	5 ppm Zn <sup>2+</sup> and PA 150 ppm	WL. PDP. EIS. SEM-EDX.	90%	265
Tryptophan (Try), tyrosine (Tyr), serine (ser)	Low alloy steel/0.2 M ammoniated citric acid	Temkin isotherm	0.06 M	PDP. EIS. EFM. OM.	86%	256
					83%	
					82%	
Tetra- <i>n</i> -butyl ammonium methioninate	Mild steel/1 M HCl	Frundlich/mixed-type inhibitor	1.59 × 10 <sup>-3</sup> M	OCP. PP. SEM-EDX.	95.1%	266
Casein	Mild steel/0.1 M HCl	Langmuir	400 ppm	WL. PDP. EIS. AFM, FTIR SEM-EDX.	96.41	236
Casein	Steel/0.1 mol L <sup>-1</sup> NaOH		9.7 × 10 <sup>-4</sup> M	PDP. EIS	97.76%	267
Gluten hydrolysate	Mild steel/1 M HCl	Physical and chemical adsorption/mixed-type inhibitor	1000 ppm	WL. PDP. EIS, FTIR	96.6%	268
Maize gluten meal extract	Carbon steel/1 M HCl	Langmuir	2000 ppm	PDP. EIS, SEM-EDS	88%	269

to the targeted metal surface by combining and/or boosting their mechanisms. Higher doses may be needed when using an individual inhibitor to reach the necessary level of inhibition. Nevertheless, it can be employed in synergy with another inhibitor to accomplish the necessary inhibiting impact at fewer dosages, saving costs in various applications. Further, the development of novel molecules or complexes amongst the inhibitors may result in synergistic interactions. These complexes can be formed either by the inhibitors interacting with the metal surface or by their chemical interactions with each other. Furthermore, synergism is a useful strategy for boosting inhibitors' suppressive potency and expanding their use in harsh circumstances. It is vital for both real-world use and the theoretical investigation of corrosion inhibitors. As mentioned in eqn (1), a synergism parameter (S1) is frequently employed to assess this impact.<sup>275</sup>

$$S1 = \frac{1 - \theta_{1+2}}{1 + \theta'_{1+2}} \quad (1)$$

The  $\theta_{1+2}$  parameter is estimated by  $=(\theta_1 + \theta_2) - (\theta_1 \times \theta_2)$ , where  $\theta_1$  represents the surface coverage of one employed inhibitor, while  $\theta_2$  is coverage of another inhibitor or other additive, and  $\theta'_{1+2}$  represents the sum of both employed materials. Whereas a value of S1 less than unity implies an antagonistic impact, a value larger than unity implies inhibitory synergism between the employed materials.

#### 4.1 Synergistic impact between inorganic substances

Numerous research studies have consistently shown that achieving the desired level of corrosion inhibition often requires the use of high concentrations of inorganic substances, leading to significant costs. Additionally, the toxicity of some inorganic compounds raised environmental concerns. However, extensive investigation has been conducted in various scientific papers to explore the benefits of utilizing a combination of two or more compounds, Table 5. This synergistic effect has been demonstrated to enhance inhibition efficiency, enabling the usage of lower concentrations of inhibitors compared to employing a single compound even in harsh circumstances. For instance, the combined action of nitrite with phosphate, chromate, zinc, or other inorganic inhibitors has been extensively examined, demonstrating significant synergistic effects. These investigations have found that mixed inhibitors containing nitrite are highly effective, even in the presence of elevated chloride levels.<sup>281,282</sup> The effectiveness matches that of using nitrite as a standalone inhibitor at higher concentrations. Further, growing environmental consciousness regarding the hazardous impact of nitrite ions has led to the need to reduce their usage. To address this concern, the blending of nitrite with non-toxic and eco-friendly inhibitors like molybdate is being pursued to minimize harmful impacts.<sup>58</sup> In one study, the impacts of zinc, nitrite, and molybdate ions on the protection of MS in chloride-containing water were



Table 5 Characteristics of some representative examples of synergistic between corrosion inhibitors

Inhibitor	Environment	Conc.	Method of corrosion monitoring	IE %	Ref.
Sodium nitrite	Carbon steel	2 g L <sup>-1</sup>		65%	58
Sodium nitrite		2 g L <sup>-1</sup>		53%	
Nitrite + molybdate		<2 g L <sup>-1</sup>		93%	
Sodium tungstate + ZnSO <sub>4</sub>	Mild steel/natural seawater	1000 ppm + 300 ppm ZnSO <sub>4</sub>	WL, EIS, PDP, XPS	84.81	66
Zinc aluminium molybdenum orthophosphate hydrate (ZAM)/zinc calcium strontium aluminium orthophosphate silicate hydrate(ZCP)	Mild steel/NaCl	1 g each of ZAM and ZCP	EIS, PDP, electrochemical noise, SEM, EDS	92%	276
Sodium nitrite	Mild steel/3.5NaCl	0.5 M NaNO <sub>2</sub>	WL	10%	277
Potassium chromate		0.5 M K <sub>2</sub> CrO <sub>4</sub>		33%	
Potassium chromate/sodium nitrite		0.5 M NaNO <sub>2</sub> + 0.5 M K <sub>2</sub> CrO <sub>4</sub>		56%	
Phenylalanine (PA) + Zn <sup>2+</sup> ions	Carbon steel/well water	5 ppm Zn <sup>2+</sup> and PA 150 ppm	WL, PDP, EIS, SEM-EDX.	90%	265
Glutamic acid with Zn <sup>2+</sup>	Carbon steel/sea water	200 ppm glutamic acid with 25 ppm Zn <sup>2+</sup>	WL, EIS, PDP, AFM, SEM	87%	258
Zn <sup>2+</sup> /sodium salt of phenyl phosphonic acid (PPA)	Neutral solution containing 60 ppm Cl <sup>-</sup>	300 ppm PPA: 50 ppm Zn <sup>2+</sup>		95%	278
Chitosan + KI	Mild steel/15% H <sub>2</sub> SO <sub>4</sub>	5 g CH + 5 mM KI	WL, DEIS, PDP, AFM, SEM and EDS	97.6	196
Sodium lignosulfonate-zinc acetate (SLZA)	Mild steel/3.5NaCl	500 ppm sodium lignosulfonate + 300 ppm zinc acetate	WL, EIS, PDP, XPS, FTIR, SEM	96%	279
Polyaspartic acid (PASP)	Mild steel/3.0 NaCl	2000 ppm PASP	WL, EIS, PDP, XPS, FTIR, SEM, AFM, MD, QC	56%	45
PASP + Zn <sup>2+</sup>		500 ppm PASP + 1 ppm Zn <sup>2+</sup>		97%	
Xanthan gum (XG)	Mild steel/1 M HCl	1000 ppm	WL, EIS, PDP, SEM	74.8%	208
Xanthan gum (XG) + SDS		1000 + 5		83.17%	
Xanthan gum (XG) + CPC		1000 + 5		75.89%	
Xanthan gum (XG) + TX		1000 + 5		82.31%	
Chondroitin sulfate derived from pig cartilage (CS-PC)		600 ppm		73.93%	
sodium alginate (SA) CS-PC + SA	400 ppm	69.03%			
Tannic acid (TA)	Mild steel/1 M HCl	400 + 400 ppm	PDP, EIS, SEM, QC	96.88	280
Galic acid (GA)		1.0 g L <sup>-1</sup>		91%2	
TA + GA		1.0 g L <sup>-1</sup>		74.5%	
		0.9 g L <sup>-1</sup> TA <sup>-1</sup> : 0.1 g L <sup>-1</sup> GA <sup>-1</sup>		93.3%	

examined.<sup>283</sup> The results demonstrated that molybdate effectively hindered corrosion with pH levels above 6. Similarly, nitrite prevents corrosion at pH levels of 4.5 and above but enhances corrosion below pH 4.5, regardless of the presence of cupric ions. However, when nitrite and molybdate are combined, they served synergistically as inhibitors with or without cupric ions at pH levels of 4.5 and above. This combination also minimized corrosion phenomena in the acidic range between pH 3.0 and 4.5, with a low level of molybdate and high levels of nitrite. The synergistic impact is accomplished by absorbing molybdate which protects the surface passive layer from aggressive anion attacks. To analyze the passive films created on MS during immersion in NaCl medium and high levels of either MoO<sub>4</sub><sup>2-</sup> or NO<sub>2</sub><sup>-</sup>, researchers employed an XPS analysis.<sup>284</sup> The results confirmed that both anions led to the development of nanometer-thick films (approximately 5 nm) on the surface, with Fe<sup>3+</sup> ions being the dominant cation. The analysis suggested that an upper sub-layer consisting of Fe<sub>2</sub>(MoO<sub>4</sub>)<sub>3</sub> was formed, followed by a layer of ferric hydroxide/

oxide, may be γ-Fe<sub>2</sub>O<sub>3</sub>. XPS data from the film created by NO<sub>2</sub><sup>-</sup> inhibitor supported the notion that it mainly comprised materials like γ-Fe<sub>2</sub>O<sub>3</sub>. Thus, the impact of NaNO<sub>2</sub> and Na<sub>2</sub>MoO<sub>4</sub> concentrations on inhibition performance was examined.<sup>58</sup> At a level of 2 g L<sup>-1</sup>, they achieved 65% and 53% inhibitions, respectively, when these inhibitors were employed individually. Interestingly, upon combined use, a synergistic impact was noticed at the same lower levels (2 g L<sup>-1</sup>), with a notable synergism value of 8.6. Moreover, the combination of these inhibitors in a ratio of 1 : 1 at lower levels significantly boosted the performance to 93%.<sup>58</sup>

#### 4.2 Synergistic impact between organic and inorganic substances

The widespread use of organic inhibitors is attributed to their eco-friendly features, cost-effectiveness, and ability to be employed in smaller quantities compared to inorganic inhibitors. As a result, these inhibitors have become the primary focus of research in various fields. However, the effectiveness of



a single organic material is significantly impacted by factors such as the temperature, condition of the metal surface and its surrounding medium, and immersion time. In certain specialized industries, a sole organic agent may not meet the stringent requirements for corrosion prevention. To address this issue, combining organic and inorganic inhibitors, as well as incorporating organic inhibitors with trace cations, alkaline earth salts, halides, or other anions, can significantly boost the anti-corrosion performance and stability of the targeted system, while also minimizing the overall usage of inhibitors.<sup>285,286</sup> As an example, the synergistic mechanism of sodium tungstate and a Mannich base ( $C_{15}H_{15}NO$ ) was examined.<sup>287</sup> Their research revealed that the Mannich base initially attaches to the targeted surface, creating a film owing to its robust adsorption energy. Following this, tungstate ions are incorporated into the defects within the created layer by Mannich base, resulting in a tightly sealed film, as well as forming hydrogen bonds with hydrogen ions, which effectively block corrosive ions from penetrating the adsorption film. This process significantly minimized the existence of corrosive ions near the employed surfaces. In a research, the synergistic impact of sodium silicate and piperazine inhibitors on ST-14 steel was explored.<sup>288</sup> The findings revealed that the combination of these two inhibitors greatly promoted the steel's resistance against corrosion, as demonstrated by PDP and EIS measurements, with improvements of approximately 87% and 76%, respectively. The most effective corrosion inhibition was achieved with a combination of 10–15 ppm sodium silicate and 2 ppm piperazine (PIP). Observing the interaction between the iron oxide layer and inhibitor molecules, it can be inferred that physical adsorption played a more prominent role in the film generation for both PIP and sodium silicate inhibitors. The researchers suggested that oxygen atoms of silica acted as bridges linking piperazine to metal ions at the surface defects. This connection enables the formation of a thicker and more impenetrable film at the anodic sites (as shown in Fig. 8a). Another study showed that the combination of sodium molybdate and benzotriazole (BTA)

resulted in a protective layer consisting primarily of BTA-Fe and  $FeMoO_4$ .<sup>290</sup> This structure enhanced the density of the  $FeMoO_4$  corrosion inhibition film and facilitated the conversion of  $FeOOH$  into a stable  $Fe_2O_3$  compound. Additionally, when the pH levels are maintained between 8.0–10.0, the inhibition performance reached 99%, and the system exhibited high stability and required a low concentration for optimal effectiveness. Furthermore, an inhibitor composed of gluconate, as well as small quantities of molybdate was reported.<sup>289</sup> The synergistic impact between gluconate and molybdate was elaborated (Fig. 8b). PDP measurements revealed that the existence of gluconate made the corrosion of tested metal kinetically and thermodynamically unfavorable, surpassing the impact of molybdate alone. The SEM, FTIR, and XPS analysis revealed that gluconate acted as a bridge between iron and molybdate, leading to the formation of a protective layer that hindered corrosion, as shown in Fig. 6b.

Numerous studies have confirmed that the inclusion of transition metal cations can greatly boost the performance of organic corrosion inhibitors. For instance, the synergistic features of sodium lignosulfonate–zinc acetate (SLZA) in hindering corrosion of employed MS in a 3.5 wt% NaCl was examined.<sup>279</sup> The findings from electrochemical data demonstrated that the joint action of ZA and SL effectively hindered uniform corrosion. The synergistic impact was quantified to be approximately 9, and the overall resistance exceeded 400  $k\Omega\text{ cm}^2$  when both SL and ZA were employed. Moreover, the SLZA system exhibited an impressive inhibition of around 96%. Based on SEM-EDS and XPS analyses, the researchers proposed that the film composed of zinc-containing compounds and SL-based complexes played a critical role in hindering corrosion, as shown in Fig. 8c. In another research, the effectiveness of PASP as an inhibitor was significantly boosted by the inclusion of zinc ions, reaching a performance of 97% at a level of 0.5  $\text{g L}^{-1}$ . By adding  $Zn^{2+}$  the performance of polyaspartic acid was noticeably boosted as it hindered the cathodic sites of the localized corrosion cells.<sup>45</sup> The zinc ions were found to adhere to the

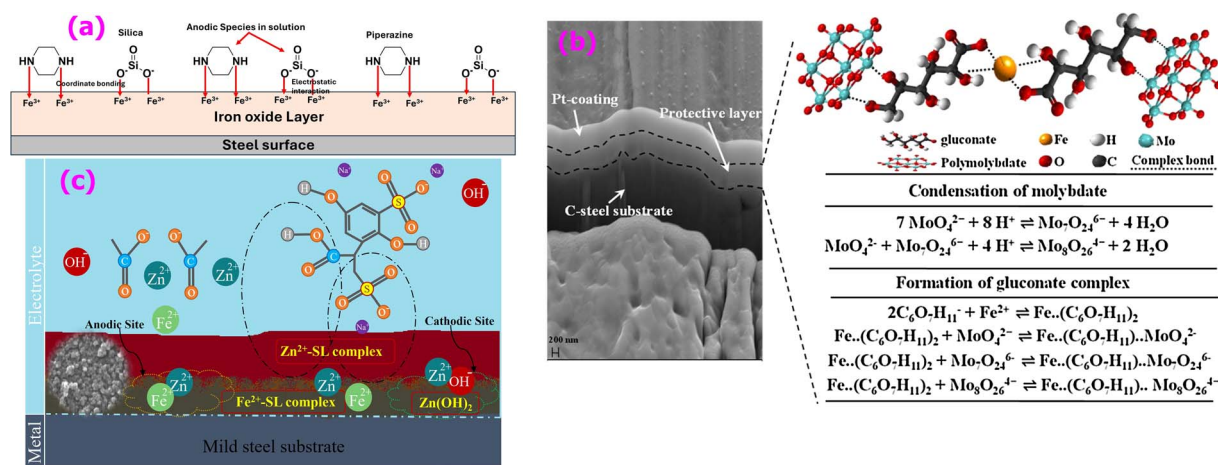


Fig. 8 Schematics of synergistic effects of mixtures of (a) piperazine and silicate, compiled from ref. 288 (b) gluconate and molybdate, reprinted with the permission of ref. 289, copyright 2024; and (c) zinc acetate and sodium lignosulfonate (SL), reprinted with the permission of ref. 279, copyright 2024.



surface, replacing  $\text{Fe}^+$  ions. This led to the inducement of a PASP-Zn complex, which created a protective layer and effectively hindered corrosion. Analysis using AFM and EDX revealed the formation of a thick layer following the inclusion of zinc ions.<sup>45</sup>

Halide ions, especially iodide ions, have been utilized to enhance the performance of organic corrosion inhibitors. The order of synergistic impacts typically follows:  $\text{Cl} < \text{Br} < \text{I}$ , where  $\text{I}^-$  ions exhibit the best synergistic impact, thanks to their larger size (216 pm) and ease of polarizability. The robust electro-negativity of halides allows for the creation of bridges between the metal surface and the positive end of the employed inhibitor. This connection helps to extend their surface coverage, resulting in better protection against corrosion. For instance, The effectiveness of CS and KI additive in inhibiting St37 steel corrosion, in a 15%  $\text{H}_2\text{SO}_4$  medium was examined.<sup>196</sup> The addition of KI significantly augmented the CS inhibitory performance, reaching 92%. PDP and EIS analysis revealed that the CS-KI film was more robust and reflected boosted effectiveness over longer immersion periods. The inhibitory performance of CS declined at elevated temperatures, while the CS-KI combination reflected a boosted trend and achieved its best inhibition of 99.72% at 60 °C. A calculated synergism emphasized that the boosted performance of CS-KI was a result of a synergistic effect.<sup>196</sup> Furthermore, the impact of KI on tannin anticorrosion performance was examined.<sup>291</sup> The findings reflected that adding just 0.025% KI to the tannin solution minimized the anodic current density ( $I_{\text{corr}}$ ) as revealed by electrochemical tests and reflected improved corrosion inhibition performance.

### 4.3 Synergism between organic inhibitors

Numerous investigations have been conducted to look at how combining organic inhibitors impacts the effectiveness of inhibition. In one study, 1000 ppm xanthan gum (XG) exhibited a 74.24% inhibition; however, the addition of low levels of surfactants, namely Triton X-100 (TX), cetyl pyridinium chloride (CPC), and sodium dodecyl sulfate (SDS), marginally boosted the corrosion inhibition efficiency.<sup>208</sup> UV-visible analysis emphasized the creation of a complex between  $\text{Fe}^{2+}$  and XG. Additionally, SEM images reflected distinct morphological changes in the presence of XG and XG-surfactant additives. Moreover, an inhibitor consisting of a combination of sodium alginate (SA) and chondroitin sulfate obtained from pig cartilage (CSPC) was developed.<sup>212</sup> The synergistic impact of these two polysaccharides on corrosion inhibition under 1 M HCl was investigated. The results suggest that the CSPC and SA mixture exhibit a robust impact, outperforming individual inhibitors (with performance of 95.18% compared to 72.78%). Furthermore, quantum mechanical calculations demonstrated that the bond creation between tested metal and tested inhibitors occurred *via* charge transfer between the CSPC, SA and iron with evidence of partial retro-donation bonding type. Furthermore, the synergism of a combination of *Anacardium occidentale* (cashew gum) and *Acacia Senegal* (Arabic gum) in corrosion protection of MS study was elaborated.<sup>292</sup> The inhibitor

adsorption followed the Langmuir isotherm, reflecting a chemisorption behavior between the metal surface and the gums. This was emphasized by the values of the free  $\Delta G$  of  $-16.47$  and  $-15.61 \text{ kJ mol}^{-1}$  at 303 K and 333 K, respectively. Dipole moment, molecular weight, and  $E_{\text{HOMO}}$  were found to affect the gum mixture binding energy, and GC-MS was used to assess the gum constituent's hydrophobicity, which was shown to be a contributing factor to its efficacy as an inhibitor in acidic environments.<sup>292</sup>

In summary, mixed corrosion inhibitors are a suitable choice when strict corrosion inhibition performance is needed in challenging processing environments. Among the available options, organic/organic systems offer the advantage of being non-toxic and biodegradable, making them environmentally preferable over organic/inorganic and inorganic/inorganic systems. However, it is crucial to mention that even though the amounts of inorganic components used in these mixtures is small, they have the potential to bioaccumulate to dangerous levels over time.

### 4.4 Synergistic corrosion-inhibition mechanisms

Synergistic corrosion inhibition mechanisms exhibited by inhibitors combinations can work *via*, the gaps-filling, bond formation between different inhibitors, cooperative and complementary adsorption, and mutual interactions of inhibitors in the bulk solution. The gaps-filling approach stipulates that different inhibitor molecules act in a complementary manner, where one type of inhibitor component fills the gaps and defects within the protective film established by the other inhibitor, thereby synergistically enhancing the overall corrosion protection. The process starts with the adsorption of the organic inhibitor compound, such as Mannich bases or polysaccharides, onto the metal surface to form a primary adsorption layer, which serves as the foundation for the development of the protective film. In a later stage, the inorganic inhibitors begin to incorporate or bind into the organic inhibitor layer while filling the gaps and defects present within the organic film, creating a more uniform and complete surface coverage.

Furthermore, the inorganic inhibitor can interact with the organic inhibitor film, leading to the formation of complex metal-organic compounds. These complex compounds contribute to the enhanced stability and protective properties of the passive layer, making it more compact, dense, and resistant to the penetration of corrosive species. The complementary adsorption and filling of the film by various inhibitor components create a synergistic effect, wherein the weaknesses or deficiencies of one inhibitor type are compensated by the strengths of the other.

On the other hand, cooperative adsorption is another key mechanism for the synergistic effect of mixed organic corrosion inhibitors. In this mechanism, the two inhibitors adsorb on the metal surface in a sequential manner, where one inhibitor first chemisorbs onto the surface, creating a foundation for the second inhibitor to then adsorb on top of the initial layer. This cooperative adsorption can lead to the formation of a more compact, stable, and protective film on the metal surface, resulting in enhanced corrosion inhibition. The synergistic



effect arises from the combined protective action of the two inhibitors, where they work in harmony to provide better coverage and protection compared to individual inhibitors.

However, complementary adsorption is another prospective mechanism for the synergistic inhibition effect, where the two inhibitors may preferentially adsorb on different sites of the metal surface, effectively covering a larger area and providing more comprehensive protection. For instance, one inhibitor may predominantly adsorb on the anodic sites, while the other inhibitor adsorbs on the cathodic sites, leading to the inhibition of both the anodic and cathodic corrosion processes. Furthermore, inhibitors mutual interactions in the bulk solution can contribute to the synergistic inhibition effect. These mutual interactions may include the formation of complex species or micelles, which can enhance the transport and adsorption of the inhibitors onto the metal surface. This improved availability and adsorption of the inhibitors on the metal surface can result in a synergistic inhibition of corrosion. Another mechanism of synergistic inhibition involves the cooperative adsorption of the mixed inhibitors on the metal surface. The adsorption of one inhibitor can modify the surface properties, creating more favorable sites for the adsorption of the other inhibitor. Additionally, the presence of multiple inhibitors can promote the formation of insoluble metal–inhibitor complexes on the metal surface. These complex species can act as a physical barrier, blocking the access of corrosive species to the metal surface and effectively inhibiting the corrosion process. In some cases, the synergistic effect may involve the combined action of anodic and cathodic inhibitors.

In summary, synergistic corrosion inhibition results in a more robust and impermeable protective barrier against corrosion, making the hybrid corrosion inhibitor system particularly ideal for harsh processing environments where strict corrosion inhibition performance is required. In addition to mutual interactions between inhibitors in the bulk solution that promote the inhibitors diffusion towards the metal surface, the underlying mechanisms governing the synergistic effect of hybrid/composite corrosion inhibitors involve complex interactions at the molecular level, such as gaps-filling, cooperative and complementary adsorptions, impermeable film formation, and the creation of inorganic–organic and organic–organic inhibitors' bonding. The nature and concentration of the inhibitors, the metal–environment system, and other variables can all affect the precise mechanism underlying the synergistic impact in mixed corrosion inhibitor systems. However, in most cases, multiple mechanisms work cooperatively.

## 5. Inhibition performance validation

### 5.1 Weight loss

The corrosion inhibitor's performance is a critical aspect of corrosion mitigation strategies.<sup>293–295</sup> Weight loss (WL) methods are commonly utilized to determine the effectiveness of corrosion inhibitors in various environments. WL analysis is a relatively simple and cost-effective method compared to other advanced techniques and provides both a quantitative measure of the corrosion rate, and a realistic simulation of the actual

corrosion conditions in a particular application. The WL method primarily involves exposing metal specimens to the corrosive environment under controlled conditions over a specific period.<sup>45,293</sup> The typical procedure involves a series of steps for the preparation and analysis of the metal sample. Initially, the sample is sanded employing emery paper to prepare it for the experiment. After that, it is dried, washed with double distilled water, and degreased with acetone. Scale with  $\pm 0.01$  mg sensitivity is employed to estimate the specimen's weight for the measurement. The recommended procedure calls for submerging the metal sample in various test solutions for a certain amount of time at a predetermined temperature. This is done with and without different concentrations of inhibitors. Following the experiment, the material is dried, cleaned, and weighed one more time.<sup>294</sup> To ensure precision, the experiments should be executed in triplicate, and the average values should be considered. The inhibition efficiency  $\eta_w$  (%), surface coverage ( $\theta$ ), and corrosion rate (Cr) can be calculated using the following equations:<sup>296,297</sup>

$$\theta = \frac{W_o - W_i}{W_o}$$

$$\eta_w = \left( \frac{Cr_0 - Cr_1}{Cr_0} \right) \times 100$$

$$Cr = \frac{(W_0 - W_1)}{(A \times t \times \rho)}$$

For instance, the WL method was used to assess the corrosion rate of MS under acidic conditions, in the presence and absence of the corrosion inhibitor.<sup>293</sup> Notably, they achieved a high inhibition efficiency of 89.5% when using 400 mg L<sup>-1</sup> inhibitor. In another study, WL monitored the inhibition performance of zinc ions and PASP at varying concentrations, where the addition of 2 mg L<sup>-1</sup> zinc ions minimized WL compared to the use of PASP alone.<sup>45</sup> Moreover, another investigation explored the impact of temperature on inhibition efficacy using the WL approach.<sup>295</sup> The study observed that higher temperatures minimized the adsorption of PESA onto the examined metal surfaces. Consequently, this resulted in minimized surface coverage and subsequently lowered efficiency. Similarly, because of severe etching and degradation or desorption of inhibitor molecules, higher temperatures caused a reduction in surface coverage.<sup>298</sup>

Overall, the WL method plays a crucial role in evaluating the performance of corrosion inhibitors. It provides valuable insights into the effectiveness of inhibitors under specific conditions, aiding in the design and optimization of corrosion protection strategies for various industrial applications.

### 5.2 Surface analysis

SEM is a powerful imaging technique that provides high-resolution images of the sample surface.<sup>299–301</sup> It utilizes a focused electron beam to scan the sample, generating



secondary electrons, backscattered electrons, and characteristic X-rays.<sup>286,302–304</sup> The secondary electron images obtained from SEM provide detailed information about the surface morphology, such as surface roughness, the presence of cracks, pits, or other corrosion features.<sup>305–307</sup> Additionally, backscattered electron imaging can reveal compositional variations on the surface, highlighting the presence of corrosion products or the distribution of the inhibitor.<sup>302</sup> EDX is used in conjunction with SEM to provide elemental analysis of the sample.<sup>308–311</sup> It detects characteristic X-rays emitted by the atoms in the sample when excited by the electron beam. In the context of evaluating corrosion inhibitors, EDX can help determine the effectiveness of the inhibitor in reducing the concentration or presence of corrosive elements, such as chloride ions or oxygen.<sup>312,313</sup> By comparing the elemental composition of metal surfaces with and without the inhibitor, changes in corrosion product formation or inhibitor adsorption can be assessed.<sup>314,315</sup>

For instance, SEM images of steel submerged in the solution without corrosion inhibitors in simulated concrete pores with chlorine revealed many pits on steel surface, revealing that the steel has been severely degraded by the  $\text{Cl}^-$  present.<sup>316</sup> Similarly, SEM pictures of the steel reveal signs of severe corrosion and comparatively extensive surface fractures.<sup>317</sup> The majority of surface flaws were the sites where corrosion started, resulting in the production of corrosion products that most likely covered specific localized regions of the whole material surface. These corrosion byproducts created a porous layer that encouraged more corrosion, leading to a serious assault with surface fractures and long void.<sup>317</sup> Furthermore, the formation of an inhibitory film on MS surface and the thickening of this film were confirmed by SEM images, which reflected the adsorption of PASP and its interaction with zinc ions.<sup>45</sup> Another research also utilized SEM images to analyze the effect of chitosan-5-HMF on the MS surface after exposure to 1 M HCl, as illustrated in Fig. 9a–d.<sup>318</sup> Without any inhibitors, the surface of MS exhibited uneven damage, characterized by the formation of pits of various sizes. Further, significant alterations were noted when mild steel was placed in a solution containing  $200 \text{ mg L}^{-1}$  of chitosan, as shown in Fig. 7b. Notably, the formation of pits and voids was eliminated. Conversely, when using the inhibitors chitosan-5-HMF1 and chitosan-5-HMF3 (Fig. 7c and d), the surface of the matrix became notably smoother and improved. This suggests that the adsorption of chitosan-5-HMF species hindered the contact between mild steel and the corrosive electrolyte, resulting in improved corrosion resistance. This inhibitory effect is further evidenced in the contact angle images. In another study, an EDX mapping examination revealed a significant presence of Cl in the affected area owing to its corrosive activity.<sup>319</sup> Conversely, a reduction in chloride signal owing to the generation of a protective layer on the MS was observed and this protective layer effectively hindered chloride ions from reaching the active sites of the MS.<sup>317</sup> Moreover, the proportion of oxygen atoms in the blank solution, which corresponds to the rate of oxide formation on the MS surface, was found to be 10.07%.<sup>320</sup> However, following the inhibitor's addition, this ratio minimized significantly to 2.87%

owing to the protective nature of adsorbed octacalcium phosphate (OCP) inhibitor molecules.

To gain quantitative insights into the surface morphology of metals, the utilization of AFM is necessary.<sup>216</sup> AFM allows for the examination of utilized specimen topography in a 3D fashion. By employing AFM, one can evaluate the surface topography of a sample and observe shifts in roughness resulting from corrosion or the presence of inhibitors.<sup>321</sup> For both protected and unprotected samples, the average roughness values, expressed in nanometers and root mean square (RMS) are calculated and compared.<sup>322</sup> The quantitative investigation demonstrates that the maximum peak-to-peak height values and the RMS roughness of the inhibitor-coated metal surface are smaller than those of the untreated metal surface.<sup>323,324</sup> For instance, the initial roughness (Ra) measurement of polished mild steel was 7.96 nm (Fig. 9e). However, immersion in a 15% HCl solution without any inhibitor for 24 hours resulted in a significant increase in Ra to 973 nm (Fig. 9f). In the presence of SA, SA-g-PMMA/ $\text{Fe}_3\text{O}_4$ , and SA-g-PMMA/ $\text{TiO}_2$ , the Ra values were measured at 414 nm, 282 nm, and 144 nm, respectively (Fig. 9g–i). Based on these findings, the SA-g-PMMA/ $\text{TiO}_2$  proved to be the most effective inhibitor, as it produced the smoothest surface. This suggests the formation of a protective layer or adsorption film on the metal surface, highlighting its superior inhibitory properties compared to the other inhibitors examined.<sup>216</sup> Similarly, it was found that the MS that corroded in soft water had a rough, non-uniform appearance with big, deep holes; however, the MS surface was smoothed up after adding the inhibitor.<sup>297</sup>

XPS is a powerful approach employed in evaluating corrosion and corrosion inhibitors. When a high-energy X-ray beam is directed at a material's surface, photoelectrons are released, which is how XPS analysis works. These photoelectrons carry data about the elemental composition and chemical states of the atoms near the surface.<sup>301</sup> XPS is useful in determining the chemical composition of the corrosion byproducts that are generated.<sup>325,326</sup> XPS can also provide information about the chemical states of these elements.<sup>146</sup> For example, iron may exist in different oxidation states as Fe(0), Fe(II), or Fe(III) species.<sup>327,328</sup> By analyzing the binding energy of the iron photoelectron peaks, one can determine the oxidation state and the presence of different iron species on the corroding surface. By comparing the XPS spectra of inhibited and uninhibited surfaces, differences in the chemical composition and bonding states of the elements can be observed. For example, the presence of a corrosion inhibitor may result in the formation of a protective layer, which is evident from the XPS spectra showing new peaks or shifts in the binding energies associated with oxygen or other relevant elements.<sup>329,330</sup> To confirm the adsorption of chemically modified hydroxyethylcellulose (CHEC) on the electrode surface, XPS analysis was conducted.<sup>331</sup> Fig. 9j displays the high-resolution plots and broad scan. The O and C bands exhibited a significant existence in the MS specimen immersed in the 15% HCl medium with  $50 \mu\text{M}$  CHEC, which is expected as they are major constituents of the inhibitor structure. The O 1s peaks at 531.74 eV and 533.22 eV correspond to the C–O and C–OH groups, respectively, that are present in



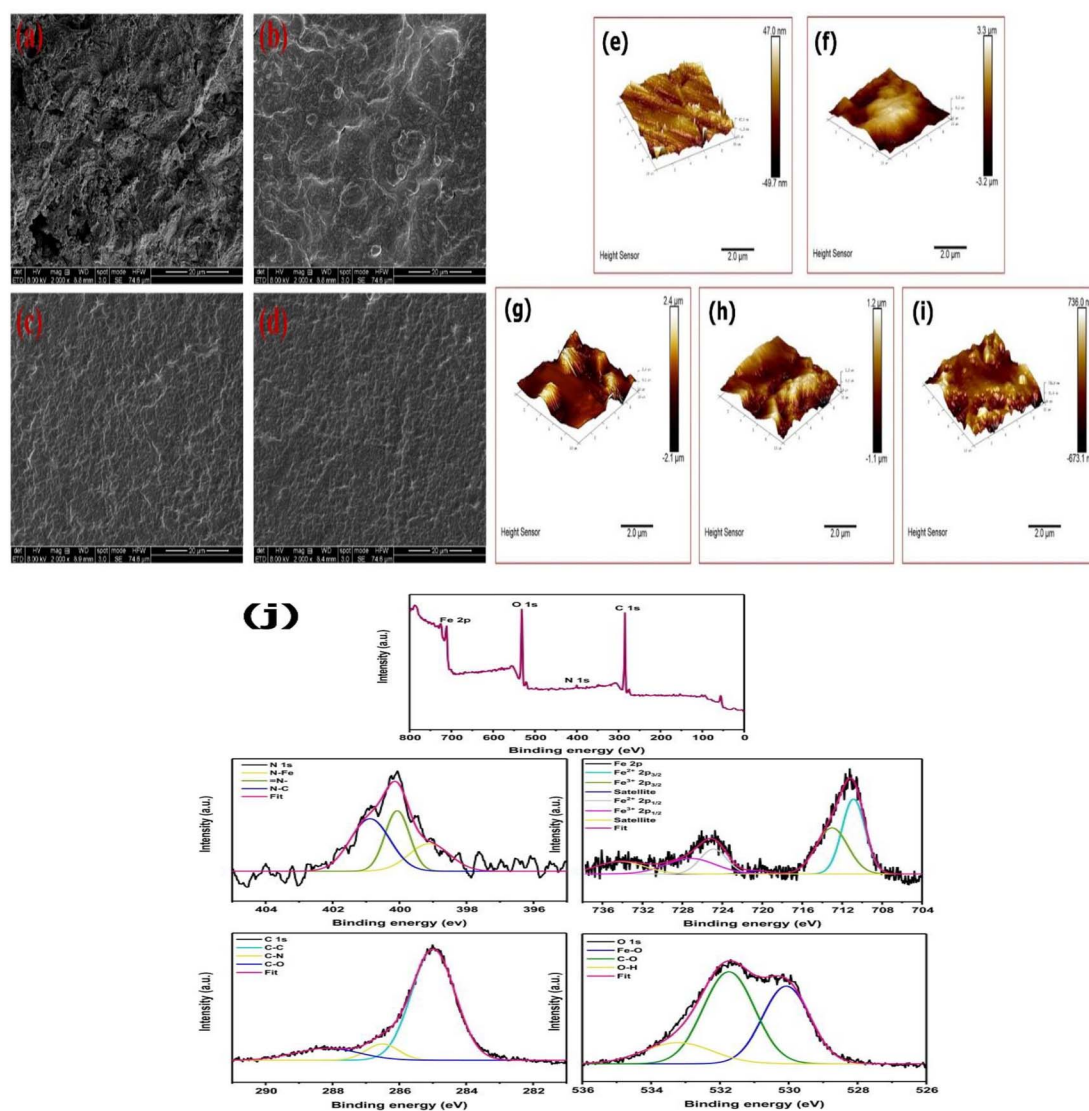


Fig. 9 SEM images of mild steel (a) 1 M HCl, (b) chitosan, (c) chitosan-5-HMF1 and (d) chitosan-5-HMF3, reprinted with the permission of ref. 318, copyright 2024, Elsevier. AFM images of mild steel surface: (e) polished, (f) blank, in presence of; (g) SA, (h) SA-g-PMMA/Fe<sub>3</sub>O<sub>4</sub>, (i) SA-g-PMMA/TiO<sub>2</sub>.<sup>183</sup> (j) XPS wide scan and high-resolution scans of Fe 2p, C 1s, O 1s, and N 1s for MS in the 15% HCl solution containing 50 μM of CHEC, reprinted with the permission of ref.<sup>283</sup>, copyright 2024, Elsevier.

the CHEC structure. The C 1s peak at 288.15 eV indicates the presence of C–O, while it is located at 285.89 eV in the uninhibited systems. The binding of inhibitor molecules on the metal surface is responsible for the C 1s peak's shift towards higher energy. Furthermore, XPS examination of the CHEC system indicates the existence of N at 399 eV, which supports interactions between carbon (C), iron (Fe), and N. These results provide compelling evidence for the efficient adsorption of CHEC molecules onto the steel surface, which blocks active sites and inhibits corrosion. The nitrogen heteroatom and the accessible orbitals in the iron's atomic structure share electron pairs during the chemical adsorption process.<sup>331</sup> Furthermore, XPS demonstrated that the adsorption of various gum-based inhibitors on MS surface involved both chemisorption and physisorption.<sup>294</sup> Similarly, the XPS analysis supports the conclusion that the adsorption of GAMo, GAMau, and GASE on

the MS surface involves both physisorption and chemisorption.<sup>294</sup> The XPS results provide strong evidence for the effective adsorption and outstanding inhibition properties of chitosan Schiff base (CS-FGA) molecules on the M.S. surface. The N 1s spectra clearly exhibit two distinct adsorption peaks, with the peak at 399.1 eV indicating the presence of N–Fe bonds. This finding further confirms the chemical adsorption between M.S. and CS-FGA.<sup>39</sup>

### 5.3 Electrochemical analysis

**5.3.1. Potentiodynamic polarization analysis.** Potentiodynamic polarization (PDP) plots, commonly referred to as Tafel curves, serve as a vital tool in assessing corrosion rates and studying inhibition mechanisms. An effective approach in corrosion analysis involves the rate of cathodic reduction and



anodic oxidation reactions may be ascertained using these graphs. The equivalent current density may be found by prolonging the linear portions of these curves until they meet. Utilizing the Tafel extrapolation method, crucial parameters such as cathodic Tafel slope ( $\beta_c$ ), corrosion potential ( $E_{\text{corr}}$ ), anodic Tafel slope ( $\beta_a$ ), and corrosion current density ( $I_{\text{corr}}$ ) can be derived. These parameters provide crucial insights into the nature of corrosion and aid in the analysis of inhibition mechanisms. When a corrosion inhibitor is present, it alters the polarization behavior of the metal electrode. In the case of an effective inhibitor, the polarization curves obtained in the presence of the inhibitor will exhibit a shift towards more positive (less active) potentials compared to the curves obtained without the inhibitor. This shift indicates a reduction in the corrosion rate and an increase in the protection efficiency. For instance, the impact of different concentrations of a specific PIL (imidazolium-derived polymeric ionic liquid) inhibitor on the corrosive behavior of MS specimens was examined under an acidic medium.<sup>332</sup> Tafel plots were used to analyze the cathodic and anodic current densities in the absence and presence of the PIL. The findings reflected a notable decline in both current densities as the concentration of the PIL inhibitor rose. This suggests that the PIL inhibitor can influence both cathodic and anodic reactions, thus affecting the overall corrosion process. Furthermore, the  $E_{\text{corr}}$  changed to greater negative values in response to the PIL inhibitor's dominant cathodic inhibition. In another investigation, the addition of PASP to a NaCl solution caused the corrosion potential to move to the positive side. Thus, PASP essentially inhibits the anodic process meanwhile doesn't significantly affect the cathodic reaction.<sup>45</sup> Similarly, the utilization of an AS inhibitor results in a significant change in the corrosion potential values ( $E_{\text{corr}}$ ), causing them to shift in a positive direction towards nobility.<sup>333</sup> In a separate investigation, the analysis of PDP data demonstrated that the introduction of Chitosan-acrylic acid-poly succinimide terpolymer caused a shift in  $I_{\text{corr}}$  values to lower levels, demonstrating the inhibition of carbon steel corrosion by the existence of CTS-AA-PSI. At higher levels (500 mg L<sup>-1</sup>), the increased amount of CTS-AA-PSI molecules resulted in enhanced coverage of the carbon steel surface, leading to a robust inhibition performance (77.84%). Furthermore, higher dosages of CTS-AA-PSI were noticed to shift  $E_{\text{corr}}$  towards more positive values and greatly minimize the corrosion rate. During this process, the value of  $\beta_c$  gradually minimized from 398.3 mV dec<sup>-1</sup> (blank) to 79.2 mV dec<sup>-1</sup> (500 mg L<sup>-1</sup>), while  $\beta_a$  minimized from 81.7 mV dec<sup>-1</sup> (blank) to 50.1 mV dec<sup>-1</sup> (500 mg L<sup>-1</sup>). Importantly, the difference in  $\Delta E_{\text{corr}}$  between the uninhibited and inhibited samples was less than 85 mV, demonstrating that CTS-AA-PSI predominantly served as a mixed-kind agent.<sup>334</sup> Fig. S4† illustrates a remarkable decline in the current densities when sucrose derivative corrosion inhibitor (CHEC) is present at all temperatures. Additionally, the  $E_{\text{corr}}$  movement according to the medium temperature reflects the significant influence of temperature on the inhibitory effect of CHEC.<sup>331</sup>

**5.3.2. Electrochemical impedance spectroscopic analysis.** EIS examines the electrical features of a material by applying alternating current (AC) signals and a range of frequencies are

utilized to obtain a spectrum.<sup>335,336</sup> Typically, EIS assessments are carried out using a standard three-electrode electrochemical cell setup. This setup consists of the working electrode (WE), counter or supplementary electrode (CE), and reference electrode (RE). The WE represents the metal sample under test.

Impedance spectroscopy is employed to determine the double-layer capacitance ( $C_{\text{dl}}$ ) and the resistance to charge transfer ( $R_{\text{ct}}$ ).<sup>337</sup> The inhibition performance can then be estimated using these parameters. Effective adsorption of the inhibitor is demonstrated by an enhancement in  $R_{\text{ct}}$  and a minimization in  $C_{\text{dl}}$  as the inhibitor amount is increased.<sup>73</sup> The impedance modulus ( $|Z|$ ) represents the overall resistance to the electrochemical processes occurring at the metal–solution interface, and a higher  $|Z|$  value indicates better corrosion inhibition. The phase angle ( $\theta$ ) provides information about the nature of the electrochemical processes, such as the presence of capacitive or inductive behavior. The EIS data is typically presented in the form of Nyquist and Bode plots, which provide a visual representation of the electrochemical impedance characteristics. The Nyquist plot shows the imaginary component of the impedance ( $Z''$ ) versus the real component ( $Z'$ ), while the Bode plot shows the logarithm of the impedance modulus ( $|Z|$ ) and the phase angle ( $\theta$ ) as a function of the logarithm of the frequency. By comparing the EIS data between the uninhibited and inhibited systems, the effectiveness of the corrosion inhibitor can be evaluated. Typically, the  $R_{\text{ct}}$  value increases, the  $C_{\text{dl}}$  value decreases, and the  $|Z|$  value increases in the presence of an effective corrosion inhibitor, indicating an improvement in the corrosion inhibition performance.

To further analyze the EIS data and gain a better understanding of the corrosion inhibition mechanism, an equivalent circuit model can be employed. The choice of the equivalent circuit model depends on the specific system and the processes occurring at the metal–solution interface. The equivalent circuit model consists of various electrical elements, such as resistors, capacitors, and inductors, which represent the different electrochemical processes and the characteristics of the inhibitor film. By fitting the experimental EIS data to the equivalent circuit model, the values of the circuit elements can be obtained, providing insights into the inhibition mechanism and the changes in the interfacial properties due to the presence of the corrosion inhibitor. Overall, the EIS analysis together with the Nyquist and Bode plots, and the use of equivalent circuit modeling, is a powerful tool for evaluating the performance and understanding the mechanisms of corrosion inhibitors.

For instance, as shown in Fig. S5a and b,† EIS was utilized to examine the electrochemical features of the MS surface in both blank and Cs-g-L-arginine containing solutions.<sup>338</sup> The Nyquist plot demonstrated a semicircle, with greater diameters noticed in the presence of Cs-g-L-arginine compared to the blank solution. Additionally, the size of the semicircle increased as the inhibitor's concentration rose. This demonstrates that Cs-g-L-arginine exhibits significant resistance to charge movement compared to the unprotected MS surface in the blank solution, attributed to its adsorption onto the Cs-g-L-arginine surface.<sup>338</sup>



## 5.4 Computational studies

Unlike the time consuming and equipment-intensive nature of experimental measurements, computational techniques provide a versatile and efficient means of evaluating the effectiveness of inhibitors. By analyzing the structural properties of corrosion inhibitors, computational approaches offer valuable insights into their potential impact. This predictive capability is particularly advantageous as it allows for the assessment of organic molecules' corrosion-inhibiting performance even before conducting time-consuming and resource-intensive experimental tests. The power of computational analysis lies in its ability to facilitate the design and development of efficient inhibitors. Through the utilization of computer software, specifically density functional theory (DFT), researchers can estimate reactivity indices and establish quantitative structure–activity relationships (QSAR). This allows for a systematic understanding of how different molecular structures correlate with inhibitor performance. Moreover, atomistic, and molecular simulations, including Monte Carlo (MC) and Molecular Dynamics (MD) simulations play a vital role in providing detailed insights. These simulations provide a deeper understanding of the likely orientations of inhibitor adsorption on the metal surface under investigation. By visualizing these interactions at the atomic and molecular levels, researchers can gain crucial information to guide the design of corrosion inhibitors with enhanced effectiveness.

**5.4.1. Quantum mechanical calculations.** A popular computer modeling approach to analyzing chemical characteristics, chemical processes, electronic structure, and charge distribution, is called density functional theory (DFT).<sup>13,175,339</sup> The frontier molecular characteristics of inhibitor molecules, namely the highest occupied molecular orbital (HOMO), the energy gap ( $\Delta E_{\text{gap}}$ ), and the lowest unoccupied molecular orbital (LUMO), are intimately related to their capacity to adsorb to metallic surfaces. DFT calculations offer valuable quantum chemical features such as  $E_{\text{HOMO}}$ ,  $E_{\text{LUMO}}$ , electron density,  $\Delta E_{\text{gap}}$ , electrostatic potential (ESP), and the quantity of migrated electrons ( $\Delta N$ ). Determining  $\Delta N$  involves employing Koopman's theorem, which relies on several parameters including electron affinity ( $A$ ), chemical softness ( $\sigma$ ), absolute chemical hardness ( $\eta$ ), electronegativity ( $\chi$ ).<sup>340</sup> Electrons tend to migrate from a system with lower electronegativity ( $\chi$ ) to one with higher electronegativity until a condition of equilibrium is reached when considering electronegativity.<sup>341</sup> An essential aspect when evaluating the stability and reactivity of molecules is absolute hardness ( $\eta$ ), as hard molecules were shown to have a significant energy gap and a limited electron-donating ability. Conversely, soft molecules possess a small energy gap and a significant ability to donate electrons, thus making them more reactive compared to their harder counterparts. Moreover, an increased dipole moment strengthens the adsorption of the inhibitor onto the metal surface, thus facilitating the process of inhibition.<sup>341</sup> Therefore, highly effective inhibition mechanisms generally exhibit elevated softness,  $E_{\text{HOMO}}$ , and dipole moment values, alongside lower electronegativity,  $E_{\text{LUMO}}$ , and hardness values.<sup>342</sup> For instance, sodium oleate (SO), and calcium

lignosulfonate (CLS) were evaluated as corrosion inhibitors.<sup>343</sup> The sulfonate groups of the CLS molecule, which functioned as electron donors, were the main contributors to the HOMO and LUMO distributions at the end of the chain, according to quantum chemical analysis. On the other hand, sites for electron acceptance were supplied by the lignin functional group, sinapyl alcohol monomer. The lengthy carbon chain's center and the chain end of the oleic acid group were home to the SO-inhibitor molecule's HOMO and LUMO, respectively. According to the  $E_{\text{HOMO}}$  and  $E_{\text{LUMO}}$  values, CLS outperformed SO inhibitor.<sup>343</sup> In another investigation, the TTA inhibitor exhibited a dispersed concentration of electron density in the middle area of its structure, which included heteroatoms like O, S, and N.<sup>344</sup> On the other hand, TTA's LUMO electron density is dispersed on both sides of the core triazole ring, suggesting that these particular molecular regions are in charge of absorbing electrons from the iron surface. The HOMO and LUMO electrons serve crucial roles in the electron donation and acceptance processes involved in the adsorption processes onto the Fe surface. The TTA inhibitor may adsorb onto the iron surface as evidenced by its strong ionization potential values and very weak electron affinity. The TTA inhibitor is predicted to have high adsorptive qualities on the Fe surface due to its high chemical softness and low hardness. Furthermore, TTA's important capacity to donate electrons to the Fe (110) surface is shown by the fraction of transferred electrons ( $\Delta N$ ) of TTA [ $\Delta N$  (TTA) = 0.0502].<sup>344</sup> Similarly, DFT calculations was employed for various type of *Boswellia serrata* gums namely xylose, arabinose, galactose, and glucuronic acid. The LUMO and HOMO iso-surfaces were noticed to be distributed over the heteroatoms and rings, this reflects that these regions are the adherent sites for the inhibitor molecules.<sup>341</sup> Positive values for quantum parameters imply that molecules are inclined to transmit electrons to the target surface. High inhibition and reactivity abilities of the molecules are shown by lower  $\Delta E$  values as well. When compared to the remaining compounds, xylose demonstrated greater reactivity.<sup>341</sup>

**5.4.2. Molecular dynamics (MD).** Molecular dynamics (MD) is a tool that allows us to study the behavior of atoms and molecules over time. In the context of adsorption, MD modeling provides valuable insights by simulating the interactions among metal surface and adsorbate molecules. One important aspect that MD modeling can assess is the orientation of the molecules on the metal surface.<sup>175,345,346</sup> How the molecules are positioned and aligned relative to the metal surface strongly influences their adsorption features. For instance, when an inhibitor molecule lies flat on the metal surface, it covers a larger region, promoting the chances of binding to active sites and granting a protective layer.<sup>231,347,348</sup> In contrast, if the inhibitor molecule adopts a vertical or non-planar orientation, its coverage on the metal surface may be minimized, limiting its effectiveness as an adsorbate. In MD simulations, the term “adsorption energy,” which is also referred to as “interaction energy,” represents the amount of energy needed or released when a group of inhibitor molecules adhere to a metallic surface. This energy is crucial to understanding the underlying mechanism of adsorption. Several key factors, namely inhibitor



valence, electronegativity, and reactive site coordination, are important variables in influencing the energy associated with adsorption.<sup>349,350</sup> The estimation of energy can be expressed as follows:<sup>351</sup>

$$E_{\text{interaction}} = E_{\text{total}} - (E_{\text{metal+solution}} + E_{\text{molecule}})$$

where  $E_{\text{metal+solution}}$  signifies the energy of the cell in the absence of any retarding substance. On the other hand,  $E_{\text{molecule}}$  stands for the energy of the applied molecules of inhibitor when it exists on the surface. Lastly,  $E_{\text{total}}$  represents the collective energy of the simulated system. A negative energy demonstrates a spontaneous and stable adsorption operation. This reflects that the inhibitor molecules are attracted to the metal surface, initiating various chemical, physical, or combined adsorption forces. A more potent inhibitory performance is achieved through increased adsorption capacity, leading to a more substantial release of energy (illustrated by a larger negative value).<sup>36</sup> The energy required to bind various systems consists of several factors including dissociation energy, electron binding energy, gravitational binding energy, and atomic binding energy. In metal surfaces, inhibitor molecules have a crucial impact on bond dissociation energy as chemical bonds are formed and broken constantly. The strength of the attraction between the inhibitor molecule and the metal has a direct effect on the interaction energy. A higher value signifies stronger bonding and increased inhibition efficiency. As a result, the  $E_{\text{binding}}$  can be calculated by taking the reciprocal of the  $E_{\text{interaction}}$  to determine its magnitude. MD simulations have found widespread application in exploring the interaction among surfaces and inhibitor molecules within various electrolytic environments. For instance, MD simulations extensively examined various surfactants-based inhibitors.<sup>352</sup> The findings from these simulations reflect a notable attraction of the target surface to the benzene ring of inhibitor, with the ring often aligning parallel to the surface. This behavior can be reasonably explained by the interaction between  $\pi$ -electrons and the metal d-orbitals. Furthermore, the adsorption features of two variants of pyridine-carboxaldehyde thiosemicarbazone (PCT), specifically 2-PCT and 4-PCT, on mild MS was examined by MD simulations that showed that both 2-PCT and 4-PCT exhibited nearly horizontal direction during the adherence process.<sup>353</sup> Furthermore, the  $\pi$ - and non-bonding electrons of the pyridine ring, along with the nitrogen and sulfur atoms of thiosemicarbazone, actively engaged in electron acceptance and a donation from the targeted metal surface. The estimated binding energies were determined to be 85.52 kcal mol<sup>-1</sup> for 2-PCT and 83.39 kcal mol<sup>-1</sup> for 4-PCT. Furthermore, an MD study examined the behavior of amphiphilic surfactant inhibitors and revealed that these molecules adhered to the metal surface in a specific arrangement, where the inhibitor's polar heads and hydrophobic tails alternate, resulting in the formation of a cohesive and uniform adherent layer.<sup>354</sup> Consequently, this process gives rise to two distinct binding energies for nitrogen atoms. The first category of molecules showcases electrostatic interaction between the metal surface and the nitrogen atom (head orientation onto the surface). On the other hand, the

second category of molecules experiences negligible surface interaction, as the head group is oriented towards the bulk medium. Furthermore, examined the adsorption patterns of 3-phenyl-1,2,4-triazole-5-thione (PTT) onto low-carbon steel was examined, focusing on the Fe(110) surface, the most stable facet of this body-centered cubic metal.<sup>355</sup> Two simulated media were employed: PTT/NaOH/Fe(110) related to a non-corrosive medium, and PTT/NaOH/NaCl/Fe(110) corresponding to a corrosive medium, as illustrated in Fig. S6a.† Analyzing the adsorption configurations of the studied molecule in both media reflected that it aligned horizontally to the metal surface, offering significant surface protection. Additionally, the investigation demonstrated that the existence of NaCl caused a decrease of around 10% in  $E_{\text{binding}}$ . This reduction highlights the detrimental impact of Cl<sup>-</sup> ions on the protective film of the molecule on the metal surface. Furthermore, MD study of the inhibitor's binding with MS in a 1 M HCl solution was performed.<sup>351</sup> As shown in Fig. S6b,† the final arrangements of the *Lavandula Mairei* Humbert extract (LM) inhibitor are illustrated after achieving equilibrium at various simulated temperatures (303, 313, 323, and 333 K).<sup>351</sup> The findings demonstrate that the LM inhibitor firmly attaches to the Fe(110) surface in a horizontally flat position, facilitated by the presence of oxygen atoms and aromatic rings within the inhibitor structure. As the temperature rises, there is a lowering in the negative interaction energy between the Fe(110) system and the LM inhibitor. This suggests that the bonding strength diminishes as the temperature rises. Further, MD simulations were employed to predict the adsorption behavior of the CHEC molecule on a Fe (110) surface in an aqueous environment. The simulations revealed that the CHEC molecule adopts a flat-lying adsorption orientation on the Fe surface, maximizing surface coverage. The binding energy ( $E_{\text{bind}}$ ) calculations showed a substantially negative value (-137.65 kJ mol<sup>-1</sup>), attributed to dispersive interactions from the  $\pi$  electron delocalization and the high polarizability of the amine N atoms. This adsorption orientation was found to be stable and consistent with experimental observations of strong corrosion inhibition performance. Additional simulations in the gas phase confirmed the orientation, showcasing the favorable interaction between the Fe (110) surface and the diphenyl and amine groups, which are significant in the adsorption process. These interactions are expected to remain intact even at elevated temperatures.<sup>331</sup>

## 5.5 Summaries of evaluation techniques

Corrosion detection and monitoring are crucial in various industries to prevent infrastructure damage and equipment failure. Electrochemical techniques provide a non-destructive and fast way to assess corrosion and evaluate the effectiveness of inhibitors. However, challenges like electrode polarization, surface roughness, and corrosion by-products can hinder these techniques. Microscopy, including SEM and AFM, offers high-resolution imaging to examine corrosion products, pitting, and surface topography. Spectroscopic approaches like infrared spectroscopy and XPS provide detailed information on molecular composition and chemical changes on material surfaces,



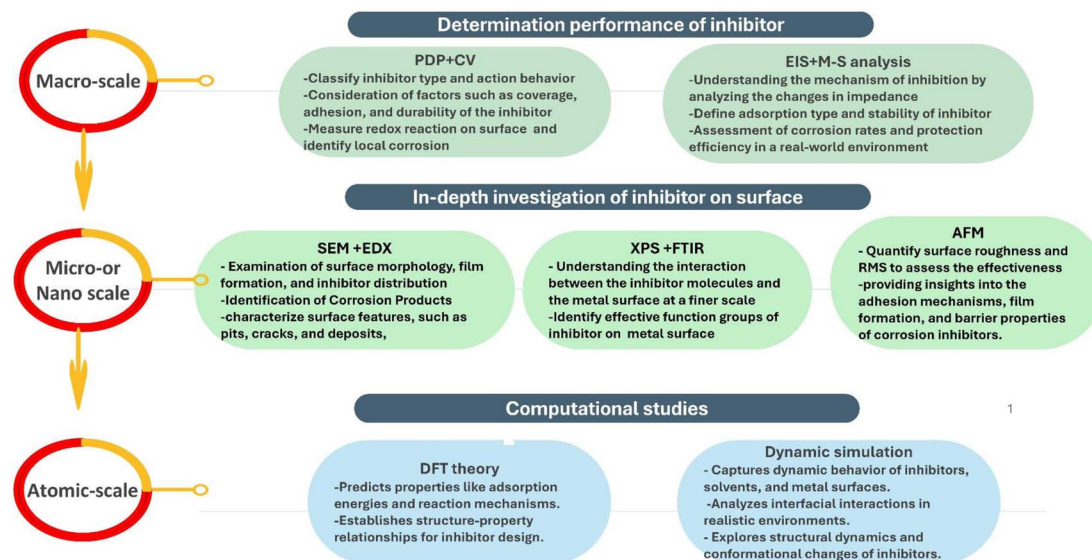


Fig. 10 Summary of inhibition performance validation approaches.

aiding in inhibitor characterization and corrosion product identification. Computational studies using DFT and MD simulations help understand atomic-level interactions between inhibitors and metal surfaces, predicting corrosion reactions' thermodynamics and kinetics. By combining electrochemical, microscopy, spectroscopic, and computational techniques, researchers and engineers can comprehensively understand corrosion processes. This multidisciplinary approach facilitates the development of more effective corrosion prevention strategies, optimization of inhibitor formulations, and informed material selection in various industries. Fig. 10. Illustrate summary of characterization techniques.

## 6. Comprehensive economic analysis of the corrosion inhibitor market

Corrosion poses a significant economic threat, resulting in substantial financial losses. According to the World Corrosion Organization, approximately 25% of steel production is impacted by corrosion yearly, equating to five tons per second or 150 million tons annually. Recent studies have shown that leading companies in the oil and gas sector are spending around \$1.372 billion yearly to address corrosion-related issues. Ignoring the issue of corrosion can have significant financial consequences for various sectors. Even highly developed states and countries with advanced technology are impacted by corrosion and its substantial impacts. For example, in 1998, the USA incurred losses of around \$276 billion as a result of corrosion-related effects, which accounted for approximately 3.1% of the gross domestic product. As of 2011, the overall estimated cost of corrosion exceeded \$2.2 trillion, rising to \$2.5 trillion by 2016, amounting to 3.4% of the global gross domestic product. In India, the yearly cost of corrosion is less than \$100 billion, with South Africa reporting a direct cost of \$9.6

billion.<sup>25,26</sup> Implementing proper corrosion protection methods could potentially reduce these losses by 15–35%.<sup>25,26</sup>

The global corrosion inhibitor market is a dynamic and rapidly expanding industry fueled by the escalating demand for effective corrosion protection across a wide range of sectors. According to recent industry analyses, the global corrosion inhibitor market was valued at US\$ 8.3 billion in 2022 and is expected to reach \$13.34 billion by 2034, with a Compound Annual Growth Rate (CAGR) of 4.1% during the forecast period. This substantial market growth is driven by the increasing focus on corrosion prevention in vital infrastructure projects, the surge in demand for corrosion protection in the oil and gas sector, and the growing emphasis on sustainable and eco-friendly solutions.

Fig. 11a and b show the development of corrosion inhibitors and its global market over time in a chronological manner. Organic corrosion inhibitors dominated the market in 2020 and accounted for over 60% of the total market share. The growing popularity of organic inhibitors, such as amines and imidazolines, is driven by their versatility and effectiveness in various applications. The organic sub-segment had the greatest corrosion inhibitors market share three years ago. The corrosion inhibitors market value for this sub-segment was 4975.5 million back then. The organic sub-segment is expected to have a CAGR of 4.13% for the period that this report covers. The inorganic corrosion inhibitors market growth rate is expected to be 4.5% for this period. Green corrosion inhibitors is projected to witness the highest CAGR during the forecast period, as there is an increasing demand for environmentally friendly and sustainable corrosion protection solutions.

In 2020, North America emerged as the dominant regional market, capturing over 34% of the global market share, primarily bolstered by its well-established industrial base and strict regulatory frameworks in the United States and Canada (Fig. 11c). On the other hand, Asia-Pacific stands out as the



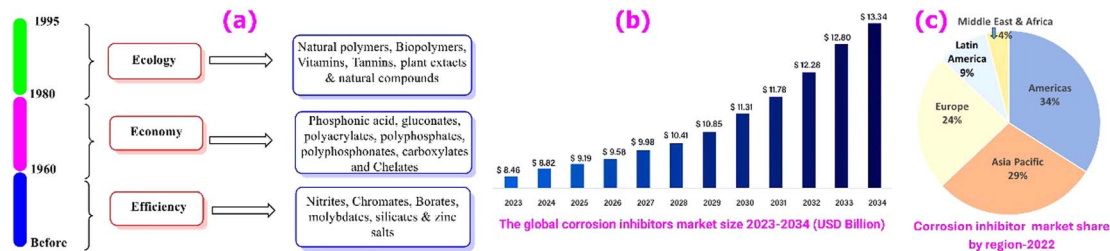


Fig. 11 (a) Development of corrosion inhibitors over year, reprinted with the permission of ref. 356, copyright 2024, Elsevier, (b) the global corrosion inhibitors market and forecast 2023–2034 (USD billion), (c) corrosion inhibitor market share by region in 2022, compiled from <https://www.precedenceresearch.com>.

fastest-growing regional market, exhibiting a remarkable CAGR of over 8% throughout the forecast period. Meanwhile, Europe ranks as the third-largest regional market, with notable market presence in countries. Moreover, the evolving regulatory landscape and mounting environmental concerns are ushering in a shift towards the adoption of less toxic and environmentally friendly corrosion inhibitor products. This trend highlights the industry's continuous evolution towards sustainable and eco-conscious practices in response to global environmental challenges.

## 7. SWOT analysis

The review highlights the potential of synergistic effects between mixed corrosion inhibitors, particularly organic/organic systems, as a viable and advantageous choice for applications requiring robust corrosion inhibition performance in challenging processing environments. These mixed inhibitors offer the benefits of low environmental risk and high efficiency, positioning them as a preferred alternative to single-system inhibitors. While the review article provides a comprehensive technical overview, it may fall short in offering detailed formulation-level insights, limiting the ability of readers to fully understand the nuances and optimization potential of these inhibitor systems. Additionally, the limited coverage of real-world application data and long-term performance evaluation could undermine the confidence of end-users in adopting the discussed inhibitor technologies. Furthermore, the review's narrow focus on the technical aspects may overlook critical factors such as regulatory, safety, and practical implementation challenges, which are crucial for the successful deployment of corrosion control solutions in the real world. This lack of a more holistic perspective could hinder the review's ability to provide a comprehensive roadmap for the widespread adoption of the discussed inhibitor technologies. Opportunities for expanding the review's scope include incorporating more diverse global perspectives, exploring hybrid and synergistic inhibitor systems, integrating life cycle assessment and sustainability analysis, establishing industry partnerships, and broadening the coverage to include alternative corrosion mitigation techniques. Addressing these areas could enhance the review's relevance and applicability across different regions and industries. Potential threats to the widespread adoption of corrosion inhibitors include regulatory and environmental concerns,

technological advancements in competing corrosion control methods, economic and market fluctuations, resistance to change in established industries, and the lack of standardized testing and evaluation protocols. Addressing these challenges will be crucial for the successful implementation of effective and sustainable corrosion inhibition strategies. Fig. 12 demonstrated the summary of SWOT analysis.

## 8. Conclusion and prospects

This review article provides a comprehensive and in-depth analysis of corrosion inhibitors, with a focus on both inorganic and organic inhibitors, as well as ecofriendly and biological macromolecules. The review highlights the inhibition mechanisms, with a particular emphasis on the efficiency of organic compounds due to the presence of heteroatoms and conjugated  $\pi$  electron systems. The review also presents case studies and investigations of corrosion inhibition, showcasing the performance and potential application of various inhibitors. One significant aspect that this review addresses is the growing trend of seeking eco-friendly alternative inhibitors derived from natural resources. The review provides a comparative evaluation of the environmentally friendly biopolymer inhibitors, considering their efficacy, compatibility, and sustainability. Furthermore, the evaluation of corrosion inhibitors is discussed, encompassing various analytical techniques such as weight loss, electrochemical, and surface analysis tools. This comprehensive evaluation enhances our understanding of inhibitor behaviors and mechanisms; however, there are some gaps that need to be filled, including:

(1) Optimizing existing inhibitors: researchers should focus on enhancing the effectiveness and stability of currently available organic, inorganic, and green corrosion inhibitors. This can be achieved through strategic molecular design, the incorporation of synergistic additives, and the development of inhibitor-based coatings and composite systems. Particular attention should be given to improving the long-term durability and reliable performance of inhibitor films under challenging environmental conditions.

(2) Synergistic inhibition in extreme environments: investigating the performance of mixed/hybrid/and composite inhibitors under harsh and demanding conditions, such as high temperatures, aggressive chemical environments, or elevated mechanical stresses, can unlock new avenues for corrosion



## SWOT Analysis Infographics



Fig. 12 SWOT analysis.

control. Demonstrating the synergistic inhibition capabilities in these extreme scenarios can expand the applicability of these systems to challenging industrial settings.

(3) Enhanced mechanistic insights: delving deeper into the mechanistic aspects of synergistic inhibition using mixed inhibitors can yield valuable scientific contributions. Elucidating the precise interactions between the inhibitors, their influence on passive film formation, and the interplay between anodic and cathodic processes can provide fundamental knowledge to guide the design of more effective corrosion mitigation strategies.

(4) Multilayered inhibitor architectures: building upon the concept of synergistic inhibition, the prospect of designing multilayered inhibitor architectures on metal surfaces presents an intriguing direction. By strategically arranging different inhibitors in tailored sequences, it may be possible to create hierarchical protective systems with enhanced durability and self-healing capabilities.

(5) Bioinspired and biomimetic inhibitors: the pursuit of green and eco-friendly corrosion inhibitors has led researchers to explore bioinspired and biomimetic approaches. Drawing inspiration from naturally occurring processes and structures, scientists are investigating the development of inhibitors that mimic the self-healing, self-cleaning, or anti-fouling properties found in biological systems. For instance, the study of marine organisms and their inherent resistance to corrosion has the potential to yield novel biomimetic inhibitor formulations with enhanced performance and environmental compatibility.

(6) Multifunctional and responsive smart inhibitors: the next generation of corrosion inhibitors is expected to exhibit multifunctional and smart capabilities, addressing not only

corrosion prevention but also other surface-related challenges, such as antifouling, anti-icing, or self-healing properties. These responsive and adaptive inhibitors would be able to sense and respond to changes in the environment, automatically adjusting their protective functions to maintain optimal performance under varying conditions.

(7) Application of computational modeling, machine learning, and artificial intelligence that significantly accelerate the discovery, optimization, and deployment of more efficient corrosion inhibitors.

(8) Scaling up green inhibitor production: to meet the growing demand for eco-friendly corrosion inhibitors, researchers and industry should collaborate to develop scalable extraction, purification, and formulation processes for naturally occurring inhibitor compounds derived from plant extracts, marine organisms, or other renewable sources. Simulation and modeling tools can play a crucial role in optimizing the production parameters and enhancing the industrial-scale viability of these green inhibitors.

(9) Sustainable production and life cycle assessment: as the focus on environmental sustainability intensifies, the development of corrosion inhibitors will need to be accompanied by sustainable production processes and comprehensive life cycle assessments. This will involve the use of renewable, biodegradable, and non-toxic raw materials, the optimization of manufacturing methods to minimize waste and energy consumption, and the implementation of circular economy principles to enable the reuse, recycling, or safe disposal of inhibitor-containing products.

In conclusion, this review article not only provides a comprehensive analysis of corrosion inhibitors but also



highlights the importance of adopting environmentally friendly alternatives. It offers valuable insights and future perspectives for researchers and industrial sectors, ultimately helping to build effective and sustainable corrosion control solutions.

## Data availability

The data analyzed in this review article are from previously published studies. The specific datasets and sources are cited throughout the manuscript and listed in the reference section. Readers can access the underlying data from the original published sources as cited. The authors confirm that they did not have any special access privileges to these datasets.

## Conflicts of interest

There are no conflicts to declare.

## References

- S. Zehra, M. Mobin and J. Aslam, An overview of the corrosion chemistry, *Environmentally Sustainable Corrosion Inhibitors*, 2022, pp. 3–23.
- C.-Q. Li, W. Yang and W. Shi, Corrosion effect of ferrous metals on degradation and remaining service life of infrastructure using pipe fracture as example, *Struct. Infrastruct. Eng.*, 2020, **16**(4), 583–598.
- M. A. Ahmed, S. A. Mahmoud and A. A. Mohamed, Unveiling the complexities of microbiologically induced corrosion: mechanisms, detection techniques, and mitigation strategies, *Front. Environ. Sci. Eng.*, 2024, **18**(10), 120.
- O. Fayomi, I. Akande and S. Odigie, Economic impact of corrosion in oil sectors and prevention: An overview, *J. Phys.: Conf. Ser.*, 2019, **1378**, 022037.
- R. Bender, *et al.*, Corrosion challenges towards a sustainable society, *Mater. Corros.*, 2022, **73**(11), 1730–1751.
- D. Lin, *et al.*, A robust and eco-friendly waterborne anti-corrosion composite coating with multiple synergistic corrosion protections, *Composites, Part B*, 2022, **232**, 109624.
- U. M. Angst, A critical review of the science and engineering of cathodic protection of steel in soil and concrete, *Corrosion*, 2019, **75**(12), 1420–1433.
- V. Chobaomsup, M. Metzner and Y. Boonyongmaneerat, Superhydrophobic surface modification for corrosion protection of metals and alloys, *J. Coat. Technol. Res.*, 2020, **17**, 583–595.
- P. Bi, *et al.*, Robust super-hydrophobic coating prepared by electrochemical surface engineering for corrosion protection, *Coatings*, 2019, **9**(7), 452.
- A. Thakur and A. Kumar, Sustainable inhibitors for corrosion mitigation in aggressive corrosive media: a comprehensive study, *J. Bio-Tribo-Corros.*, 2021, **7**, 1–48.
- C. Pan, *et al.*, Effects of corrosion inhibitor and functional components on the electrochemical and mechanical properties of concrete subject to chloride environment, *Constr. Build. Mater.*, 2020, **260**, 119724.
- C. Verma, *et al.*, Phthalocyanine, naphthalocyanine and their derivatives as corrosion inhibitors: A review, *J. Mol. Liq.*, 2021, **334**, 116441.
- M. Goyal, *et al.*, Organic corrosion inhibitors for industrial cleaning of ferrous and non-ferrous metals in acidic solutions: A review, *J. Mol. Liq.*, 2018, **256**, 565–573.
- P. D. Desai, *et al.*, Corrosion inhibitors for carbon steel: A review, *Vietnam J. Chem.*, 2023, **61**(1), 15–42.
- J. Haque, *et al.*, Experimental and quantum chemical analysis of 2-amino-3-((4-((S)-2-amino-2-carboxyethyl)-1H-imidazole-2-yl) thio) propionic acid as new and green corrosion inhibitor for mild steel in 1 M hydrochloric acid solution, *J. Mol. Liq.*, 2017, **225**, 848–855.
- M. A. Ahmed, M. A. Ahmed and A. A. Mohamed, Adsorptive removal of tetracycline antibiotic onto magnetic graphene oxide nanocomposite modified with polyvinylpyrrolidone, *React. Funct. Polym.*, 2023, **191**, 105701.
- K. Hu, *et al.*, Influence of biomacromolecule DNA corrosion inhibitor on carbon steel, *Corros. Sci.*, 2017, **125**, 68–76.
- Y. M. Panchenko and A. Marshakov, Long-term prediction of metal corrosion losses in atmosphere using a power-linear function, *Corros. Sci.*, 2016, **109**, 217–229.
- M. Murmu, *et al.*, Nitrate as corrosion inhibitor, in *Inorganic Anticorrosive Materials*, Elsevier, 2022, pp. 269–296.
- E. De Ketelaere, *et al.*, Sodium silicate corrosion inhibition behaviour for carbon steel in a dynamic salt water environment, *Corros. Sci.*, 2023, **217**, 111119.
- C. M. Fernandes, *et al.*, Study of three new halogenated oxoquinolinecarbohydrazide N-phosphonate derivatives as corrosion inhibitor for mild steel in acid environment, *Surf. Interfaces*, 2020, **21**, 100773.
- B. Maranescu, N. Plesu and A. Visa, Phosphonic acid vs. phosphonate metal organic framework influence on mild steel corrosion protection, *Appl. Surf. Sci.*, 2019, **497**, 143734.
- C. Verma, *et al.*, Aqueous phase environmental friendly organic corrosion inhibitors derived from one step multicomponent reactions: a review, *J. Mol. Liq.*, 2019, **275**, 18–40.
- H. Wei, *et al.*, Green inhibitors for steel corrosion in acidic environment: state of art, *Mater. Today Sustain.*, 2020, **10**, 100044.
- S. A. Umoren, *et al.*, Exploration of natural polymers for use as green corrosion inhibitors for AZ31 magnesium alloy in saline environment, *Carbohydr. Polym.*, 2020, **230**, 115466.
- Z. Shang and J. Zhu, Overview on plant extracts as green corrosion inhibitors in the oil and gas fields, *J. Mater. Res. Technol.*, 2021, **15**, 5078–5094.
- A. Mahmood, *et al.*, Recent progress in biopolymer-based hydrogel materials for biomedical applications, *Int. J. Mol. Sci.*, 2022, **23**(3), 1415.
- R. Ganjoo, *et al.*, Heteropolysaccharides in sustainable corrosion inhibition: 4E (Energy, Economy, Ecology, and



- Effectivity) dimensions, *Int. J. Biol. Macromol.*, 2023, 123571.
- 29 M. A. Quraishi, D. S. Chauhan and V. S. Saji, Heterocyclic biomolecules as green corrosion inhibitors, *J. Mol. Liq.*, 2021, **341**, 117265.
- 30 Y. Zhang, *et al.*, Self-healing coatings based on stimuli-responsive release of corrosion inhibitors: a review, *Front. Mater.*, 2022, **8**, 795397.
- 31 S. Zhu, *et al.*, New insights into the capture performance and mechanism of hazardous metals  $\text{Cr}^{3+}$  and  $\text{Cd}^{2+}$  onto an effective layered double hydroxide based material, *J. Hazard. Mater.*, 2022, **426**, 128062.
- 32 F. Zhao, *et al.*, An overview on the corrosion mechanisms and inhibition techniques for amine-based post-combustion carbon capture process, *Sep. Purif. Technol.*, 2023, **304**, 122091.
- 33 C. B. Verma, M. Quraishi and A. Singh, 2-Aminobenzene-1, 3-dicarbonitriles as green corrosion inhibitor for mild steel in 1 M HCl: Electrochemical, thermodynamic, surface and quantum chemical investigation, *J. Taiwan Inst. Chem. Eng.*, 2015, **49**, 229–239.
- 34 A. A. Shalaby and A. A. Mohamed, Determination of acid dissociation constants of Alizarin Red S, Methyl Orange, Bromothymol Blue and Bromophenol Blue using a digital camera, *RSC Adv.*, 2020, **10**(19), 11311–11316.
- 35 Y. Boughoues, *et al.*, Adsorption and corrosion inhibition performance of some environmental friendly organic inhibitors for mild steel in HCl solution via experimental and theoretical study, *Colloids Surf., A*, 2020, **593**, 124610.
- 36 S. Donkor, *et al.*, An overview of computational and theoretical studies on analyzing adsorption performance of phytochemicals as metal corrosion inhibitors, *J. Mol. Liq.*, 2022, **359**, 119260.
- 37 I. W. Ma, *et al.*, A concise review on corrosion inhibitors: types, mechanisms and electrochemical evaluation studies, *J. Coat. Technol. Res.*, 2022, 1–28.
- 38 M. M. Y. Modwi, *et al.*, Eco-friendly Corrosion Inhibitor of Q235 carbon steel in 1.0 M HCl by Isatin/Chitosan Schiff Base, *J. Mol. Struct.*, 2024, 139592.
- 39 L. Wang, *et al.*, Adsorption mechanism of quaternary ammonium corrosion inhibitor on carbon steel surface using ToF-SIMS and XPS, *Corros. Sci.*, 2023, **213**, 110952.
- 40 M. Bouanis, *et al.*, Corrosion inhibition performance of 2, 5-bis (4-dimethylaminophenyl)-1, 3, 4-oxadiazole for carbon steel in HCl solution: Gravimetric, electrochemical and XPS studies, *Appl. Surf. Sci.*, 2016, **389**, 952–966.
- 41 F. Dou, *et al.*, Exploration of novel polyaspartic acid derivatives as fluorescent eco-friendly corrosion inhibitors for the carbon steel: Electrochemical, surface analysis (SEM/XPS) and theoretical calculation, *Colloids Surf., A*, 2023, **658**, 130606.
- 42 H. A. Rasheed, *et al.*, A review on the use of carboxymethyl cellulose in oil and gas field operations, *Cellulose*, 2023, **30**(16), 9899–9924.
- 43 H. Assad and A. Kumar, Understanding functional group effect on corrosion inhibition efficiency of selected organic compounds, *J. Mol. Liq.*, 2021, **344**, 117755.
- 44 D. E. Arthur, *et al.*, A review on the assessment of polymeric materials used as corrosion inhibitor of metals and alloys, *Int. J. Ind. Chem.*, 2013, **4**, 1–9.
- 45 A. Zeino, *et al.*, Mechanistic study of polyaspartic acid (PASP) as eco-friendly corrosion inhibitor on mild steel in 3% NaCl aerated solution, *J. Mol. Liq.*, 2018, **250**, 50–62.
- 46 J. Chen, *et al.*, Corrosion inhibition performance of threonine-modified polyaspartic acid for carbon steel in simulated cooling water, *J. Appl. Polym. Sci.*, 2019, **136**(15), 47242.
- 47 H. Gerengi, *et al.*, Experimental and quantum chemical evaluation of 8-hydroxyquinoline as a corrosion inhibitor for copper in 0.1 M HCl, *Ind. Eng. Chem. Res.*, 2016, **55**(36), 9614–9624.
- 48 G. Palanisamy, Corrosion inhibitors, *Corros. Inhib.*, 2019, 1–24.
- 49 R. Sabzi and R. Arefinia, Investigation of zinc as a scale and corrosion inhibitor of carbon steel in artificial seawater, *Corros. Sci.*, 2019, **153**, 292–300.
- 50 R. A. Anaee, Sodium silicate and phosphate as corrosion inhibitors for mild steel in simulated cooling water system, *Arabian J. Sci. Eng.*, 2014, **39**, 153–162.
- 51 M. Gobara, *et al.*, Corrosion protection mechanism of Ce 4+/organic inhibitor for AA2024 in 3.5% NaCl, *RSC Adv.*, 2020, **10**(4), 2227–2240.
- 52 J. Zhao, *et al.*, Corrosion of N80 Steel in a Concentrated Tetrapotassium Pyrophosphate Solution and Corrosion Control by Vanadates, *Int. J. Electrochem. Sci.*, 2019, **14**(7), 6209–6222.
- 53 H. Khani and R. Arefinia, Inhibition mechanism of nitrite on the corrosion of carbon steel in simulated cooling water systems, *Mater. Corros.*, 2018, **69**(3), 337–347.
- 54 K. Kim, *et al.*, Corrosion inhibiting mechanism of nitrite ion on the passivation of carbon steel and ductile cast iron for nuclear power plants, *Adv. Mater. Sci. Eng.*, 2015, 2015.
- 55 M. Hayyan, *et al.*, Utilizing of sodium nitrite as inhibitor for protection of carbon steel in salt solution, *Int. J. Electrochem. Sci.*, 2012, **7**(8), 6941–6950.
- 56 S. Karim, *et al.*, Effect of nitrate ion on corrosion inhibition of mild steel in simulated cooling water, *Chem. Eng. Res. Bull.*, 2010, **14**(2), 87–91.
- 57 D. Y. Lee, W. C. Kim and J. G. Kim, Effect of nitrite concentration on the corrosion behaviour of carbon steel pipelines in synthetic tap water, *Corros. Sci.*, 2012, **64**, 105–114.
- 58 M. Shaglouf, *et al.*, Influence of Nitrite and Molybdate Blend on Carbon Steel Inhibition in Chloride Containing Solutions, *Sirte University Scientific Journal*, 2022, **12**(1), 108–121.
- 59 G. Mu, *et al.*, Molybdate and tungstate as corrosion inhibitors for cold rolling steel in hydrochloric acid solution, *Corros. Sci.*, 2006, **48**(2), 445–459.
- 60 M. Tommaselli, N. Mariano and S. Kuri, Effectiveness of corrosion inhibitors in saturated calcium hydroxide solutions acidified by acid rain components, *Constr. Build. Mater.*, 2009, **23**(1), 328–333.



- 61 Y. T. Tan, S. L. Wijesinghe and D. J. Blackwood, Effect of molybdate on the passivation of carbon steel in alkaline solutions under open-circuit conditions, *J. Electrochem. Soc.*, 2016, **163**(10), C649.
- 62 H. Bensabra, *et al.*, Inhibitive effect of molybdate ions on the electrochemical behavior of steel rebar in simulated concrete pore solution, *Metall. Mater. Trans. A*, 2017, **48**, 412–424.
- 63 K. Yee, *et al.*, Corrosion inhibition of molybdate and nitrite for carbon steel corrosion in process cooling water, *J. Eng. Sci. Technol.*, 2019, **14**(4), 2431–2444.
- 64 G. A. Gaber, H. A. Aly and L. Z. Mohamed, Effect of sodium tungstate on the corrosion behavior of Fe-base alloy in H<sub>2</sub>SO<sub>4</sub> solution, *Int. J. Electrochem. Sci.*, 2020, **15**(8), 8229–8240.
- 65 V. Deepak and J. Bhattarai, Effect of sodium tungstate as a green corrosion inhibitor on the passivation behavior of mild steel sheet in aggressive media, *Int. J. Appl. Sci. Biotechnol.*, 2016, **4**(2), 183–190.
- 66 J. Zhang, *et al.*, Synergistic Inhibition Effect of Sodium Tungstate and Zinc Sulphate on Mild Steel Corrosion in Seawater, *Int. J. Electrochem. Sci.*, 2018, **13**(7), 6522–6536.
- 67 S. kareem Mohammed, Effect Use of Two Chemical Compounds Sodium Nitrate and Sodium Silicate as Corrosion Inhibitor to Steel Reinforcement, *Al-Khwarizmi Engineering Journal*, 2018, **14**(2), 123–128.
- 68 F. B. Mainier, *et al.*, The use of sodium silicate as a corrosion inhibitor in a saline drilling fluid: a nonaggressive option to the environment, *J. Environ. Prot.*, 2016, **7**(13), 2025.
- 69 M. Rizvi, *et al.*, Sodium nitrite as a corrosion inhibitor of copper in simulated cooling water, *Sci. Rep.*, 2021, **11**(1), 8353.
- 70 Y. Song, *et al.*, Research progress of nitrite corrosion inhibitor in concrete, *Int. J. Corros.*, 2019, 3060869.
- 71 M. B. Valcarce and M. Vázquez, Carbon steel passivity examined in solutions with a low degree of carbonation: The effect of chloride and nitrite ions, *Mater. Chem. Phys.*, 2009, **115**(1), 313–321.
- 72 P. Garcés, *et al.*, Effect of nitrite in corrosion of reinforcing steel in neutral and acid solutions simulating the electrolytic environments of micropores of concrete in the propagation period, *Corros. Sci.*, 2008, **50**(2), 498–509.
- 73 M. A. Amin, H. H. Hassan and S. S. Abd El Rehim, On the role of NO<sub>2</sub><sup>-</sup> ions in passivity breakdown of Zn in deaerated neutral sodium nitrite solutions and the effect of some inorganic inhibitors: potentiodynamic polarization, cyclic voltammetry, SEM and EDX studies, *Electrochim. Acta*, 2008, **53**(5), 2600–2609.
- 74 H. H. Uhlig and R. W. Revie, *Corrosion and Corrosion Control*, 1985.
- 75 Z. Cao, M. Hibino and H. Goda, Effect of nitrite ions on steel corrosion induced by chloride or sulfate ions, *Int. J. Corros.*, 2013, 853730.
- 76 Y. Zhou and Y. Zuo, The inhibitive mechanisms of nitrite and molybdate anions on initiation and propagation of pitting corrosion for mild steel in chloride solution, *Appl. Surf. Sci.*, 2015, **353**, 924–932.
- 77 A. Al-Refai, *et al.*, Photoelectron spectroscopy study of the inhibition of mild steel corrosion by molybdate and nitrite anions, *Corros. Sci.*, 2010, **52**(2), 422–428.
- 78 Z. Xu, *et al.*, Properties of sodium molybdate-based compound corrosion inhibitor for hot-dip galvanized steel in marine environment, *Corros. Rev.*, 2023, **41**(2), 225–235.
- 79 A. Rokni, R. Zakeralhosseini and M. H. Moayed, An investigation on the effect of molybdenum alloy element and molybdate inhibitor on the stable and metastable pits and its correlation with the pit morphology, *J. Taiwan Inst. Chem. Eng.*, 2023, **153**, 105203.
- 80 Y. Liu and J. Shi, Design of a smart protective coating with molybdate-loaded halloysite nanotubes towards corrosion protection in reinforced concrete, *Cem. Concr. Compos.*, 2023, 105419.
- 81 X. Li, S. Deng and H. Fu, Sodium molybdate as a corrosion inhibitor for aluminium in H<sub>3</sub>PO<sub>4</sub> solution, *Corros. Sci.*, 2011, **53**(9), 2748–2753.
- 82 M. Ali, C. Mustafa and M. Habib, Effect of molybdate, nitrite and zinc ions on the corrosion inhibition of mild steel in aqueous chloride media containing cupric ions, *J. Sci. Res.*, 2009, **1**(1), 82–91.
- 83 T. D. Nguyen, *et al.*, Molybdate intercalated hydrotalcite/graphene oxide composite as corrosion inhibitor for carbon steel, *Surf. Coat. Technol.*, 2020, **399**, 126165.
- 84 Y. T. Tan, S. L. Wijesinghe and D. J. Blackwood, Inhibition of bicarbonate-chloride corrosion and passivation of carbon steel under open-circuit conditions by molybdate, *J. Electrochem. Soc.*, 2017, **164**(9), C505.
- 85 S. P. Rey and M. Gary, Molybdate and Non-Molybdate Options for Closed Systems, *Molybdate and Non-molybdate Options for Closed Systems*, Association of Water Technologies (AWT), 2005.
- 86 S. Refaey, *et al.*, Inhibition of chloride localized corrosion of mild steel by PO<sub>4</sub><sup>3-</sup>, CrO<sub>4</sub><sup>2-</sup>, MoO<sub>4</sub><sup>2-</sup>, and NO<sub>2</sub><sup>-</sup> anions, *Appl. Surf. Sci.*, 2000, **158**(3–4), 190–196.
- 87 M. Deyab and S. Abd El-Rehim, Inhibitory effect of tungstate, molybdate and nitrite ions on the carbon steel pitting corrosion in alkaline formation water containing Cl<sup>-</sup> ion, *Electrochim. Acta*, 2007, **53**(4), 1754–1760.
- 88 V. S. Sastri, *Green Corrosion Inhibitors: Theory and Practice*, John Wiley & Sons, 2012.
- 89 K. Ogura and T. Ohama, Pit formation in the cathodic polarization of passive iron IV. Repair mechanism by molybdate, chromate and tungstate, *Corrosion*, 1984, **40**(2), 47–51.
- 90 W. J. Lorenz, Der einfluss von halogenidionen auf die anodische auflösung des eisens, *Corros. Sci.*, 1965, **5**(2), 121–131.
- 91 J.-R. Chen, *et al.*, Studies on carbon steel corrosion in molybdate and silicate solutions as corrosion inhibitors, *Surf. Sci.*, 1991, **247**(2–3), 352–359.
- 92 C. Wang, *et al.*, Modified chitosan-oligosaccharide and sodium silicate as efficient sustainable inhibitor for



- carbon steel against chloride-induced corrosion, *J. Cleaner Prod.*, 2019, **238**, 117823.
- 93 K. Aramaki, Self-healing mechanism of an organosiloxane polymer film containing sodium silicate and cerium (III) nitrate for corrosion of scratched zinc surface in 0.5 M NaCl, *Corros. Sci.*, 2002, **44**(7), 1621–1632.
- 94 H. Gao, *et al.*, Study of the corrosion inhibition effect of sodium silicate on AZ91D magnesium alloy, *Corros. Sci.*, 2011, **53**(4), 1401–1407.
- 95 M. E. Mohorich, *et al.*, Electrochemical studies on silicate and bicarbonate ions for corrosion inhibitors, *Metall. Mater. Trans. A*, 2010, **41**, 2563–2574.
- 96 J. Qiu, *et al.*, Synergistic effect of molybdate or tungstate and water soluble thiol on the corrosion protection of copper, *Appl. Surf. Sci.*, 2024, **654**, 159418.
- 97 H. Li, *et al.*, Cutting fluid corrosion inhibitors from inorganic to organic: Progress and applications, *Korean J. Chem. Eng.*, 2022, **39**(5), 1107–1134.
- 98 F. Kandemirli and S. Sagdinc, Theoretical study of corrosion inhibition of amides and thiosemicarbazones, *Corros. Sci.*, 2007, **49**(5), 2118–2130.
- 99 C.-B. Zheng, *et al.*, The inhibition effect of the molybdate on hydrogen permeation of 2205 duplex stainless steel, *Surf. Coat. Technol.*, 2016, **287**, 153–159.
- 100 B. Lin, *et al.*, Study on synergistic corrosion inhibition effect between calcium lignosulfonate (CLS) and inorganic inhibitors on Q235 carbon steel in alkaline environment with Cl<sup>-</sup>, *Molecules*, 2020, **25**(18), 4200.
- 101 D. A. Meier, B. Chen and C. Myers, Cooling water systems: An overview, *Water-Formed Deposits*, 2022, 239–267.
- 102 Y. Chen, *et al.*, Impact of phosphate corrosion inhibitors on chloride binding and release in cement pastes, *Constr. Build. Mater.*, 2020, **236**, 117469.
- 103 D. M. Bastidas, *et al.*, Corrosion inhibition mechanism of steel reinforcements in mortar using soluble phosphates: A critical review, *Materials*, 2021, **14**(20), 6168.
- 104 M. Pryor and M. Cohen, The mechanism of the inhibition of the corrosion of iron by solutions of sodium orthophosphate, *J. Electrochem. Soc.*, 1951, **98**(7), 263.
- 105 I. Zin, S. Lyon and V. Pokhmurskii, Corrosion control of galvanized steel using a phosphate/calcium ion inhibitor mixture, *Corros. Sci.*, 2003, **45**(4), 777–788.
- 106 Y. Morozov, *et al.*, Epoxy coatings modified with a new cerium phosphate inhibitor for smart corrosion protection of steel, *Corros. Sci.*, 2019, **159**, 108128.
- 107 M. Reffass, *et al.*, Effects of phosphate species on localised corrosion of steel in NaHCO<sub>3</sub>+ NaCl electrolytes, *Electrochim. Acta*, 2009, **54**(18), 4389–4396.
- 108 A. Mohagheghi and R. Arefinia, Corrosion inhibition of carbon steel by dipotassium hydrogen phosphate in alkaline solutions with low chloride contamination, *Constr. Build. Mater.*, 2018, **187**, 760–772.
- 109 M. Pryor and M. Cohen, The inhibition of the corrosion of iron by some anodic inhibitors, *J. Electrochem. Soc.*, 1953, **100**(5), 203.
- 110 S. Gypser, *Identification of Phosphate Adsorption Mechanisms on Fe-And Al-Hydroxides and the Influence of Inorganic and Organic Compounds to Reduce Long-Term Phosphorus Fixation on Mineral Surfaces*, BTU Cottbus-Senftenberg, 2019.
- 111 I. Sieber, *et al.*, Investigations on the passivity of iron in borate and phosphate buffers, pH 8.4, *Corros. Sci.*, 2006, **48**(11), 3472–3488.
- 112 Z. Szklarska-Smialowska and R. Staehle, Ellipsometric study of the formation of films on iron in orthophosphate solutions, *J. Electrochem. Soc.*, 1974, **121**(11), 1393.
- 113 L. Yohai, M. Vázquez and M. Valcarce, Phosphate ions as corrosion inhibitors for reinforcement steel in chloride-rich environments, *Electrochim. Acta*, 2013, **102**, 88–96.
- 114 S. Abd El Haleem, *et al.*, Environmental factors affecting the corrosion behavior of reinforcing steel. IV. Variation in the pitting corrosion current in relation to the concentration of the aggressive and the inhibitive anions, *Corros. Sci.*, 2010, **52**(5), 1675–1683.
- 115 H. Uhlig, D. Triadis and M. Stern, Effect of oxygen, chlorides, and calcium ion on corrosion inhibition of iron by polyphosphates, *J. Electrochem. Soc.*, 1955, **102**(2), 59.
- 116 Z. Szklarska-Smialowska and J. Mankowski, *Le mecanisme de l'action des polyphosphates comme inhibiteurs de la corrosion de l'acier par l'eau*, Centre Belge D'etude Et De Documentation Des Eaux, 1967, vol. 20(288), pp. 474–480.
- 117 B. Andrzejczek, Mechanism of Action of Acidified Sodium Phosphate Solution as a Corrosion Inhibitor of Iron in Tap Water, *Br. Corros. J.*, 1979, **14**(3), 176–178.
- 118 S. Rajappa, T. Venkatesha and B. Praveen, Chemical treatment of zinc surface and its corrosion inhibition studies, *Bull. Mater. Sci.*, 2008, **31**, 37–41.
- 119 M. A. Ahmed and A. A. Mohamed, Evaluation and optimization of antiscalant substances for enhanced reverse osmosis performance, *J. Saudi Chem. Soc.*, 2024, 101923.
- 120 J. Telegdi, History of phosphorus-containing corrosion inhibitors: From the beginning till the present time, in *Water-Formed Deposits*, Elsevier, 2022, pp. 49–68.
- 121 A. Paszternák, *et al.*, Surface analytical characterization of passive iron surface modified by alkyl-phosphonic acid layers, *Electrochim. Acta*, 2010, **55**(3), 804–812.
- 122 M. Salasi, *et al.*, The electrochemical behaviour of environment-friendly inhibitors of silicate and phosphonate in corrosion control of carbon steel in soft water media, *Mater. Chem. Phys.*, 2007, **104**(1), 183–190.
- 123 A. Chirkunov and Y. Kuznetsov, Corrosion inhibitors in cooling water systems, in *Mineral Scales and Deposits*, Elsevier, 2015, pp. 85–105.
- 124 E. Kalman, *et al.*, The effect of calcium ions on the adsorption of phosphonic acid: a comparative investigation with emphasis on surface analytical methods, *Electrochim. Acta*, 1994, **39**(8–9), 1179–1182.
- 125 F. Karman, *et al.*, The role of oxide layer formation during corrosion inhibition of mild steel in neutral aqueous media, *Electrochim. Acta*, 1998, **43**(1–2), 69–75.
- 126 K. D. Demadis, M. Papadaki, and D. Varouchas, Metal-phosphonate anticorrosion coatings, *Green Corrosion*



- Chemistry and Engineering: Opportunities and Challenges*, Wiley, New Jersey, 2012.
- 127 M. Prabakaran, *et al.*, Corrosion protection of mild steel by a new phosphonate inhibitor system in aqueous solution, *Egypt. J. Pet.*, 2014, **23**(4), 367–377.
- 128 M. Prabakaran, *et al.*, Corrosion inhibition behavior of propyl phosphonic acid–Zn<sup>2+</sup> system for carbon steel in aqueous solution, *Appl. Surf. Sci.*, 2013, **276**, 592–603.
- 129 C. Verma, *et al.*, Sulfur and phosphorus heteroatom-containing compounds as corrosion inhibitors: An overview, *Heteroat. Chem.*, 2018, **29**(4), e21437.
- 130 L. K. Goni, *et al.*, Bioinspired heterocyclic compounds as corrosion inhibitors: a comprehensive review, *Chem.–Asian J.*, 2021, **16**(11), 1324–1364.
- 131 T. Harvey, *et al.*, The effect of inhibitor structure on the corrosion of AA2024 and AA7075, *Corros. Sci.*, 2011, **53**(6), 2184–2190.
- 132 M. Ouakki, *et al.*, Insights into corrosion inhibition mechanism of mild steel in 1 M HCl solution by quinoxaline derivatives: electrochemical, SEM/EDAX, UV-visible, FT-IR and theoretical approaches, *Colloids Surf., A*, 2021, **611**, 125810.
- 133 M. Yadav, *et al.*, Corrosion inhibition effect of spiropyrimidinethiones on mild steel in 15% HCl solution: insight from electrochemical and quantum studies, *RSC Adv.*, 2015, **5**(87), 70832–70848.
- 134 C. Verma, *et al.*, Principles and theories of green chemistry for corrosion science and engineering: design and application, *Green Chem.*, 2024, **26**(8), 4270–4357.
- 135 R. Tuir, *et al.*, Study of phosphonate addition and hydrodynamic conditions on ordinary steel corrosion inhibition in simulated cooling water, *Mater. Chem. Phys.*, 2010, **122**(1), 1–9.
- 136 N. N. Hau and D. Q. Huong, Effect of aromatic rings on mild steel corrosion inhibition ability of nitrogen heteroatom-containing compounds: Experimental and theoretical investigation, *J. Mol. Struct.*, 2023, **1277**, 134884.
- 137 K. J. Thomas, Electro analytical and gravimetric investigations on corrosion inhibition properties of pyridine-carbaldehyde derivatives on carbon steel, *Chem. Sci. Rev. Lett.*, 2017, **6**, 2300–2308.
- 138 A. Ismail, *et al.*, Electrochemical corrosion performance of aromatic functionalized imidazole inhibitor under hydrodynamic conditions on API X65 carbon steel in 1 M HCl solution, *Arabian J. Sci. Eng.*, 2019, **44**(6), 5877–5888.
- 139 E.-S. M. Sherif, *et al.*, Corrosion of high strength steel in concentrated sulfuric acid pickling solutions and its inhibition by 3-amino-5-mercapto-1, 2, 3-triazole, *Int. J. Electrochem. Sci.*, 2015, **10**(2), 1777–1791.
- 140 N. Wazzan, I. Obot and T. M. Fagieh, The role of some triazoles on the corrosion inhibition of C1020 steel and copper in a desalination descaling solution, *Desalination*, 2022, **527**, 115551.
- 141 O. I. El Mouden, *et al.*, Anti-corrosive properties of two new green heterocyclic azole derivatives on C38 steel in 1 M (HCl) medium, experimental and theoretical study, *Results Chem.*, 2023, **5**, 100641.
- 142 A. Berisha, Experimental, Monte Carlo and molecular dynamic study on corrosion inhibition of mild steel by pyridine derivatives in aqueous perchloric acid, *Electrochem*, 2020, **1**(2), 188–199.
- 143 J. Wen, *et al.*, Exploration of imidazole-4-methylimine thiourea as effective corrosion inhibitor for mild steel in hydrochloric medium: Experimental and theoretical studies, *Colloids Surf., A*, 2023, **674**, 131895.
- 144 A. A. Mohamed, *et al.*, A novel kinetic determination of dissolved chromium species in natural and industrial waste water, *Talanta*, 2006, **70**(2), 460–467.
- 145 A. T. Mubarak, *et al.*, A novel kinetic determination of nitrite based on the perphenazine-bromate redox reaction, *Microchim. Acta*, 2007, **157**, 99–105.
- 146 M. A. Ahmed, M. A. Ahmed and A. A. Mohamed, Fabrication of NiO/g-C<sub>3</sub>N<sub>4</sub> Z-scheme heterojunction for enhanced photocatalytic degradation of methylene blue dye, *Opt. Mater.*, 2024, **151**, 115339.
- 147 M. Adel, M. A. Ahmed and A. A. Mohamed, Effective removal of cationic dyes from aqueous solutions using reduced graphene oxide functionalized with manganese ferrite nanoparticles, *Compos. Commun.*, 2020, **22**, 100450.
- 148 M. A. Ahmed and A. A. Mohamed, Advances in ultrasound-assisted synthesis of photocatalysts and sonophotocatalytic processes: A review, *Iscience*, 2023, **27**(1), 108583.
- 149 M. A. Ahmed and A. A. Mohamed, A systematic review of layered double hydroxide-based materials for environmental remediation of heavy metals and dye pollutants, *Inorg. Chem. Commun.*, 2023, **148**, 110325.
- 150 M. A. Ahmed and A. A. Mohamed, Recent progress in semiconductor/graphene photocatalysts: synthesis, photocatalytic applications, and challenges, *RSC Adv.*, 2023, **13**(1), 421–439.
- 151 A. Valdés and M. C. Garrigós, Carbohydrate-based advanced biomaterials for food sustainability: a review, in *Materials Science Forum*, Trans Tech Publ., 2016.
- 152 J. Liu, S. Willför and C. Xu, A review of bioactive plant polysaccharides: Biological activities, functionalization, and biomedical applications, *Bioact. Carbohydr. Diet. Fibre*, 2015, **5**(1), 31–61.
- 153 M. A. Ahmed and A. A. Mohamed, The use of chitosan-based composites for environmental remediation: A review, *Int. J. Biol. Macromol.*, 2023, 124787.
- 154 Q. Zhang, *et al.*, Two novel chitosan derivatives as high efficient eco-friendly inhibitors for the corrosion of mild steel in acidic solution, *Corros. Sci.*, 2020, **164**, 108346.
- 155 S. A. Al Kiey, M. S. Hasanin and S. Dacrory, Potential anticorrosive performance of green and sustainable inhibitor based on cellulose derivatives for carbon steel, *J. Mol. Liq.*, 2021, **338**, 116604.
- 156 C. Verma and M. A. Quraishi, Chelation capability of chitosan and chitosan derivatives: Recent developments in sustainable corrosion inhibition and metal decontamination applications, *Curr. Res. Green Sustain. Chem.*, 2021, **4**, 100184.



- 157 C. Verma, *et al.*, Corrosion inhibition potential of chitosan based Schiff bases: Design, performance and applications, *Int. J. Biol. Macromol.*, 2021, **184**, 135–143.
- 158 X. Luo, *et al.*, Zwitterion modified chitosan as a high-performance corrosion inhibitor for mild steel in hydrochloric acid solution, *Int. J. Biol. Macromol.*, 2024, **267**, 131429.
- 159 K. Ansari, *et al.*, Chitosan Schiff base: an environmentally benign biological macromolecule as a new corrosion inhibitor for oil & gas industries, *Int. J. Biol. Macromol.*, 2020, **144**, 305–315.
- 160 V. Zargar, M. Asghari and A. Dashti, A review on chitin and chitosan polymers: structure, chemistry, solubility, derivatives, and applications, *ChemBioEng Rev.*, 2015, **2**(3), 204–226.
- 161 A. M. Kumar, *et al.*, Water-soluble chitosan salt as ecofriendly corrosion inhibitor for N80 pipeline steel in artificial sea water: Experimental and theoretical approach, *Int. J. Biol. Macromol.*, 2024, **254**, 127697.
- 162 M. A. Ahmed, M. A. Ahmed and A. A. Mohamed, Synthesis, characterization and application of chitosan/graphene oxide/copper ferrite nanocomposite for the adsorptive removal of anionic and cationic dyes from wastewater, *RSC Adv.*, 2023, **13**(8), 5337–5352.
- 163 A. K. Singh, *et al.*, Relation of alkyl chain length and corrosion inhibition efficiency of N-Acylated Chitosans over mild steel in acidic medium, *J. Environ. Chem. Eng.*, 2024, 113179.
- 164 X. Dou, *et al.*, Research progress on chitosan and its derivatives in the fields of corrosion inhibition and antimicrobial activity, *Environ. Sci. Pollut. Res.*, 2024, 1–17.
- 165 S. A. Umoren, *et al.*, Inhibition of mild steel corrosion in HCl solution using chitosan, *Cellulose*, 2013, **20**, 2529–2545.
- 166 N. K. Gupta, *et al.*, Chitosan: A macromolecule as green corrosion inhibitor for mild steel in sulfamic acid useful for sugar industry, *Int. J. Biol. Macromol.*, 2018, **106**, 704–711.
- 167 Y. Wang, *et al.*, Novel chitosan-oligosaccharide derivatives as fluorescent green corrosion inhibitors for P110 steel, *Carbohydr. Polym.*, 2024, 122475.
- 168 N. Rossi, C. Grosso and C. Delerue-Matos, Shrimp Waste Upcycling: Unveiling the Potential of Polysaccharides, Proteins, Carotenoids, and Fatty Acids with Emphasis on Extraction Techniques and Bioactive Properties, *Mar. Drugs*, 2024, **22**(4), 153.
- 169 M. Sankar, R. Karthikeyan and S. Vigneshkumar, Synthesis and Characterization of Chitosan Acetylcholine Nanoparticles for Neural Disorders Associated with Cancer Treatment, *J. Inorg. Organomet. Polym. Mater.*, 2023, **33**(8), 2465–2484.
- 170 G. Cui, *et al.*, Chitosan oligosaccharide derivatives as green corrosion inhibitors for P110 steel in a carbon-dioxide-saturated chloride solution, *Carbohydr. Polym.*, 2019, **203**, 386–395.
- 171 K. El Mouaden, *et al.*, Chitosan polymer as a green corrosion inhibitor for copper in sulfide-containing synthetic seawater, *Int. J. Biol. Macromol.*, 2018, **119**, 1311–1323.
- 172 V. Srivastava, *et al.*, PEG-functionalized chitosan: A biological macromolecule as a novel corrosion inhibitor, *ChemistrySelect*, 2018, **3**(7), 1990–1998.
- 173 C. Verma, *et al.*, Recent developments in sustainable corrosion inhibitors: design, performance and industrial scale applications, *Mater. Adv.*, 2021, **2**(12), 3806–3850.
- 174 O. Egbuhuzor, *et al.*, Adsorption behavior and corrosion rate model of sodium carboxymethyl cellulose (NA-CMC) polymer on aluminium in hcl solution, *Niger. J. Technol.*, 2020, **39**(2), 369–378.
- 175 A. Shahmoradi, *et al.*, Studying the adsorption/inhibition impact of the cellulose and lignin compounds extracted from agricultural waste on the mild steel corrosion in HCl solution, *J. Mol. Liq.*, 2020, **304**, 112751.
- 176 M. Mobin and M. Rizvi, Adsorption and corrosion inhibition behavior of hydroxyethyl cellulose and synergistic surfactants additives for carbon steel in 1 M HCl, *Carbohydr. Polym.*, 2017, **156**, 202–214.
- 177 S. A. Umoren, *et al.*, Evaluation of chitosan and carboxymethyl cellulose as ecofriendly corrosion inhibitors for steel, *Int. J. Biol. Macromol.*, 2018, **117**, 1017–1028.
- 178 S. Umoren, *et al.*, Synergistic and antagonistic effects between halide ions and carboxymethyl cellulose for the corrosion inhibition of mild steel in sulphuric acid solution, *Cellulose*, 2010, **17**, 635–648.
- 179 A. Dastpak, *et al.*, Solubility study of lignin in industrial organic solvents and investigation of electrochemical properties of spray-coated solutions, *Ind. Crops Prod.*, 2020, **148**, 112310.
- 180 S. Yahya, N. Othman and M. Ismail, Corrosion inhibition of steel in multiple flow loop under 3.5% NaCl in the presence of rice straw extracts, lignin and ethylene glycol, *Eng. Failure Anal.*, 2019, **100**, 365–380.
- 181 M. M. Rahman, *et al.*, Phenolation of potassium hydroxide lignin and its effect on copolymerization with acrylic acid, *Biomass Convers. Biorefin.*, 2023, 1–9.
- 182 L. A. Z. Torres, *et al.*, Lignin as a potential source of high-added value compounds: A review, *J. Cleaner Prod.*, 2020, **263**, 121499.
- 183 P. Jędrzejczak, *et al.*, The role of lignin and lignin-based materials in sustainable construction – a comprehensive review, *Int. J. Biol. Macromol.*, 2021, **187**, 624–650.
- 184 C. Gao, *et al.*, Construction of a novel lignin-based quaternary ammonium material with excellent corrosion resistant behavior and its application for corrosion protection, *Materials*, 2019, **12**(11), 1776.
- 185 A. Dehghani, B. Ramezanzadeh and M. Mahdavian, Current applications of fatty acids, lignin, and lipids as green corrosion inhibitors, *Handbook of Biomolecules*, 2023, pp. 535–550.
- 186 N. Aissiou, M. Bounoughaz and A. Djeddi, Lignin-phenylhydrazone as a corrosion inhibitor of API X52 carbon steel in 3.5% NaCl and 0.1 mol/L HCl medium, *Chem. Res. Chin. Univ.*, 2021, **37**, 718–728.



- 187 J. Wang, *et al.*, Smart lignin-based polyurethane conjugated with corrosion inhibitor as bio-based anticorrosive sublayer coating, *Ind. Crops Prod.*, 2022, **188**, 115719.
- 188 A. Dastpak, *et al.*, A sustainable two-layer lignin-anodized composite coating for the corrosion protection of high-strength low-alloy steel, *Prog. Org. Coat.*, 2020, **148**, 105866.
- 189 P. Rahayu, C. Sundari, and I. Farida, Corrosion inhibition using lignin of sugarcane bagasse, in *IOP Conference Series: Materials Science and Engineering*, IOP Publishing, 2018.
- 190 M. A. Abu-Dalo, N. A. Al-Rawashdeh and A. A. Mutlaq, Green approach to corrosion inhibition of mild steel by lignin sulfonate in acidic media, *J. Iron Steel Res. Int.*, 2016, **23**(7), 722–732.
- 191 C. Gao, *et al.*, Construction of eco-friendly corrosion inhibitor lignin derivative with excellent corrosion-resistant behavior in hydrochloric acid solution, *Mater. Corros.*, 2020, **71**(11), 1903–1912.
- 192 M. M. El-Deeb, E. N. Ads and J. R. Humaidi, Evaluation of the modified extracted lignin from wheat straw as corrosion inhibitors for aluminum in alkaline solution, *Int. J. Electrochem. Sci.*, 2018, **13**, 4123–4138.
- 193 P. Kulkarni, *et al.*, Lignin from termite frass: A sustainable source for anticorrosive applications, *J. Appl. Electrochem.*, 2021, **51**, 1491–1500.
- 194 T. Rabizadeh and S. Khameneh Asl, Chitosan as a green inhibitor for mild steel corrosion: Thermodynamic and electrochemical evaluations, *Mater. Corros.*, 2019, **70**(4), 738–748.
- 195 A. Okoronkwo, S. Olusegun and O. Oluwasina, The inhibitive action of chitosan extracted from *Archachatina marginata* shells on the corrosion of plain carbon steel in acid media, *Anti-Corros. Methods Mater.*, 2015, **62**(1), 13–18.
- 196 M. M. Solomon, *et al.*, Synergistic inhibition of St37 steel corrosion in 15% H<sub>2</sub>SO<sub>4</sub> solution by chitosan and iodide ion additives, *Cellulose*, 2017, **24**, 931–950.
- 197 P. Kong, *et al.*, Polyaniline/chitosan as a corrosion inhibitor for mild steel in acidic medium, *RSC Adv.*, 2019, **9**(16), 9211–9217.
- 198 R. Menaka and S. Subhashini, Chitosan Schiff base as effective corrosion inhibitor for mild steel in acid medium, *Polym. Int.*, 2017, **66**(3), 349–358.
- 199 D. S. Chauhan, *et al.*, Chitosan-cinnamaldehyde Schiff base: A bioinspired macromolecule as corrosion inhibitor for oil and gas industry, *Int. J. Biol. Macromol.*, 2020, **158**, 127–138.
- 200 J. Haque, *et al.*, Microwave-induced synthesis of chitosan Schiff bases and their application as novel and green corrosion inhibitors: experimental and theoretical approach, *ACS Omega*, 2018, **3**(5), 5654–5668.
- 201 R. G. M. de Araújo Macedo, *et al.*, Water-soluble carboxymethylchitosan used as corrosion inhibitor for carbon steel in saline medium, *Carbohydr. Polym.*, 2019, **205**, 371–376.
- 202 I. Arukalam, *et al.*, Acid corrosion inhibition and adsorption behaviour of ethyl hydroxyethyl cellulose on mild steel corrosion, *J. Mater.*, 2014, **2014**, 1–11.
- 203 T. Sathiyapriya, G. Rathika and M. Dhandapani, In depth analysis of anti corrosion behaviour of eco friendly gum exudate for mild steel in sulphuric acid medium, *J. Adhes. Sci. Technol.*, 2019, **33**(22), 2443–2461.
- 204 N. B. Iroha and O. Akaranta, Experimental and surface morphological study of corrosion inhibition of N80 carbon steel in HCl stimulated acidizing solution using gum exudate from *Terminalia Mentaly*, *SN Appl. Sci.*, 2020, **2**(9), 1514.
- 205 H. F. Chahul, E. Maji and T. B. Danat, Adsorptive, inhibitive and thermodynamics studies on the corrosion of mild steel in the presence of *Mangifera indica* gums, *Ovidius Univ. Ann. Chem.*, 2019, **30**(2), 75–80.
- 206 V. Rajeswari, *et al.*, Physicochemical studies of glucose, gellan gum, and hydroxypropyl cellulose—Inhibition of cast iron corrosion, *Carbohydr. Polym.*, 2013, **95**(1), 288–294.
- 207 K. Azzaoui, *et al.*, Eco friendly green inhibitor Gum Arabic (GA) for the corrosion control of mild steel in hydrochloric acid medium, *Corros. Sci.*, 2017, **129**, 70–81.
- 208 M. Mobin and M. Rizvi, Inhibitory effect of xanthan gum and synergistic surfactant additives for mild steel corrosion in 1 M HCl, *Carbohydr. Polym.*, 2016, **136**, 384–393.
- 209 K. Kamburova, *et al.*, Chitosan–Alginate Nanocontainers with Caffeine as Green Corrosion Inhibitors for Protection of Galvanized Steel, *Crystals*, 2024, **14**(7), 660.
- 210 L. Muthulakshmi, *et al.*, Sodium Alginate: Grafted Alginates as Sustainable Corrosion Inhibitors, *Grafted Biopolymers as Corrosion Inhibitors: Safety, Sustainability, and Efficiency*, 2023, pp. 365–382.
- 211 M. Rbaa, *et al.*, Chemically Modified Natural Alginate Polysaccharide as Green Corrosion Inhibitors, in *Biopolymers in Sustainable Corrosion Inhibition*, CRC Press, pp. , pp. 131–147.
- 212 W. Zhang, *et al.*, Inhibition of mild steel corrosion in 1 M HCl by chondroitin sulfate and its synergistic effect with sodium alginate, *Carbohydr. Polym.*, 2021, **260**, 117842.
- 213 M. Madsen, *et al.*, Impact of alginate mannuronic-guluronic acid contents and pH on protein binding capacity and complex size, *Biomacromolecules*, 2021, **22**(2), 649–660.
- 214 L. Muthulakshmi, *et al.*, Sodium Alginate, *Grafted Biopolymers as Corrosion Inhibitors: Safety, Sustainability, and Efficiency*, 2023.
- 215 S. A. Umoren and M. M. Solomon, Green Corrosion Inhibitors: Natural Polymers and Amino Acids, in *Corrosion Science*, Apple Academic Press, 2023, pp. 483–518.
- 216 P. Kesari, G. Udayabhanu and A. Roy, Biopolymer sodium alginate based titania and magnetite nanocomposites as natural corrosion inhibitors for mild steel in acidic medium, *J. Ind. Eng. Chem.*, 2023, **122**, 303–325.
- 217 E. De Ketelaere, *et al.*, Investigation of an eco-friendly sodium alginate-sodium silicate inhibitor blend for carbon steel in a dynamic salt water environment, *Corros. Sci.*, 2024, **231**, 111991.



- 218 I. Nadi, *et al.*, Sargassum muticum extract based on alginate biopolymer as a new efficient biological corrosion inhibitor for carbon steel in hydrochloric acid pickling environment: Gravimetric, electrochemical and surface studies, *Int. J. Biol. Macromol.*, 2019, **141**, 137–149.
- 219 H. Eghbaljoo, *et al.*, Advances in plant gum polysaccharides; Sources, techno-functional properties, and applications in the food industry-A review, *Int. J. Biol. Macromol.*, 2022, **222**, 2327–2340.
- 220 M. Tanwar, R. K. Gupta and A. Rani, Natural gums and their derivatives based hydrogels: in biomedical, environment, agriculture, and food industry, *Crit. Rev. Biotechnol.*, 2024, **44**(2), 275–301.
- 221 N. R. Vaidya, P. Aklujkar and A. R. Rao, Modification of natural gums for application as corrosion inhibitor: a review, *J. Coat. Technol. Res.*, 2022, **19**(1), 223–239.
- 222 A. Peter, S. K. Sharma and I. B. Obot, Anticorrosive efficacy and adsorptive study of guar gum with mild steel in acidic medium, *J. Anal. Sci. Technol.*, 2016, **7**, 1–15.
- 223 Y. Cao, *et al.*, Green corrosion inhibitor of  $\beta$ -cyclodextrin modified xanthan gum for X80 steel in 1 M H<sub>2</sub>SO<sub>4</sub> at different temperature, *J. Mol. Liq.*, 2021, **341**, 117391.
- 224 C. Verma and M. Quraishi, Gum Arabic as an environmentally sustainable polymeric anticorrosive material: Recent progresses and future opportunities, *Int. J. Biol. Macromol.*, 2021, **184**, 118–134.
- 225 U. J. Timothy, *et al.*, An appraisal of the utilization of natural gums as corrosion inhibitors: Prospects, challenges, and future perspectives, *Int. J. Biol. Macromol.*, 2023, 126904.
- 226 M. Manickam, *et al.*, Corrosion Inhibition of Mild Steel in 1 mol L<sup>-1</sup> HCl Using Gum Exudates of *Azadirachta indica*, *Adv. Phys. Chem.*, 2016, 5987528.
- 227 N. Eddy, *et al.*, Physicochemical study and corrosion inhibition potential of *Ficus tricopoda* for aluminium in acidic medium, *Port. Electrochim. Acta*, 2013, **31**(2), 79–93.
- 228 N. O. Eddy, *et al.*, Adsorption and quantum chemical studies on the inhibition of the corrosion of aluminum in HCl by *Gloriosa superba* (GS) gum, *Chem. Eng. Commun.*, 2014, **201**(10), 1360–1383.
- 229 P. O. Ameh and N. O. Eddy, Commiphora pedunculata gum as a green inhibitor for the corrosion of aluminium alloy in 0.1 M HCl, *Res. Chem. Intermed.*, 2014, **40**, 2641–2649.
- 230 M. Ramesh and L. Rajeshkumar, Case-studies on green corrosion inhibitors, *Sustainable Corrosion Inhibitors*, 2021, **107**, 204–221.
- 231 Q. Wang, *et al.*, Insight into anti-corrosion behavior of protein extract as eco-friendly corrosion inhibitor, *Sustainable Chem. Pharm.*, 2023, **34**, 101177.
- 232 J. A. Patel and H. Kim, The TIMELESS effort for timely DNA replication and protection, *Cell. Mol. Life Sci.*, 2023, **80**(4), 84.
- 233 L. Noll, S. Zhang and W. Wanek, Novel high-throughput approach to determine key processes of soil organic nitrogen cycling: Gross protein depolymerization and microbial amino acid uptake, *Soil Biol. Biochem.*, 2019, **130**, 73–81.
- 234 A. S. Ismail and A. A. Farag, Experimental, theoretical and simulation studies of extracted crab waste protein as a green polymer inhibitor for carbon steel corrosion in 2 M H<sub>3</sub>PO<sub>4</sub>, *Surf. Interfaces*, 2020, **19**, 100483.
- 235 A. Siebert, *et al.*, Synthesis and antimicrobial activity of amino acid and peptide derivatives of mycophenolic acid, *Eur. J. Med. Chem.*, 2018, **143**, 646–655.
- 236 T. Rabizadeh and S. K. Asl, Casein as a natural protein to inhibit the corrosion of mild steel in HCl solution, *J. Mol. Liq.*, 2019, **276**, 694–704.
- 237 A. Pal, S. Dey and D. Sukul, Effect of temperature on adsorption and corrosion inhibition characteristics of gelatin on mild steel in hydrochloric acid medium, *Res. Chem. Intermed.*, 2016, **42**, 4531–4549.
- 238 B. El Ibrahimy, *et al.*, Amino acids and their derivatives as corrosion inhibitors for metals and alloys, *Arabian J. Chem.*, 2020, **13**(1), 740–771.
- 239 C. Verma, M. Quraishi and K. Y. Rhee, Aqueous phase polymeric corrosion inhibitors: Recent advancements and future opportunities, *J. Mol. Liq.*, 2022, **348**, 118387.
- 240 L. Hamadi, *et al.*, The use of amino acids as corrosion inhibitors for metals: A review, *Egypt. J. Pet.*, 2018, **27**(4), 1157–1165.
- 241 C. Verma, *et al.*, Heterocyclic amino acids-based green and sustainable corrosion inhibitors: Adsorption, bonding and corrosion control, *J. Cleaner Prod.*, 2024, 141186.
- 242 S. Pour-Ali, R. Tavangar and S. Hejazi, Comprehensive assessment of some l-amino acids as eco-friendly corrosion inhibitors for mild steel in HCl: Insights from experimental and theoretical studies, *J. Phys. Chem. Solids*, 2023, **181**, 111550.
- 243 H. H. Rasul, *et al.*, Theoretical investigation on corrosion inhibition efficiency of some amino acid compounds, *Comput. Theor. Chem.*, 2023, **1225**, 114177.
- 244 L. Matějovský, *et al.*, Amines as steel corrosion inhibitors in ethanol-gasoline blends, *Fuel*, 2024, **361**, 130681.
- 245 H. Ashassi-Sorkhabi, M. Majidi and K. Seyyedi, Investigation of inhibition effect of some amino acids against steel corrosion in HCl solution, *Appl. Surf. Sci.*, 2004, **225**(1–4), 176–185.
- 246 Q. Zhang, *et al.*, Comparison of the synergistic inhibition mechanism of two eco-friendly amino acids combined corrosion inhibitors for carbon steel pipelines in oil and gas production, *Appl. Surf. Sci.*, 2022, **583**, 152559.
- 247 R. H. Jacob, *et al.*, Chelated amino acids: biomass sources, preparation, properties, and biological activities, *Biomass Convers. Biorefin.*, 2024, **14**(3), 2907–2921.
- 248 B. E. Ibrahimy, L. Bazzi and S. E. Issami, The role of pH in corrosion inhibition of tin using the proline amino acid: theoretical and experimental investigations, *RSC Adv.*, 2020, **10**(50), 29696–29704.
- 249 E. Li, *et al.*, Amino acid imidazole ionic liquids as green corrosion inhibitors for mild steel in neutral media: Synthesis, electrochemistry, surface analysis and theoretical calculations, *J. Electroanal. Chem.*, 2023, **944**, 117650.



- 250 A. Vander Zee, *et al.*, Effect of Amino Acids on the Corrosion and Metal Release from Copper and Stainless Steel, *J. Electrochem. Soc.*, 2023, **170**(2), 021501.
- 251 R. Aslam, *et al.*, Proline nitrate ionic liquid as high temperature acid corrosion inhibitor for mild steel: Experimental and molecular-level insights, *J. Ind. Eng. Chem.*, 2021, **100**, 333–350.
- 252 J. Wang, C. Liu and B. Qian, A novel l-histidine based ionic liquid (LHIL) as an efficient corrosion inhibitor for mild steel, *RSC Adv.*, 2022, **12**(5), 2947–2958.
- 253 M. Moura, *et al.*, Study of the Efficiency of the Amino Acid L-Histidine as a Corrosion Inhibitor of 1018 Carbon Steel in Saline Solution Without and with CO<sub>2</sub> Saturation, *Mater. Res.*, 2024, **27**(suppl. 1), e20240135.
- 254 A. Dehghani, *et al.*, Improvement of the anti-corrosion ability of a silane film with  $\beta$ -cyclodextrin-based nanocontainer loaded with L-histidine: Coupled experimental and simulations studies, *Prog. Org. Coat.*, 2021, **157**, 106288.
- 255 D. Q. Huong, N. L. M. Linh and D. T. Quang, Corrosion Inhibition Ability of L-tryptophan and 5-hydroxy-L-tryptophan for Mild Steel: A Combination of Experimental and Theoretical Methods, *Phys. Chem. Chem. Phys.*, 2024, **26**, 21712–21726.
- 256 H. T. Abdel-Fatah, *et al.*, Adsorption and inhibitive properties of Tryptophan on low alloy steel corrosion in acidic media, *Arabian J. Chem.*, 2017, **10**, S1164–S1171.
- 257 N. Makarenko, U. Kharchenko and L. Zemnukhova, Effect of amino acids on corrosion of copper and steel in acid medium, *Russ. J. Appl. Chem.*, 2011, **84**, 1362–1365.
- 258 S. Gowri, *et al.*, Corrosion inhibition of carbon steel in sea water by Glutamic acid-Zn<sup>2+</sup> system, *Chem. Sci. Trans.*, 2013, **2**, 275–281.
- 259 D. Bouzidi, *et al.*, Electrochemical corrosion behaviour of iron rotating disc electrode in physiological medium containing amino acids and amino esters as an inhibitors, *Int. J. Electrochem. Sci.*, 2012, **7**(3), 2334–2348.
- 260 A. A. F. Sabirneeza, S. Subhashini and R. Rajalakshmi, Water soluble conducting polymer composite of polyvinyl alcohol and leucine: an effective acid corrosion inhibitor for mild steel, *Mater. Corros.*, 2013, **64**(1), 74–82.
- 261 H. Cang, *et al.*, Experimental and theoretical study for corrosion inhibition of mild steel by L-Cysteine, *Int. J. Electrochem. Sci.*, 2012, **7**(10), 10121–10131.
- 262 B. Qian, *et al.*, Synergistic effect of polyaspartic acid and iodide ion on corrosion inhibition of mild steel in H<sub>2</sub>SO<sub>4</sub>, *Corros. Sci.*, 2013, **75**, 184–192.
- 263 P. Singh, K. Bhrara and G. Singh, Adsorption and kinetic studies of L-leucine as an inhibitor on mild steel in acidic media, *Appl. Surf. Sci.*, 2008, **254**(18), 5927–5935.
- 264 M. Yadav, S. Kumar and L. Gope, Experimental and theoretical study on amino acid derivatives as eco-friendly corrosion inhibitor on mild steel in hydrochloric acid solution, *J. Adhes. Sci. Technol.*, 2014, **28**(11), 1072–1089.
- 265 A. S. Raja, S. Rajendran and P. Satyabama, Inhibition of corrosion of carbon steel in well water by DL-Phenylalanine-Zn<sup>2+</sup> System, *J. Chem.*, 2013, 720965.
- 266 E. Kowsari, *et al.*, In situ synthesis, electrochemical and quantum chemical analysis of an amino acid-derived ionic liquid inhibitor for corrosion protection of mild steel in 1M HCl solution, *Corros. Sci.*, 2016, **112**, 73–85.
- 267 A. Zomorodian, R. Bagonyi and A. Al-Tabbaa, The efficiency of eco-friendly corrosion inhibitors in protecting steel reinforcement, *J. Build. Eng.*, 2021, **38**, 102171.
- 268 P. Roy, *et al.*, Adsorption behaviour of gluten hydrolysate on mild steel in 1 M HCl and its role as a green corrosion inhibitor, *RSC Adv.*, 2015, **5**(75), 61170–61178.
- 269 Z. Zhang, H. Ba and Z. Wu, Sustainable corrosion inhibitor for steel in simulated concrete pore solution by maize gluten meal extract: Electrochemical and adsorption behavior studies, *Constr. Build. Mater.*, 2019, **227**, 117080.
- 270 N. Sahakyan, *et al.*, Bioavailability of tannins and other oligomeric polyphenols: A still to be studied phenomenon, *Curr. Pharmacol. Rep.*, 2020, **6**, 131–136.
- 271 C. S. Proença, *et al.*, Evaluation of tannins as potential green corrosion inhibitors of aluminium alloy used in aeronautical industry, *Metals*, 2022, **12**(3), 508.
- 272 B. Zhao, *et al.*, Corrosion inhibition performance of tannins for mild steel in hydrochloric acid solution, *Res. Chem. Intermed.*, 2018, **44**, 407–423.
- 273 A. A. Rahim, *et al.*, Mangrove tannins and their flavanoid monomers as alternative steel corrosion inhibitors in acidic medium, *Corros. Sci.*, 2007, **49**(2), 402–417.
- 274 M. T. de Sampaio, *et al.*, Evaluation of aqueous extract of *Mandevilla fragrans* leaves as environmental-friendly corrosion inhibitor for mild steel in acid medium, *J. Bio-Tribo-Corros.*, 2021, **7**, 1–11.
- 275 A. Kokalj, Considering the concept of synergism in corrosion inhibition, *Corros. Sci.*, 2023, **212**, 110922.
- 276 R. Naderi, S. Arman and S. Fouladvand, Investigation on the inhibition synergism of new generations of phosphate-based anticorrosion pigments, *Dyes Pigm.*, 2014, **105**, 23–33.
- 277 A. S. Afolabi, Synergistic inhibition of potassium chromate and sodium nitrite on mild steel in chloride and sulphide media, *Leonardo Electron. J. Pract. Technol.*, 2007, **11**, 143–154.
- 278 S. Rajendran, B. Apparao and N. Palaniswamy, Corrosion inhibition by phenyl phosphonate and Zn<sup>2+</sup>, *Anti-Corros. Methods Mater.*, 1998, **45**(3), 158–161.
- 279 M. Ahangar, *et al.*, The synergistic effect of zinc acetate on the protective behavior of sodium lignosulfonate for corrosion prevention of mild steel in 3.5 wt% NaCl electrolyte: Surface and electrochemical studies, *J. Mol. Liq.*, 2020, **314**, 113617.
- 280 I. Obot and A. Madhankumar, Enhanced corrosion inhibition effect of tannic acid in the presence of gallic acid at mild steel/HCl acid solution interface, *J. Ind. Eng. Chem.*, 2015, **25**, 105–111.
- 281 J. K. Das and B. Pradhan, Study on influence of nitrite and phosphate based inhibiting admixtures on chloride interaction, rebar corrosion, and microstructure of concrete subjected to different chloride exposures, *J. Build. Eng.*, 2022, **50**, 104192.



- 282 G. D. Eyu, *et al.*, The synergistic effect of iodide and sodium nitrite on the corrosion inhibition of mild steel in bicarbonate–chloride solution, *Materials*, 2016, **9**(11), 868.
- 283 M. Ali, C. Mustafa and M. Habib, Effect of molybdate, nitrite and zinc ions on the corrosion inhibition of mild steel in aqueous chloride media containing cupric ions, *J. Sci. Res.*, 2009, **1**(1), 82–91.
- 284 A. Al-Refaie, R. A. Cottis, and R. Lindsay, *Impact of Molybdate and Nitrite Anions on the Corrosion of Mild Steel*, NACE International Corrosion Conference Series, NACE, 2009.
- 285 S. A. Umoren and M. M. Solomon, Synergistic corrosion inhibition effect of metal cations and mixtures of organic compounds: a review, *J. Environ. Chem. Eng.*, 2017, **5**(1), 246–273.
- 286 D. Baskaran, *et al.*, Trends of Chemical Engineering Applications in the Last Three Decades: A Scientometric and Retrospective Review, *Korean J. Chem. Eng.*, 2024, 1–23.
- 287 J. Hu, *et al.*, Investigation on the synergy mechanism of mixed inhibitors–Mannich base and Na<sub>2</sub>WO<sub>4</sub> on Fe surface by molecules dynamic simulation, *Mol. Simul.*, 2019, **45**(11), 927–934.
- 288 S. Ghaffari, M. Aliofkhaezrai and A. S. Rouhaghdam, Corrosion Inhibition of Sodium Silicate and Piperazine and Their Synergistic Effect on Carbon Steel in Soft Water Media, *Prot. Met. Phys. Chem. Surf.*, 2019, **55**, 1195–1206.
- 289 H.-H. Ou, Q. T. P. Tran and P.-H. Lin, A synergistic effect between gluconate and molybdate on corrosion inhibition of recirculating cooling water systems, *Corros. Sci.*, 2018, **133**, 231–239.
- 290 Y. Zhou, Y. Zuo and B. Lin, The compounded inhibition of sodium molybdate and benzotriazole on pitting corrosion of Q235 steel in NaCl+ NaHCO<sub>3</sub> solution, *Mater. Chem. Phys.*, 2017, **192**, 86–93.
- 291 O. Benali, *et al.*, Green corrosion inhibitor: inhibitive action of tannin extract of *Chamaerops humilis* plant for the corrosion of mild steel in 0.5 M H<sub>2</sub>SO<sub>4</sub>, *J. Mater. Environ. Sci.*, 2013, **4**(1), 127–138.
- 292 D. E. Arthur, Computational and experimental study on corrosion inhibition potential of the synergistic 1: 1 combination of Arabic and cashew gums on mild steel, *Pet. Res.*, 2020, **5**(2), 170–180.
- 293 A. Berrissoul, *et al.*, Assessment of corrosion inhibition performance of origanum compactum extract for mild steel in 1 M HCl: Weight loss, electrochemical, SEM/EDX, XPS, DFT and molecular dynamic simulation, *Ind. Crops Prod.*, 2022, **187**, 115310.
- 294 M. El Azzouzi, *et al.*, Moroccan, Mauritania, and senegalese gum Arabic variants as green corrosion inhibitors for mild steel in HCl: Weight loss, electrochemical, AFM and XPS studies, *J. Mol. Liq.*, 2022, **347**, 118354.
- 295 A. Zeino, *et al.*, Mechanistic study of polyepoxy succinic acid (PESA) as green corrosion inhibitor on carbon steel in aerated NaCl Solution, *Mater. Today Commun.*, 2021, **29**, 102848.
- 296 Z. Bensouda, *et al.*, Extraction, characterization and anticorrosion potential of an essential oil from orange zest as eco-friendly inhibitor for mild steel in acidic solution, *J. Bio-Tribo-Corros.*, 2019, **5**, 1–20.
- 297 H. Zheng, *et al.*, Improved corrosion resistance of carbon steel in soft water with dendritic-polymer corrosion inhibitors, *Chem. Eng. J.*, 2023, **452**, 139043.
- 298 R. Shanmugapriya, *et al.*, Electrochemical and Morphological investigations of *Elettaria cardamomum* pod extract as a green corrosion inhibitor for Mild steel corrosion in 1 N HCl, *Inorg. Chem. Commun.*, 2023, **154**, 110958.
- 299 M. Adel, *et al.*, Removal of heavy metals and dyes from wastewater using graphene oxide-based nanomaterials: A critical review, *Environ. Nanotechnol., Monit. Manage.*, 2022, **18**, 100719.
- 300 M. Adel, M. A. Ahmed and A. A. Mohamed, Synthesis and characterization of magnetically separable and recyclable crumbled MgFe<sub>2</sub>O<sub>4</sub>/reduced graphene oxide nanoparticles for removal of methylene blue dye from aqueous solutions, *J. Phys. Chem. Solids*, 2021, **149**, 109760.
- 301 M. Adel, M. A. Ahmed and A. A. Mohamed, Effective removal of indigo carmine dye from wastewaters by adsorption onto mesoporous magnesium ferrite nanoparticles, *Environ. Nanotechnol., Monit. Manage.*, 2021, **16**, 100550.
- 302 N. B. Iroha, *et al.*, Linagliptin drug molecule as corrosion inhibitor for mild steel in 1 M HCl solution: Electrochemical, SEM/XPS, DFT and MC/MD simulation approach, *Colloids Surf., A*, 2023, **660**, 130885.
- 303 M. A. Ahmed, S. Amin and A. A. Mohamed, Fouling in reverse osmosis membranes: monitoring, characterization, mitigation strategies and future directions, *Heliyon*, 2023, **9**(4), e14908.
- 304 M. A. Ahmed, S. A. Mahmoud and A. A. Mohamed, Nanomaterials-modified reverse osmosis membranes: a comprehensive review, *RSC Adv.*, 2024, **14**(27), 18879–18906.
- 305 C. Jiang, *et al.*, Quantitative characterization of reinforcement cross-sectional roughness and prediction of cover cracking based on machine learning under the influence of pitting corrosion, *Measurement*, 2023, **220**, 113322.
- 306 S. Oh, *et al.*, The effect of surface roughness on re-passivation and pitting corrosion of super duplex stainless steel UNS S 32760, *Int. J. Electrochem. Sci.*, 2023, **18**(12), 100351.
- 307 M. A. Ahmed, S. A. Mahmoud and A. A. Mohamed, Unveiling the photocatalytic potential of graphitic carbon nitride (gC 3 N 4): a state-of-the-art review, *RSC Adv.*, 2024, **14**(35), 25629–25662.
- 308 M. A. Ahmed, M. A. Ahmed and A. A. Mohamed, Removal of 4-nitrophenol and indigo carmine dye from wastewaters by magnetic copper ferrite nanoparticles: Kinetic, thermodynamic and mechanistic insights, *J. Saudi Chem. Soc.*, 2023, **27**(6), 101748.
- 309 M. A. Ahmed, M. A. Ahmed and A. A. Mohamed, Facile adsorptive removal of dyes and heavy metals from wastewaters using magnetic nanocomposite of zinc



- ferrite@ reduced graphene oxide, *Inorg. Chem. Commun.*, 2022, **144**, 109912.
- 310 M. Adel, *et al.*, Characterization of fouling for a full-scale seawater reverse osmosis plant on the Mediterranean sea: membrane autopsy and chemical cleaning efficiency, *Groundw. Sustain. Dev.*, 2021, **16**, 100704.
- 311 M. Adel, M. A. Ahmed and A. A. Mohamed, A facile and rapid removal of cationic dyes using hierarchically porous reduced graphene oxide decorated with manganese ferrite, *FlatChem*, 2021, **26**, 100233.
- 312 A. Chraka, *et al.*, Electrochemical explorations, SEM/EDX analysis, and quantum mechanics/molecular simulations studies of sustainable corrosion inhibitors on the Cu-Zn alloy in 3% NaCl solution, *J. Mol. Liq.*, 2023, **387**, 122715.
- 313 K. E. Mouaden, *et al.*, Thiocarbonylhydrazide-crosslinked chitosan as a bioinspired corrosion inhibitor for protection of stainless steel in 3.5% NaCl, *Sustainable Chem. Pharm.*, 2020, **15**, 100213.
- 314 H. Didouh, *et al.*, Investigating the use of Moringa Oleifera leaf extract as an environment-friendly corrosion inhibitor for API 5L X52 steel in 1 M HCl, *J. Mol. Liq.*, 2023, **390**, 122910.
- 315 M. Rbaa, *et al.*, Green synthesis of novel carbohydrate polymer chitosan oligosaccharide grafted on d-glucose derivative as bio-based corrosion inhibitor, *J. Mol. Liq.*, 2021, **322**, 114549.
- 316 Q. Wang, *et al.*, Evaluation for Fatsia japonica leaves extract (FJLE) as green corrosion inhibitor for carbon steel in simulated concrete pore solutions, *J. Build. Eng.*, 2023, **63**, 105568.
- 317 F.-Z. Eddahhaoui, *et al.*, Experimental and computational aspects of green corrosion inhibition for low carbon steel in HCl environment using extract of Chamaerops humilis fruit waste, *J. Alloys Compd.*, 2024, **977**, 173307.
- 318 W. Zhang, *et al.*, High-performance corrosion resistance of chemically-reinforced chitosan as ecofriendly inhibitor for mild steel, *Bioelectrochemistry*, 2023, **150**, 108330.
- 319 N. I. F. Idelfitri, *et al.*, Synthesis, characterisation and corrosion inhibitory study of Meldrum's acid Thiosemicarbazone: Weight Loss, SEM-EDX and DFT, *Inorg. Chem. Commun.*, 2023, **150**, 110485.
- 320 N. Ferraa, *et al.*, Investigation of the inhibition behavior of an octacalcium phosphate as a green corrosion inhibitor against carbon steel in 3% NaCl medium, *Inorg. Chem. Commun.*, 2023, **157**, 111343.
- 321 P. Kesari, *et al.*, Chitosan based titanium and iron oxide hybrid bio-polymeric nanocomposites as potential corrosion inhibitor for mild steel in acidic medium, *Int. J. Biol. Macromol.*, 2023, **225**, 1323–1349.
- 322 A. A. Begum, *et al.*, Corrosion mitigation on orthodontic wire made of SS 18/8 alloy using esomeprazole tablet (Esiloc-40 mg) in artificial saliva, *J. Saudi Chem. Soc.*, 2023, **27**(4), 101681.
- 323 R. C. Nascimento, L. B. Furtado, and M. J. O. Guimarães, Biopolymers as Corrosion Inhibitors: Relative Inhibition Potential of Biopolymers and Grafted Biopolymers, *Grafted Biopolymers as Corrosion Inhibitors: Safety, Sustainability, and Efficiency*, 2023, pp. 21–55.
- 324 R. M. Nair, B. Bindhu and R. R. Isaac, Boron nitride nanosheets dispersed biopolymer solution as an effective copper corrosion inhibitor in acidic medium, *Polym. Bull.*, 2023, **80**(12), 12849–12863.
- 325 W. Sassi, *et al.*, New green advanced biopolymer as a repairer of aged AA-5083 alloy immersed into dead seawater, *J. Polym. Res.*, 2020, **27**, 1–18.
- 326 H. Khosravi, R. Naderi and B. Ramezanzadeh, Synthesis and application of molybdate-doped mussel-inspired polydopamine (MI-PDA) biopolymer as an effective sustainable anti-corrosion substance for mild steel in NaCl solution, *Biomass Convers. Biorefin.*, 2022, 1–17.
- 327 M. Galai, *et al.*, Surface analysis and interface properties of a newly synthesized quinoline-derivative corrosion inhibitor for mild steel in acid pickling bath: Mechanistic exploration through electrochemical, XPS, AFM, contact angle, SEM/EDS, and computational studies, *J. Phys. Chem. Solids*, 2024, **184**, 111681.
- 328 K. Dahmani, *et al.*, Evaluating the efficacy of synthesized quinoline derivatives as Corrosion inhibitors for mild steel in acidic environments: An analysis using electrochemical, computational, and surface techniques, *J. Mol. Struct.*, 2024, **1295**, 136514.
- 329 B.-I. Lin, *et al.*, Experimental and theoretical study on corrosion inhibition and adsorption performance of Ipomoea batatas L. leaf extract for mild steel, *Arabian J. Chem.*, 2024, **17**(1), 105410.
- 330 K. Subbiah, *et al.*, Unraveling the anti-corrosion mechanisms of a novel hydrazone derivative on steel in contaminated concrete pore solutions: An integrated study, *J. Adv. Res.*, 2024, **58**, 211–228.
- 331 A. Farhadian, *et al.*, Modified hydroxyethyl cellulose as a highly efficient eco-friendly inhibitor for suppression of mild steel corrosion in a 15% HCl solution at elevated temperatures, *J. Mol. Liq.*, 2021, **338**, 116607.
- 332 E. K. Ardakani, E. Kowsari and A. Ehsani, Imidazolium-derived polymeric ionic liquid as a green inhibitor for corrosion inhibition of mild steel in 1.0 M HCl: Experimental and computational study, *Colloids Surf., A*, 2020, **586**, 124195.
- 333 A. A. Abdulridha, *et al.*, Corrosion inhibition of carbon steel in 1 M H<sub>2</sub>SO<sub>4</sub> using new Azo Schiff compound: Electrochemical, gravimetric, adsorption, surface and DFT studies, *J. Mol. Liq.*, 2020, **315**, 113690.
- 334 Y. Zheng, *et al.*, Chitosan-acrylic acid-polysuccinimide terpolymer as environmentally friendly scale and corrosion inhibitor in artificial seawater, *Desalination*, 2021, **520**, 115367.
- 335 X. Li, *et al.*, Cassava starch ternary graft copolymer as a corrosion inhibitor for steel in HCl solution, *J. Mater. Res. Technol.*, 2020, **9**(2), 2196–2207.
- 336 T. W. Quadri, *et al.*, Grafted Starch Used as Sustainable Corrosion Inhibitors, *Grafted Biopolymers as Corrosion Inhibitors: Safety, Sustainability, and Efficiency*, 2023, pp. 313–335.



- 337 A. Rahimi, *et al.*, Novel sucrose derivative as a thermally stable inhibitor for mild steel corrosion in 15% HCl medium: An experimental and computational study, *Chem. Eng. J.*, 2022, **446**, 136938.
- 338 S. N. Dalhatu, *et al.*, L-arginine grafted chitosan as corrosion inhibitor for mild steel protection, *Polymers*, 2023, **15**(2), 398.
- 339 Z. Jiang, *et al.*, Dramatic improvement in corrosion inhibition effect of carboxymethyl cellulose by modified with levodopa: Experimental study and first-principles calculations, *Corros. Sci.*, 2024, 112037.
- 340 S. H. M. Jessima, *et al.*, Experimental and Theoretical Approach of Evaluating Chitosan Ferulic Acid Amide as an Effective Corrosion Inhibitor, *J. Bio- Tribo-Corros.*, 2023, **9**(4), 80.
- 341 M. Mobin, M. Basik and J. Aslam, Boswellia serrata gum as highly efficient and sustainable corrosion inhibitor for low carbon steel in 1 M HCl solution: experimental and DFT studies, *J. Mol. Liq.*, 2018, **263**, 174–186.
- 342 K. Bijapur, *et al.*, Recent trends and progress in corrosion inhibitors and electrochemical evaluation, *Appl. Sci.*, 2023, **13**(18), 10107.
- 343 Y. Wang and Y. Zuo, The adsorption and inhibition behavior of two organic inhibitors for carbon steel in simulated concrete pore solution, *Corros. Sci.*, 2017, **118**, 24–30.
- 344 M. Damej, *et al.*, New epoxy resin as a corrosion inhibitor for the protection of carbon steel C38 in 1 M HCl. experimental and theoretical studies (DFT, MC, and MD), *J. Mol. Struct.*, 2022, **1254**, 132425.
- 345 C. Gao, *et al.*, Lignin copolymers as corrosion inhibitor for carbon steel, *Ind. Crops Prod.*, 2021, **168**, 113585.
- 346 S. Gong, *et al.*, Glutamic Acid Enhances the Corrosion Inhibition of Polyaspartic Acid on Q235 Carbon Steel, *ACS Omega*, 2023, **8**(42), 39709–39719.
- 347 Y. Chen, X. Chen and Y. Liang, Synthesis of polyaspartic acid/graphene oxide grafted copolymer and evaluation of scale inhibition and dispersion performance, *Diamond Relat. Mater.*, 2020, **108**, 107949.
- 348 H. Adelnia, *et al.*, Metal ion chelation of poly (aspartic acid): From scale inhibition to therapeutic potentials, *Int. J. Biol. Macromol.*, 2023, **229**, 974–993.
- 349 X. Li, *et al.*, Synergistic inhibition effect of walnut green husk extract and sodium lignosulfonate on the corrosion of cold rolled steel in phosphoric acid solution, *J. Taiwan Inst. Chem. Eng.*, 2020, **114**, 263–283.
- 350 S. K. Saha, M. Murmu, and P. Banerjee, Computational modelings and software applications for corrosion inhibition, in *Electrochemical and Analytical Techniques for Sustainable Corrosion Monitoring*, Elsevier, 2023, pp. 155–190.
- 351 A. Berrissoul, *et al.*, Evaluation of Lavandula mairei extract as green inhibitor for mild steel corrosion in 1 M HCl solution. Experimental and theoretical approach, *J. Mol. Liq.*, 2020, **313**, 113493.
- 352 M. R. Khan, *et al.*, Direct Observation of Adsorption Morphologies of Cationic Surfactants at the Gold Metal-Liquid Interface, *J. Phys. Chem. Lett.*, 2020, **11**(22), 9901–9906.
- 353 B. Xu, *et al.*, Experimental and theoretical evaluation of two pyridinecarboxaldehyde thiosemicarbazone compounds as corrosion inhibitors for mild steel in hydrochloric acid solution, *Corros. Sci.*, 2014, **78**, 260–268.
- 354 X. Ko and S. Sharma, Adsorption and self-assembly of surfactants on metal-water interfaces, *J. Phys. Chem. B*, 2017, **121**(45), 10364–10370.
- 355 M. Doubi, *et al.*, A synthesis 3-phenyl-1, 2, 4-triazole-5-thione as an inhibitor against low carbon steel corrosion in simulated reinforced concrete: Experimental and theoretical studies, *Chem. Data Collect.*, 2023, **44**, 100989.
- 356 C. Verma, A. Thakur, R. Ganjoo, S. Sharma, H. Assad, A. Kumar, M. A. Quraishi and A. Alfantazi, Coordination bonding and corrosion inhibition potential of nitrogen-rich heterocycles: Azoles and triazines as specific examples, *Coord. Chem. Rev.*, 2023, **488**, 215177.

